Identification of Genomic Alterations in Castration Resistant Prostate Cancer using Next Generation Sequencing

Thesis

Submitted for a Doctoral Degree in Natural Sciences
(Dr. rer. nat)

Faculty of Mathematics and Natural Sciences
Rheinische Friedrich-Wilhelms-Universität Bonn

Submitted by

Roopika Menon

from Chandigarh, India

Bonn 2013

Prepared with the consent of the Faculty of Mathematics and Natural Sciences at the Rheinische Friedrich-Wilhelms- Universität Bonn

1. Reviewer: Prof. Dr. Sven Perner
2. Reviewer: Prof. Dr. Hubert Schorle

Date of examination: 19 November 2013
Year of Publication: 2014

Declaration

I solemnly declare that the work submitted here is the result of my own investigation, except where otherwise stated. This work has not been submitted to any other University or Institute towards the partial fulfillment of any degree.

Roopika Menon; Author

Acknowledgements

This thesis would not have been possible without the help and support of many people. I would like to dedicate this thesis to all the people who have helped make this dream a reality.

This thesis would have not been possible without the patience, support and guidance of my supervisor, Prof. Dr. Sven Perner. It has truly been an honor to be his first PhD student. He has both consciously and unconsciously made me into the researcher that I am today. My PhD experience has truly been the 'best' because of his time, ideas, funding and most importantly his incredible sense of humor. He encouraged and gave me the opportunity to travel around the world to develop as a scientist. I cannot thank him enough for this immense opportunity, which stands as a stepping-stone to my career in science. I would also like to thank Prof. Roman Thomas and Prof. Hubert Schorle for their advice on my thesis and their support. I would also like to thank Dr. Christine Schuberth who played an integral part in guiding me through the PhD process.

I would then like to thank my family members: my mother, father, and brother who have been pillars of support at every step of the way and have stood by me throughout this wonderful journey. I would like to thank them for your advice, guidance, love, and for being a major source of inspiration throughout my life. Words cannot describe all that you have done for me, and what you mean to me. I truly believe that my grandparents' blessings and good wishes have made me who I am and brought me to this stage in my life. I would like to thank Dinker Uncle, Pranati Aunty, Brahma Uncle, Hardi Aunty and Sudhaka for believing in me and for their kinds words of encouragement.

My fiancé, Vinay, has been a tremendous support during all my times of frustration. His patience and understanding helped me tackle every hurdle with courage and strength. My achievements were always his pride. His family has been an incredible source of encouragement, showering me with words of appreciation and instilling in me enough faith to carry this journey forward, till the end.

More importantly, I could not have completed my thesis without my ‘German family’. I would like to specifically thank Diana and Alina for being my ‘besties’. They were the first people I would run to for sharing all my PhD and non-PhD related happiness and sorrows. They truly share a very special place in my life. Wenzel’s presence in the lab brought a smile to my face on each and every day. My students, Kerstin and Fried, made science a fun and exciting experience. Mario’s bioinformatic analysis was the heart to my thesis, in him I found a great friend and a wonderful colleague. I would like to thank Silke, Karen, Anne, Angela, and Michael for their encouragement. I must mention Zaki Shaikhibrahim, who has been a mentor and a true friend through every step of the way. His advice and support on every topic has been invaluable. I must also thank Barny for making my time in the lab memorable and amusing. Thanks to my ‘German family’, my time in Germany has been a wonderful experience.

I would like to specifically thank Lynnette Fernandez Cuesta who was a constant source of optimism through this whole process. She not only guided me professionally, but has also been a close confidant through the past three years. Her advice and compassionate attitude have been priceless, and instrumental in my success. I shall treasure our interactions forever.

I would like to thank all my collaborators, both national and international, all members of the Institute of Pathology at Tuebingen and Bonn.

I would also like to thank all my friends in Tuebingen and Bonn for the wonderful time spent in these beautiful cities.

Table of Contents

1. Summary.....1

2. Introduction.....3
- 2.1 The Prostate.....4
- 2.2 Cancer Stages and Cancer Types.....5
- 2.3 Genomic Events Leading to PCa Initiation and Progression.....7
- 2.4 Processes Promoting PCa Progression 11
- 2.5 Androgen Receptor and PCa.....13
- 2.6 Available Treatments Options for PCa.....14
- 2.7 Pathology Archiving of PCa Samples.....16
- 2.8 Next Generation Sequencing 17
- 2.9 Next Generation Sequencing Approaches.....19
- 2.10 Next Generation Sequencing and PCa.....20

3. Aims of the Study.....23

4. List of Abbreviations.....25

5. Materials and Methods.....27
- 5.1 Reagents.....27
- 5.2 Apparatus.....28
- 5.3 Consumables.....29
- 5.4 Kits.....30
- 5.5 Cell Culture Reagents.....30
- 5.6 Cell Lines.....31
- 5.7 Antibodies.....31
- 5.8 Primers.....31
- 5.9 siRNA.....32
- 5.10 Buffers and Solutions.....32
- 5.11 BAC Clones.....33

6. Methods.....34
- 6.1 Next Generation Sequencing (SOLiD4).....37
- 6.2 Fixation Protocols 37
- 6.3 Fluorescent In-Situ Hybridization.....38
- 6.4 Cell Culture.....40
- 6.5 Protein Analysis.....42
- 6.6 Functional Assays.....44

7. Results.....49
- 7.1 Objective I.....49
- 7.2 Objective II.....58
- 7.3 Objective III 66

8. Discussion.....86

9. Conclusion.....94

10. References……..95

11. Appendix I……..104

12. Appendix II ……..111

13. List of Publications ……..115

14. Curriculum Vitae ……..116

1. Summary

Castration resistant prostate cancer (CRPC) is the most aggressive form of prostate cancer (PCa). For the development of novel therapeutic targets for CRPC, it is key to decipher the molecular alterations underlying this lethal disease. Next generation sequencing (NGS) technologies have revolutionized cancer research by detecting genomic alterations, nucleotide substitutions, insertions, deletions and copy number alterations. This project was focused on identifying novel genes involved in CRPC by assessing somatic copy number alterations (SCNA) using whole exome sequencing on five CRPC and paired normal formalin fixed paraffin embedded (FFPE) samples by the SOLiD4 next generation sequencing platform.

The central aim of this study was the identification of therapeutic targets for CRPC. Due to the unavailability and scarcity of fresh frozen CRPC material for research purposes, the primary aim of this study was to compare the DNA, RNA and protein integrity in fixed tissues obtained from pathology archives. Secondly, validity of formalin fixed paraffin embedded (FFPE) and fresh frozen PCa tissue, from the same patient, was determined by whole exome sequencing. A large data overlap between both fixed tissue types was observed. This eventually led to the main objective of the study involving the identification of therapeutic targets for CRPC.

FFPE and HOPE fixed specimen were comparable in DNA quality for downstream research purposes. Furthermore, FFPE tumor and fresh frozen tumor exome sequencing data, from the same patient, showed an overlap in the SNV analysis. This led to the central aim which included the analysis of somatic copy number alterations (SCNA) using whole exome sequencing on five CRPC and paired normal FFPE samples by the SOLiD4 next generation sequencing platform. The sequencing data identified two genes, *YWHAZ* and *PTK2*. Both genes, located on chromosome 8, were

amplified on all five sequenced patients. Furthermore, the amplification frequency of both genes increased depending on the stage of PCa: prostate confined or localized PCa, lymph node metastasized PCa and CRPC. *YWHAZ* knockdown in the PC-3 cell line impaired proliferation and migration. Similarly, *PTK2* inhibition, using a pharmacological inhibitor, TAE226 inhibitor, significantly affected both cell migration and proliferation at a concentration of 10 μM. Overall, these findings suggest that inhibiting both *YWHAZ* and *PTK2* could potentially delay cancer progression in patients harboring the amplification of the latter genes. Furthermore, FFPE tissue could be used as a promising alternative to fresh frozen tissue for NGS technologies.

2. Introduction

Prostate cancer (PCa) is the second largest cause of cancer related death in men of the western world, accounting for more than 250,000 deaths a year (**Figure 1**) (1). It has been reported that 1 out of every 6 men will be diagnosed with PCa and 1 out of every 3 diagnosed men will die of this disease (2). Various genetic alterations such as amplifications, deletions, mutations, substitutions, and rearrangements, have been studied to trigger the onset of disease. Unfortunately, due to its poorly understood molecular mechanisms, in addition to its highly heterogeneous and complex nature, treatment options for this disease remain a challenge (3).

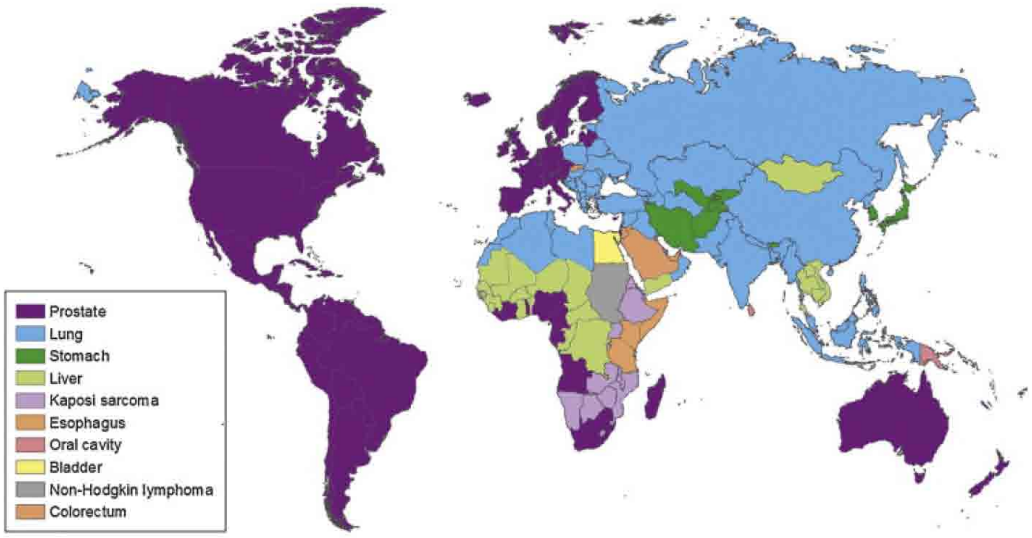

Figure 1: Prostate cancer diagnosis world wide.
The most commonly diagnosed cancer among men worldwide in 2008. Prostate cancer (purple) is the second largest cause of death in men of the western world. (adapted from Ferlay *et al*. 2010). (4)

2.1 The Prostate

The prostate is a walnut sized exocrine gland of the male reproductive organ. It surrounds the urethra and located at the base of the urinary bladder. The function of the prostate is the secretion of semen, with spermatozoa and seminal vesicle fluid. The secretions from the seminal make semen alkaline in nature, which aids in prolonging the lifespan of sperm (5). The prostate is architecturally defined as having four zones: the central, periurethral transition, peripheral, and fibromuscular stroma (6). These prostate zones consist of parenchymal cells, namely luminal epithelial cells, basal epithelial cells and fibromuscular stromal cells. The luminal epithelial cells express high levels of androgen receptor (AR). The basal epithelial cells express AR at low undetectable levels. A rare subset of cells known as the neuroendocrine cells expressing endocrine markers are also present (7).

In brief, the prostate is regulated by androgens, namely testosterone and 5-alpha-di hyrdotestosterone, produced by the male testicles. These hormones belong to the group of steroid hormones. The conversion of cholesterol to testosterone involves various steps (**Figure 2**) and studies have shown that 5% of testosterone is converted to dihydrotestosterone (DHT) through the 5-alpha-reductase catalyzed conversion in the cells of the external male genitalia, the prostate and the bulbourethral glands. DHT also exhibits a higher affinity to AR then testosterone. Furthermore, this highly active metabolite binds to several DNA sequences to initiate transcription. This results in the development and differentiation of the prostate (8).

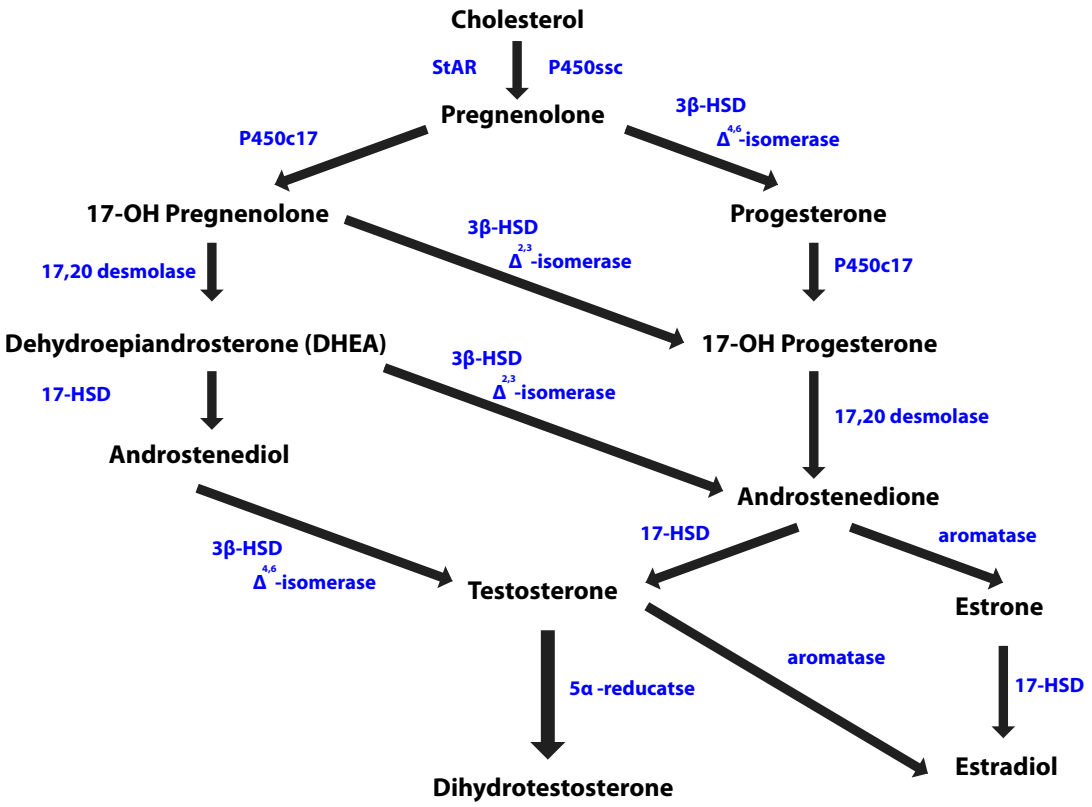

Figure 2: Conversion of cholesterol to testosterone.
DHT plays an active role in prostate cancer development and progression (adapted from Chen *et al*, 2006) . (9)

2.2 Cancer Stages and Types

PCa can be broadly categorized into three stages: localized PCa, lymph node metastasized PCa and distant metastasized PCa (**Figure 3**). Localized PCa is cancer that is confined to the prostate gland and is curable in majority of the cases. Lymph node metastasized PCa includes the spreading of the cancer through the lymph system consisting of lymph nodes and lymph vessels. The most lethal form of this disease is distant metastasized PCa, also known as castration resistant prostate cancer (CRPC), where the cancer has spread to distant tissues through the blood stream (10). The bone is the most frequent site of metastasis for PCa.

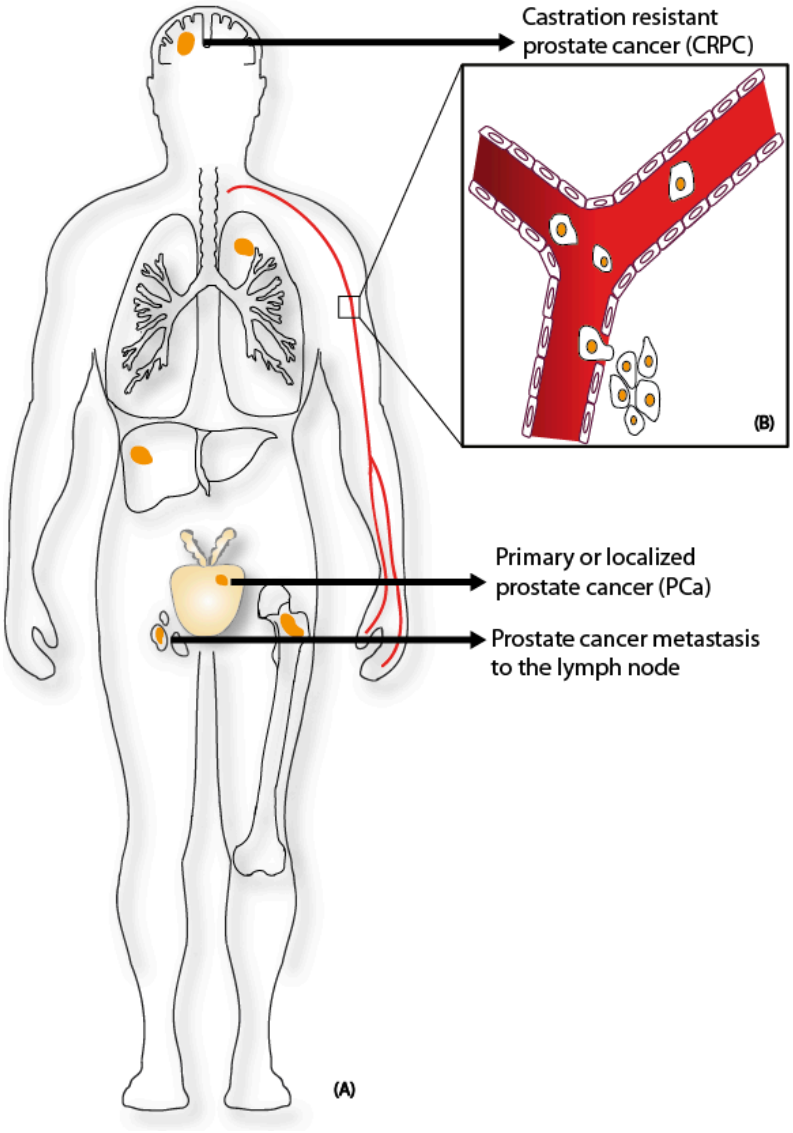

Figure 3: Prostate cancer types.
(A) Human schematic representing localized PCa, lymph node metastasized PCa and distant metastasis to the brain. (B) Metastasis of tumor cells from the site of origin to different locations in the body via the bloodstream (adapted from Braun et al. 2010) (11)

Additionally, PCa is commonly seen to occur in two types, namely adenocarcinoma and small cell carcinoma. Adenocarcinoma is the most common form of PCa, which arises from the cells of the glands. As most of the cells in the prostate are glandular cells, adenocarcinoma has a tendency to develop metastatic potential. The rare but highly aggressive form of PCa is small cell carcinoma. Small cell carcinomas are

aggressive because they are AR negative and patients do not benefit from hormone treatments (12).

2.3 Genomic Events Leading to PCa Initiation and Progression

In-depth analysis using comparative genomic hybridization (CGH) studies has identified various somatic alterations in PCa. These alterations include chromosomal losses at 3p, 8p,10q, 13q, and 17p. The 8q region is seen to be extensively amplified in PCa patients (13). Many genes lie in the regions of gains and losses known to be key players in PCa initiation and progression such as *NKX3.1* deletion, *MYC* amplification, *PTEN* (phosphatase and tensin homolog) deletion, *EZH2* up-regulation, and *TMRPSS2-ERG* gene fusions.

a) *NKX3.1* deletion: The *NKX3.1* homeobox gene located on 8p is frequently seen to be down regulated in advanced PCa. Through the progression of PCa, several studies indicate the complete loss of the gene or a reduction in protein expression. In mice, *NKX3.1* regulates prostate epithelial differentiation and stem cell function. In humans, the gene protects against DNA damage and regulates inflammation (14). Therefore, the absence or decrease of NKX3.1 expression in PCa progression suggests a role as a potential tumor suppressor in PCa.

b) *MYC* amplification: *MYC* is an oncogene situated in the 8q24 chromosomal region and is frequently amplified and over-expressed in advanced PCa. This gene is a transcription factor regulating metabolism, development, apoptosis, cell proliferation and differentiation (15). *MYC* amplifications often occur in combination with other genetic alterations leading to a cumulative negative effect (16). Studies have also shown that forced expression of *MYC* produces immortalized nontumorigenic human prostate epithelial cells (17).

c) *PTEN* (phosphatase and tensin homolog) deletion: *PTEN* is a potential tumor suppressor gene situated on 10q23. This gene is reported to be frequently deleted in various cancers. Previous publications have reported that the loss of *PTEN* activates the AKT and JNK signaling pathways therefore leading to the development of CRPC (18, 19). In PCa, conflicting data regarding the single allelic deletion of *PTEN*, mutation of the second allele, and the reduced expression of PTEN have been published (20). Interestingly, through the progression of PCa, *PTEN* copy number loss correlates to the aggressive nature of the disease. *PTEN*, *MYC* and *NKX3*.1 genetic alterations often occur together exhibiting a cumulative negative effect on patient health. With reference to cancer cell lines, human cell lines exhibiting decreased PTEN expression and *PTEN* deleted mouse cell PCa lines develop a castration resistant phenotype (21). The molecular mechanisms behind PTEN alterations in PCa remain to be investigated.

d) *EZH2* up-regulation: The up-regulation of *EZH2* through amplification is a common event in advanced PCa (22). The gene is part of the Polycomb family and codes for histone lysine methyltransferase. *EZH2* targets, which also include *NKX3.1*, play an active role in metastasis by the activation of the Ras and NF-$_K$B pathways (23). The polycomb family of genes function as inhibitors of gene expression by forming multimeric complexes of proteins. These structures alter chromatin structure. This family of genes regulates expression of cell cycle genes and *HOX* genes. These latter genes regulate proliferation (24).

e) *TMRPSS2-ERG* gene fusions: The most commonly occurring gene fusions in PCa involve the ETS transcription factors. The ETS transcription factors regulate DNA binding, both positively and negatively, to transcriptional regulatory properties on the same domain. Many ETS domain proteins are linked to cancer via various

mechanisms, which include their function in chromosomal translocations or overexpression/down-regulation in cancers. Similarly, the family of transcription factors also regulate proto-oncogenes or tumor suppressor proteins by their ability to transduce signals from oncogenically activated signaling cascades (25). The *TMPRSS2-ERG* gene fusion is the most common gene fusion occurring in 15-80% of PCa patients. The large variation is due to the ethnicity, age, family history etc. The *TMPRSS2* gene codes for a serine protease that is expressed in the epithelium of the prostate (26). The fusion occurs between the 5'exon of *TMPRSS2* and the coding sequence of *ERG*. The exact location of the fusion is on 21q22.2-22.3 resulting in two products, an insertion through deletion or a translocation (**Figure 4**).

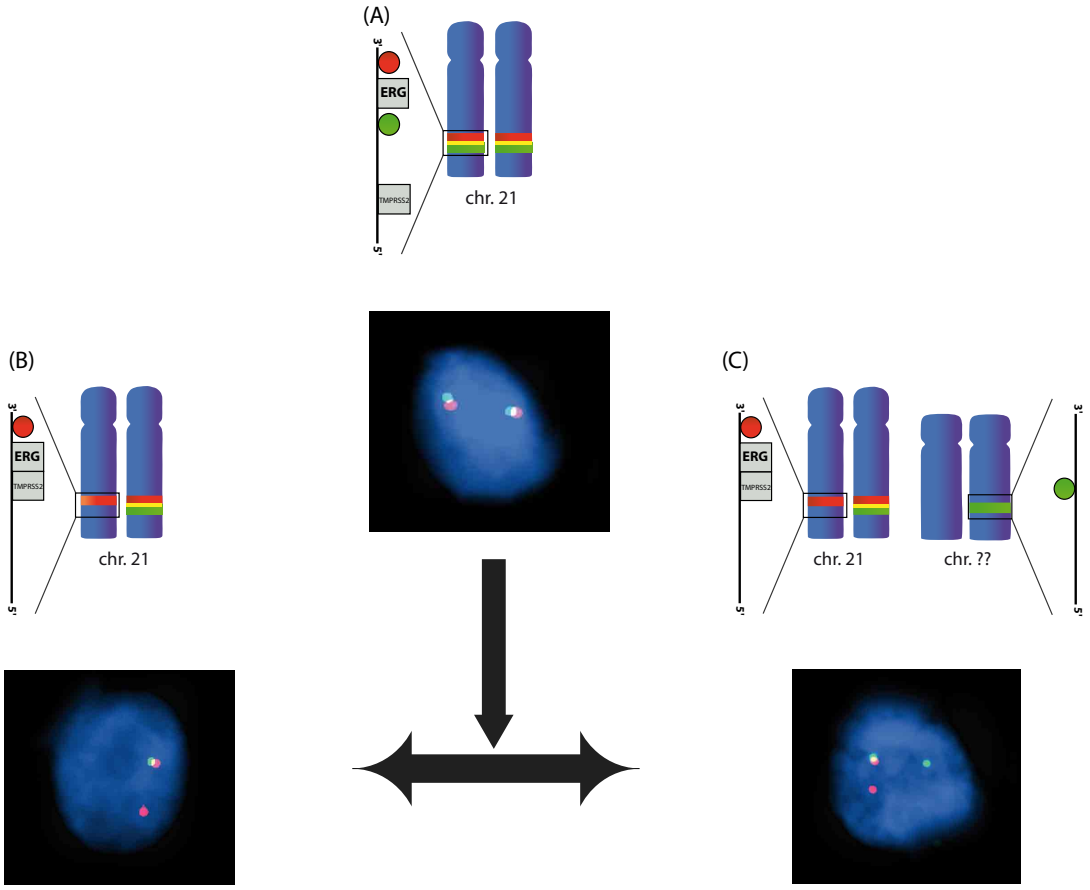

Figure 4: *ERG* rearrangement.
Dual colored fluorescent in situ hybridization (FISH) assay to detect *ERG* break-apart. (A) A wild type *ERG* rearranged nucleus. (B) *ERG* rearrangement through deletion. (C) *ERG* rearrangement through insertion (adapted from Braun *et al*., 2011). (27)

Studies show that in patients harboring the fusion, the *TMPRSS2* promoter contains the responsive promoter elements thus leading to androgen dependent *ETS* gene overexpression (28). This fusion may be a result of radiation and other genotoxic stress leading to double stranded breaks within the DNA. *TMPRSS2* is also seen to fuse with *ETV1, ETV4* and *ETV5*. Another gene fusion seen in very low frequencies is *SLC45A3* gene fusions with *ERG, ETV1* and *ETV5*(29).

The most commonly seen *TMPRSS2-ERG* gene results in the *TMPRSS2* exon 1 fusing with *ERG* exon 4, referred to as Type III isoform. This is seen in 80-90% of the gene fusions. The second most common isoform results in the fusion between *TMPRSS2* exon 2 and *ERG* exon 4, referred to as Type IV (**Figure 5**). The Type IV fusion result in enhanced proliferation and invasion of PCa epithelial cells (30).

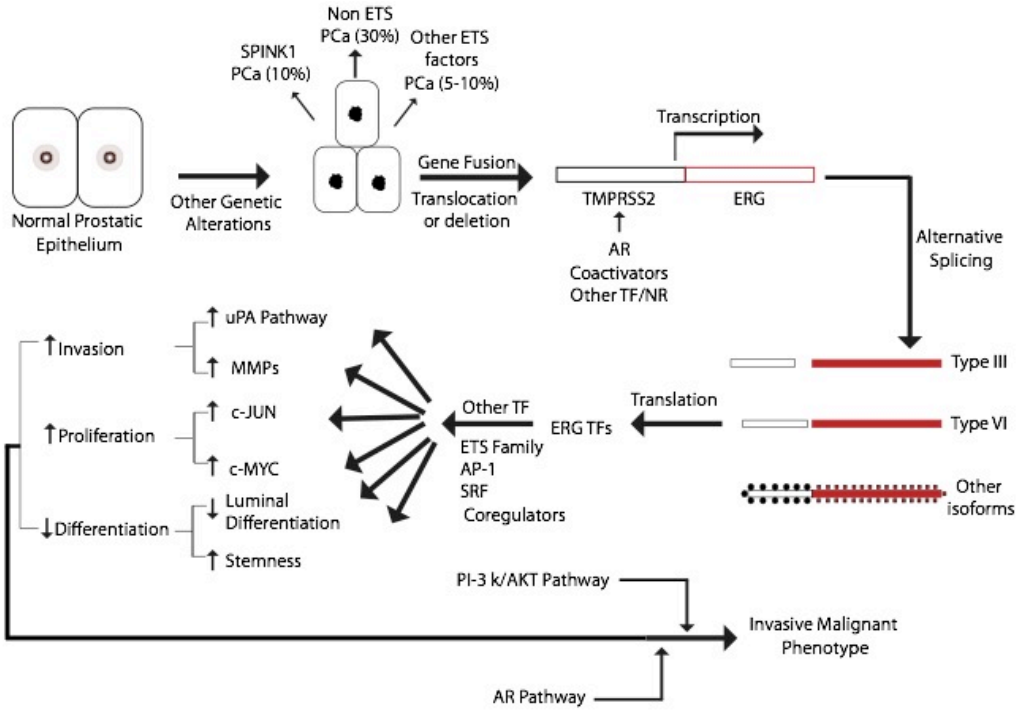

Figure 5: Role of TMPRSS2-*ERG* gene fusions.
The most commonly seen isoforms of the gene fusion include the Type III and Type IV. These fusions lead to the up and down-regulations of various pathways involved in PCa progression (adapted from Tindall *et al,* 2011) . (31)

Extensive studies on the *ERG* gene have shown its role in acting as an oncogene and promoting tumor formation. It interacts with the c-JUN and AP-1 pathways to promote growth, therefore indication the role of the gene fusion in the same (30). The VCaP cell line, a PCa cell line derived from a vertebral metastatic lesion, is the only cell line harboring the Type III gene rearrangement. Furthermore, studies have shown that the Type III isoform induces increased invasion, proliferation and motility and decreased differentiation (30).

e) Altered Pathways in PCa: One significant pathway that is altered in PCa is the up-regulation of the PI3K/AKT/mTOR signaling cascade. The tumor suppressor gene *PTEN* negatively regulates this pathway and loss of PTEN results in increase of cell growth, proliferation, and survival (32). In addition, the ERK/MAPK signaling pathway is also frequently activated in advanced PCa. Similarly, the RAS and RAF pathways are also up-regulated, possibly via mutations, in PCa (32). Inhibition of the above mentioned pathways has decreased tumor cell development and enhanced apoptosis. These characteristics have enhanced the role of these pathways as potential combinational therapeutic targets for treated PCa (33, 34).

2.4 Processes Promoting Prostate Cancer Progression

Various factors lead to PCa progression in men. Amongst these factors, age is considered to be the most significant risk factor leading to the development of PCa. Along with age, several environmental and physiological processes contribute to the progression of the disease. Several studies have identified inflammation, oxidative stress, telomere shortening and cell senescence also to play a key role in promoting PCa (7, 35, 36) .

a) Inflammation: Chronic inflammation in the presence of the expression of various chemokines has been reported to be linked to PCa progression (37). In older men, regions of frequent inflammation have been referred to as "proliferative inflammatory atrophy (PIA). These regions exhibit increased epithelial proliferation (38).

b) Oxidative Stress: An imbalance in the detoxifying enzymes and the reactive oxygen species (ROS) leads to lipid, DNA and protein damage, which is a major cause of oxidative stress. It is speculated that the prostate gland is highly vulnerable to oxidative stress due to the processes such as inflammation, hormonal dysregulation, diet, and epigenetic modifications. The epigenetic silencing of the gene, *GSTP1*, belonging to the glutathione S-transferase family is a classic example. The function of this gene is to initiate the detoxification of the ROS. In PCa, the gene is inactivated due to promoter hypermethylation thereby subjecting DNA to further genome damaging stress that may lead to malignant cancer progression. Another example is APE/Ref 1, a multifunctional enzyme controlling other enzymes involved in detoxification and base excision repair. This enzyme is up-regulated in PCa, but, PCa patients harboring a polymorphism in the *APE* gene are susceptible to developing cancer due to the loss of function of the gene (39).

c) Telomere shortening: Telomeres are repetitive sequencing situated on the ends of chromosomes to denote chromosomal stability. Studies have correlated the effects of telomere shortening during prostate carcinogenesis, but the exact mechanism of action still remains unclear (40).

d) Senescence: In PCa, oncogene driven senescence plays a key role in tumor suppression. Oncogenes, such as *FOXm1*, *p53*, *Rb, c-Myc*, drive senescence through replicative stress or the formation of ROS. Several senescence markers such as SA-β-Gal, $p14^{arf}$, $p16^{ink4a}$ are used to identify indolent phenotype from the aggressive (41).

2.5 Androgen Receptor and PCa

AR plays a key role in prostate cancer. The AR gene is part of the steroid hormone receptor superfamily of genes. It is a nuclear transcription factor located on the X chromosome. Structurally, it consists of 8 exons and is divided into three distinct domains: the N terminal domain (NTD), the deoxyribonucleic acid (DNA) binding domain, and the ligand binding domain (LBD). The "hinge domain" links the LBD to the DBD (42) (**Figure 6**).

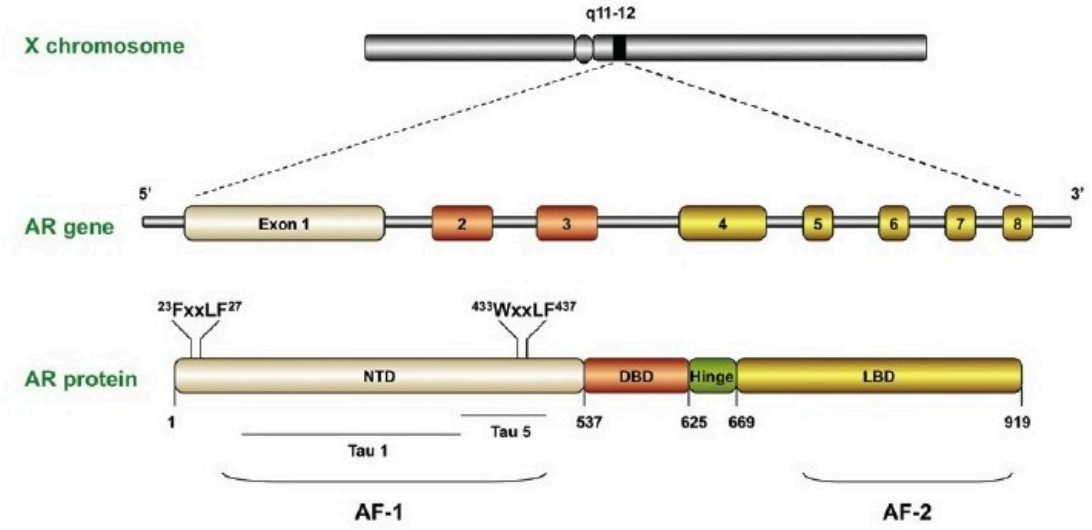

Figure 6: Schematic representation of *AR* on Chromosome X. (43)

Upon the binding of testosterone or DHT to the *AR* on the target cell, several heat shock proteins are dissociated to the cytoplasm. This is followed by a conformational change in the structure of the receptor resulting in its translocation to the nucleus. In the nucleus the receptor binds to specific DNA sequences and dimerizes resulting in the recruitment of coactivators such as ARA70, ARA55, ARA54, ARA267-α, Smad-3,and AIB1 (44). These steps lead to the activation of transcription of target genes such Prostate Specific Antigen (PSA) in the prostate, cyclin-dependent kinase

inhibitor 1A, Ezrin, Matrix metalloproteinase and SREBF chaperone. *AR* also recruits co-repressors such as *Cyclin D1, RAD9* homologs, Nuclear receptor co-repressor 1 and others (45-52). Therefore, *AR* is essential in maintaining homeostasis in both the epithelial and stromal tissues of the normal prostate.

Apart from the ligand binding activity of *AR*, several post translational modifications also play a major role in *AR* function. *AR* phosphorylation initiates the activation of growth factors, which are important for prostate epithelial cell growth and function. Acetylation of the *AR* is required for PCa proliferation and survival. This modification allows for the recruitment of co-regulators of the target genes and inhibits apoptosis mediated by *MEKK1* and *JNK* (53). Sumoylation of *AR* is necessary for the localization, degradation and activation of *AR*. Furthermore, AR ubiquitination plays a major role in enhancing the transcriptional of *AR* in the LNCaP cells (54).

More generalized function of the *AR* include the regulation of the cell cycle. *AR* up-regulates genes such as *Skp2, Cyclin D1, CDK1,* and *mTOR*; and down-regulates genes such as *p21*, and *p27*, thereby facilitating cellular replication and G1/S cell cycle transition. *AR* also regulates *Cyclin A* and *CDK2* activity by triggering the S and G2 phases of the cell cycle (55). Another important function of *AR* is the inhibition of apoptosis. It up-regulates Fas/FasL associated death domain protein like inhibitory protein (FLIP) that in turn inhibits the death induced signaling complex (DISC). Furthermore, the Wnt pathway downstream modulator, Beta-catenin, also interacts with *AR* and enhances gene transcription.

2.6 Available Treatment Options for PCa

PCa can be detected by a digital rectal exam, increased PSA levels in blood, MRI, CT scan, and surgery. PSA is a part of the kallikrein family and is an androgen regulated

serine protease that is secreted by both malignant and benign prostate epithelial cells. PSA values are influenced by several factors such as age, cancer, race and inflammation (56). Based on tumor growth and spread, the cancer is characterized based on the TNM system. T(umor) – measures the size of the tumor, N(odes)- accounts for spreading of the cancer to the lymph nodes and M(etastasis) – describes spreading of the cancer to various distant tissues through the blood stream. Furthermore, PCa stages I-IV describe the aggressiveness of the disease, with I denoting cancer confined to the prostate and IV denoting a highly aggressive and lethal form PCa (57).

Early stage treatment options for the PCa include radiation and surgery (radical prostatectomy). When closely monitored, 50% of patients benefit from this treatment. On the other hand, the lethal form of the disease, CRPC, has very limited treatment options and an average survival rate of a few months to a couple of years (58, 59). Thus, much needs to be done in developing treatment options for CRPC patients, as it still remains a major challenge.

The current and most commonly used treatment option for CRPC is androgen ablation therapy. The therapy is aimed at blocking the production of androgen that in turn regresses the growth and spread of PCa cells. Some FDA approved drugs include Abiraterone, a CYP17 inhibitor decreasing testosterone levels, and MDV-3100, an AR antagonist (60-62). Initially, patients respond well to treatment, but they are never completely cured of the disease, eventually resulting in recurrence and cancer related death. The major challenge involving the androgen ablation therapy is the ability of the PCa cell to survive and proliferate in the absence of androgen. To escape the androgen blockade, approximately one third of CRPC patient tumors develop AR amplifications (63). Other studies have shown that androgen ablation therapy results

in a gain of function mutation in the *AR* resulting in increased protein stability, sensitivity to minute amounts of androgens, sensitivity to other steroid hormones and increased recruitment of other AR coactivator proteins. Alternative splice forms of active AR variants often develop in CRPC (64). Lastly, another escape mechanism is the production of endogenously expressed androgen synthetic enzymes resulting in the *de* novo androgen synthesis and conversion of weaker androgens to testosterone and dihydrotestosterone.

2.7 Pathology Archiving of PCa Samples

For research purposes, PCa samples can be obtained in three forms: fresh frozen, formalin fixed paraffin embedded (FFPE) and hepes-glutamic acid (buffer mediated organic solvent protection effect (HOPE) fixation.

Fresh frozen samples are known to be the ideal source of material for genomic and proteomic analysis, with the least amount of degradation. Unfortunately, they are sparsely available and require labor-intensive protocols for storage and handling. Thus, storing fresh frozen material is a very tedious and cost intensive process. On the other hand, FFPE material is abundantly available in pathology archives. They are easy to handle and store but their research related applications remain limited (65-68). Recently, several studies have validated the use of FFPE tissue for DNA, RNA and protein related research (69, 70).

A promising new alternative is HOPE fixation. This fixation protocol may combine the benefits of both FFPE and fresh frozen material. The HOPE technique consists of a solution containing organic buffer, meant to serve as a protectant. Acetone acts as the dehydrating agent on the tissue, in combination with pure paraffin at 52-54°C melting temperature. The tissue is passed through the buffer to minimize degradation,

then dehydrated and fixed for long term use (71). HOPE fixed material has been used for several DNA and RNA based studies with promising results (71-73).

With regards to CRPC samples, the availability of fresh frozen CRPC material is limited. This is mainly because patients with advanced PCa do not undergo biopsies of metastasis as part of routine medical care (69). And the availably CRPC samples are FFPE fixed and stored in pathology archives. Due to the fixation protocols, there are major limitations and hurdles faced in performing a broad spectrum of molecular analysis with such material.

2.8 Next Generation Sequencing

Next generation sequencing (NGS) has revolutionized science in the past few years. It has made a profound impact on the understanding of genetics and biology. In research, NGS has enabled the study of the complete human genome, exome, transcriptiome and epigenomics, unlike earlier methods, which allowed the study of only select regions of the genome, exome and transcriptome. The new generations of sequencing platforms have improved sequencing productivity at an exponential growth rate, enabling fast, cheap and accurate ways to analyze sequences. The well known sequencing platforms include the Roche 454 Genome Sequencer, the Illumina Genome Analyzer and the Life Technologies SOLiD System. Each system has advantages and disadvantages with reference to its wide range of applications.

The Life Technologies SOLiD system functions on the principle of sequencing by ligation (74). It utilizes an average read length of 50 bp (base pairs). As FFPE samples are highly degraded, the short sequencing read length of 50 bp is optimal. In brief, a library of DNA/RNA fragments is prepared from the sample desired to be sequenced. The average size for SOLiD sequencing is 50-75 bp. These fragments are then

hybridized to beads. Each bead contains one fragment consisting of a universal P1 adapter sequence. This is to maintain homogeneity within all the beads containing the same P1 adapter sequence. This method uses the beads to generate amplified products by emulsion polymerase chain reaction (PCR) using the necessary PCR reagents. After the PCR reaction, the emulsion is broken and the beads containing amplified products are then immobilized on a substrate, a glass slide (**Figure 7**).

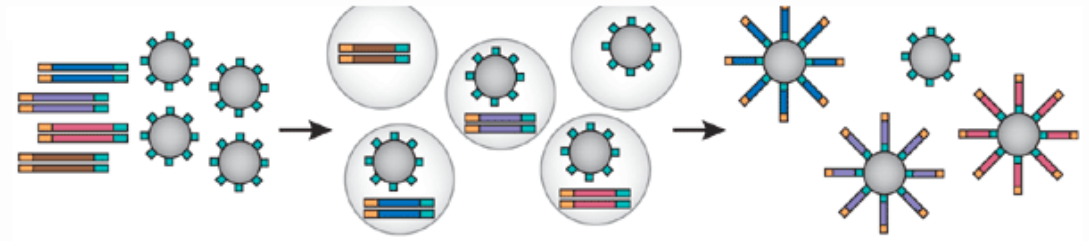

Figure 7: Emulsion PCR for the SOLiD platform
An adaptor flanked shotgun library is amplified by PCR that includes beads in water in oil emulsion reaction. The primer goes and attaches to the surface of the bead. PCR amplicons are captured on the bead surface that can be enriched after breaking the emulsion. (adapted from Shendure *et a*l. 2008). (75)

The sequencing occurs on the glass slide where primers that hybridize to the P1 adapter are used. To this reaction, dibase probes, probes consisting of two specific base pair combinations, compete for ligation to the primer sequence. Next, fluorescently labeled octamers are added to the mixture. Based on the position of the nucleotide in the octamer, a fluorescent signals is produced, determining the sequence of the fragment (**Figure 8**). Five sets of primers compete for each sequence. Through the sequencing process, to reduce the sequencing error, each base is read by two different primers in two independent ligation reactions. Therefore, the advantageous dual base encoding technology using dibase probes inherently corrects errors.

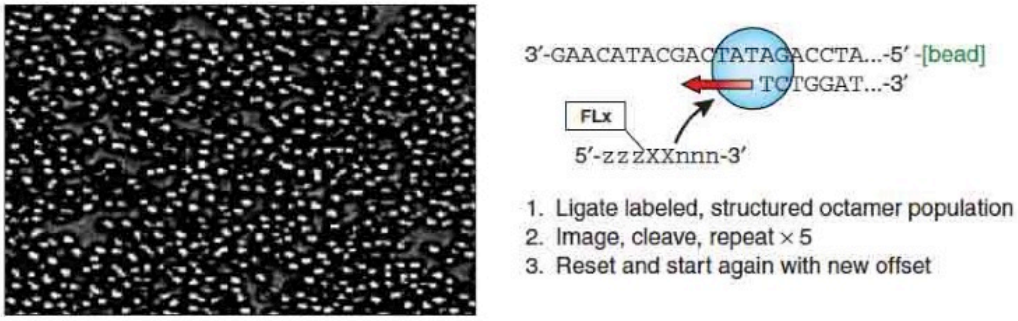

Figure 8: SOLiD Sequencing
Clonal amplification is performed on beads, to which fluorescently labeled octamers are added in cycles. After binding, cleavage occurs between position 5 and 6 and a new octamer is incorporated. This process is repeated in several cycles (adapted from Shendure *et a*l. 2008). (75)

Working with FFPE fixed tissue samples is a challenge due to cross linkage of biomolecules caused by the fixation protocols (76). Furthermore, nucleic acids are degraded into fragments. Due to above mentioned FFPE characteristics, using FFPE samples for NGS would require a platform that is capable of sequencing short fragments of DNA/RNA approximately 50-75bp in length. Therefore,, the ideal NGS platform is the SOLiD4 system, having an average read length of 50 base pairs and enabling an accurate capture of fragmented genomic DNA from FFPE tissues.

2.9 Next Generation Sequencing Approaches

Depending on the research question of interest, various approaches can be applied to NGS. Some of the most commonly used sequencing approaches have been described below:

a) Genome sequencing- Genome sequencing refers to the sequencing of all chromosomes including the mitochondrial DNA of an organism. Due to the large amount of data that is generated through genome sequencing, efficient computational skills and large storage is required. The data generated from genome sequencing identifies somatic and autosomal variations in an individual. Unfortunately, whole

genome sequencing is currently an expensive tool, but with the introduction of new sequencing platforms in the market, the cost is drastically reducing (77).

ii) Exome sequencing- The human exome makes up 1% of the genome and codes for proteins. The exome is composed of exons that are transcribed sequences that are part of the mRNA after the removal of introns. Previous studies have shown that the exome contains 85% of disease causing mutations in humans (78). There are approximately 180,000 exons in the human genome that are translated to 30 megabases in length (79). The primary aim of performing exome sequencing is to identify the functional disease specific variation in humans.

iii) Targeted resequencing- This method involves the sequencing of a particular region or gene of an individual's chromosome. Genes identified through genome, exome and transcriptome sequencing are validated by targeted resequencing approaches with a high level of accuracy. Targeted resequencing is widely used in clinical settings to identify causative mutations within populations, or to identify low frequency SNVs, single nucleotide variations, or various structural variants

2.10 Next Generation Sequencing and Prostate Cancer

With reference to patient care, NGS paved way to personalized therapeutics medicine. Whole genome, exome and transcriptome sequencing have identified tumor specific mutations and genes that could serve as potential therapeutic targets for cancer therapy. The tremendous amount of data generated from sequencing has aided in understanding the development and progression of various cancers by identifying tumor specific genes that up regulate cancer specific pathways and processes. Additionally, worldwide collaborative efforts have been made in the form of the

International Cancer Genome Consortium (ICGC) and The Cancer Genome Atlas (TCGA) Project to study the genomic landscape of thousands of cancers (80, 81).

Various studies have been aimed at understanding the molecular mechanism behind PCa initiation, development and progression through NGS technologies (69, 82-85). The aim of the studies is to capture a molecular signature for PCa at various stages to identify genes that have a potential role in tumorigenesis.

The paradigm-shifting discovery of the *TMRPSS2-ERG* recurrent gene fusion in approximately 50% of primary PCa became a basis for stratifying patients into fusion positive and fusion negative patients. Unfortunately, its role as a therapeutic target is still not clear and is under development (26).

In early 2011, in an attempt to perform an in-depth study on primary PCa, seven primary PCa samples were subjected to whole genome sequencing. Recurrent gene fusions involving *CADM2* (cell adhesion molecule 2) and *MAG12* (myelin associated glycoprotein) were reported to occur specifically in primary PCa, in addition to the *TMPRSS2-ERG* gene fusion (83). Exome sequencing on primary PCa also revealed the recurrent mutation of *SPOP* (speckle-type POZ protein), *FOXA1* (forkhead box AQ), and *MED12* (mediator complex subunit 12) (86). Furthermore, a deep mutational analysis was performed on mice xenografts of advanced and lethal PCa. *TP53* (tumor protein p53), *DLK2* (delta like 2 homolog), *GPC6* (glypican 6) and *SDF4* (stromal cell derived factor 4) were recurrently mutated in these samples (84).

Patients suffering from CRPC, being the most lethal form of the disease, are in an urgent need to identify potential therapeutic targets to block or delay the progress of cancer. Various CRPC studies describing the structural and epigenetic changes, and the mutational landscape have reported alterations in the advanced form of the disease

(69, 82, 85). But, functionally, much remains to be done to validate the therapeutic targets and provide the commercially available inhibitors for patient care.

3. Aims of the Study

Scientific Problem

The number of PCa related deaths is increasing each year, which has resulted in an over-diagnosis or over-treatment of men suffering from the disease. A major challenge in CRPC is the limited availability of promising treatment options. Currently, the most effective treatment option is androgen deprivation therapy, but in due course of time, most men develop resistance to this hormonal approach. Therefore, there is an urgent need to identify biomarkers and potential therapeutic targets to delay or inhibit the progression of cancer from an indolent to a highly aggressive stage.

Chromosome 8q amplification is a very common event in localized PCa. This chromosomal region consists of oncogenes such as *cMYC, eIF3* and *PSCA* that play an active role in cancer initiation. Deletion of various tumor suppressors such as *PTEN, NKX3.1* all together enhance cancer progression. The discovery of the *TMRPSS2-ERG* rearrangement became a plausible basis for patient stratification but its function as a therapeutic target is under investigation.

Aims

The overall aim of this study is to decode the molecular and genetic alternations using novel high throughput sequencing approaches on a clinically well-defined cohort of hormone refractory prostate cancer (CRPC) patients to identify novel therapeutic targets. This aim was subdivided into three objectives-

Objective I: Determining the DNA, RNA and protein integrity of fresh-frozen, FFPE and HOPE fixed tissue to identify the optimal tissue for sequencing and functional studies.

Objective II: Determining the sequencing efficiency of FFPE tissue, in comparison to fresh-frozen tissue, both obtained from the same patient, using the SOLiD4 sequencing platform.

Objective III: Identification of novel therapeutic targets for castration resistant prostate cancer by whole exome sequencing, and functional validation of the identified targets.

4. List of Abbreviations

%	percent
AR	androgen receptor
bp	base pairs
BSA	bovine serum albumin
°C	temperature in degree Celsius
cDNA	complementary DNA
cMYC	c-myc avian myelocytomatosis viral oncogene homolog
CRPC	castration resistant prostate cancer
DAPI	4'-6-Diamidino-2-phenylindole
DMEM	dulbecco's modified eagle medium
DMSO	dimethyl sulfoxide
DNAse	desoxyribonuclease
dNTP	deoxynucleotidetriphosphate
EDTA	ethylenediaminetetraacetic acid
ERG	v-ets erythroblastosis virus E26 oncogene homolog (avian)
FBS	foetal bovine serum
FFPE	formalin fixed paraffin embedded
FISH	fluorescent in situ hybridization
g	gram
HE	Hematoxylin and eosin
HEPES	4-(2-hydroxyethyl)-1-piperazineethanesulfonic acid
IHC	immunohistochemistry
kb	kilobases
kDa	kilodalton
L	liter
LN	lymph node
m	milli
M	mol L^{-1}
µ	micro
mRNA	messenger RNA
NGS	next generation sequencing
NKX3.1	Homeobox protein NK-3 homolog A
OD	optical density
PAGE	polyacrylamide gelelectrophoresis
PBS	phosphate-buffered saline
PCa	prostate cancer
PCR	polymerase chain reaction
PFA	paraformaldehyde
PTEN	phosphatase and tensin homolog
PTK2	protein tyrosine kinase 2
PVDF	polyvinylidene fluoride
qRT-PCR	quantitative real-time polymerase chain reaction
RNase	ribonuclease

x g	centrifugal force
SCNA	somatic copy number alterations
SDS	sodium dodecyl sulfate
siRNA	short interference ribonucleic acid
SNV	single nucleotide variations
SOLiD	Sequencing by oligonucleotide ligation and sequencing
Temed	N,N,N',N'-tetramethylethylendiamine
TMA	tissue microarray
Tris	Tris-(hydroxymethyl)-aminomethane
UV	ultra violet
YWHAZ	tyrosine 3-monooxygenase/tryptophan 5-monooxygenase activation protein, zeta polypeptide

5. Materials

5.1 Reagents

Chemicals	Manufacturer	Location
2-Propanol	AppliChem	Gablingen
Acetone	AppliChem	Gablingen
Ammonium persulfate	Carl Roth	Karlsruhe
Ampicillin	Sigma Aldrich	Steinheim
Bovine serum albumin standard	Sigma Aldrich	Steinheim
CAS-Block	Life Technologies	Darmstadt
Centromeric probe (Chr. 8)	Metasystems	Altussheim
Chloramphenicol	Sigma Aldrich	Steinheim
Cot Human DNA	Roche	Mannheim
DEPC, treated water	Carl Roth	Karlsruhe
Developer	Fujifilm	Düsseldorf
Dextran Sulfate, Sodium Salt	Merck	Darmstadt
di Natriumhydrogenphosphate	Merck	Darmstadt
Digest-All 3	Invitrogen	Karlsruhe
Digoxigenin	Roche	Mannheim
Dimethyl sulfoxide	Sigma Aldrich	Steinheim
Ethanol	AppliChem	Gablingen
Ethidium Bromide	Sigma Aldrich	Steinheim
Ethylenediaminetetraacetic acid (EDTA)	Sigma Aldrich	Steinheim
EtOH 100%	Merck	Darmstadt
Fixer	Fujifilm	Düsseldorf
Formamide	Merck	Darmstadt
Glycerol	AppliChem	Gablingen
Glycine	Carl Roth	Karlsruhe
Glycogen, Ultra Pure	Invitrogen	Karlsruhe
Hoechst 33342	Invitrogen	Karlsruhe
HOPE® Fixative System I	Polysciences, Inc.	Eppelheim
HOPE® Fixative System II	Polysciences, Inc.	Eppelheim
Human Cot-1 DNA	Invitrogen	Karlsruhe
Hydrochloric acid	Merck	Darmstadt
Igepal CA 630	Sigma Aldrich	Steinheim
Illustra MicroSpin S-200 HR Columns	GE Healthcare	Munich
Potassium chloride	Merck	Darmstadt
Potassium hydrogen phosphate	Merck	Darmstadt
Laemmli loading buffer	Carl Roth	Karlsruhe
LB- Agar	Merck	Darmstadt
LB-Medium	AppliChem	Gablingen
Lipfectamine siRNA MAX	Invitrogen	Karlsruhe
Luria Broth - agar	AppliChem	Gablingen
Luria Broth - medium	AppliChem	Gablingen

Methanol	AppliChem	Gablingen
Nonfat dried milk powder	AppliChem	Gablingen
Normal Goat Serum	Dianova	Hamburg
Page ruler protein ladder	Thermo Scientific,	Karlsruhe
Phosphatase inhibitor cocktail 2 and 3	Sigma Aldrich	Steinheim
Ponceau S	Sigma Aldrich	Steinheim
ProLong Gold antifade reagent with DAPI	Invitrogen	Karlsruhe
Phenylmethanesulfonyl fluoride	Sigma Aldrich	Steinheim
Protease inhibitor	Sigma Aldrich	Steinheim
Revertaid H-Minus First Strand cDNA Kit	Fermentas	Karlsruhe
RNAase zap	Ambion	Karlsruhe
RNase A	AppliChem	Gablingen
Roti load 4x concentrate	Carl Roth	Karlsruhe
Sodium acetate	Sigma Aldrich	Steinheim
Sodium azide	Carl Roth	Karlsruhe
Sodium chloride (NaCl)	Merck	Darmstadt
Sodium dodecyl sulfate	Carl Roth	Karlsruhe
Spot Light CISH Translocation Kit	Invitrogen	Karlsruhe
Streptavidin, Alexa Flour 594 conjugate 2 mg/ml	Invitrogen	Karlsruhe
Streptavidin, Rhodamine Red-x conjugate	Invitrogen	Karlsruhe
Tetramethylethylenediamine	Carl Roth	Karlsruhe
Tris(hydroxymethyl)-aminomethane	Carl Roth	Karlsruhe
Tris(hydroxymethyl)-aminomethane	Carl Roth	Karlsruhe
Tween® 20	Merck	Darmstadt
Western Blot detection reagent	GE Healthcare	Munich
Xylene	AppliChem	Gablingen
Xylol	ProLabo	Cologne
Yo PRO	Invitrogen	Karlsruhe
β-mercaptoethanol	Alfa Aesar	Karlsruhe

5.2 Apparatus

Apparatus	Manufacturer	Location
Bacterial Shaker	B. Braun Biotech International	Melsungen
BBD 6220 CO_2 Incubator	Thermo Scientific	Karlsruhe
Covaris™ S2	Life Technologies GmbH	Darmstadt
ELISA reader	Biotek	Bad Friedrichshall
Gel Doc X	Biorad	Munich
IKA Vortex Genius 3	IKA	Staufen
Inverted Microscope	Olympus	Hamburg
Light Cycler® 480 Real Time PCR	Roche	Mannheim

System		
Magnetic Shaker	IKA	Staufen
Microtome	Zeiss	Oberkochen
Millipore Milli Q	Millipore	Schwalbach
Mini PROTEAN tetra electrophoresis system	BioRad	Munich
Multifuge 1L-R centrifuge	Thermo Scientific	Karlsruhe
NanoDrop 2000c	Thermo Scientific	Karlsruhe
Nikon Eclipse 80i	Nikon	Düsseldorf
PCR system	Applied Biosystems	Darmstadt
PCR work station	Peqlab	Erlangen
pH meter	PCE Deutschland	Meschede
PowerPac power supply	BioRad	Munich
Semiautomatic tissue array instrument	Beecher Instruments	Sun Prairie, WI, USA
Sorvall Legend Centrifuge	Ependorf	Hamburg
Sterile Bench	Scanlaf	Denmark
Thermo mixer	Eppendorf	Hamburg
Thermocycler	Applied Biosystems	Darmstadt
Trans blot SD semi dry electrophoretic Transfer Cell	BioRad	Munich
Waterbath	Memmert	Schwabach
Weighing Scale	Thermo Scientific	Karlsruhe
Xcelligence	Roche	Mannheim
Zeiss, Oberkochen Imager.Z1	Zeiss	Oberkochen

5.3 Consumables

Consumables	Manufacturer	Location
1.5 ml tubes	Fisher Scientific GmbH	Schwerte
2 ml tubes	Fisher Scientific GmbH	Schwerte
6 well cell culture plates	VWR International GmbH	Darmstadt
12 well cell culture plates	VWR International GmbH	Darmstadt
24 well cell culture plates	VWR International GmbH	Darmstadt
96 well cell culture plates	VWR International GmbH	Darmstadt
15 ml falcon	Labomedic GmbH	Bonn
50 ml falcon	Labomedic GmbH	Bonn
15 ml falcon	Labomedic GmbH	Bonn

25T cell culture flask	VWR International GmbH	Darmstadt
75T cell culture flask	Greiner Bio	Frickenhausen
Cell scraper	TPP	Switzerland
Cryo tubes	Labomedic GmbH	Bonn
PCR tubes	Fisher Scientific GmbH	Schwerte
Pipette tips	Nerbe Plus	Winsen/Luhe
Sterile filter 0.2 µm	VWR International GmbH	Darmstadt

5.4 Kits

Kits	Manufacturer	Location
Agencour AMPure XP	Beckman Coulter	Krefeld
Agilent RNA 6000 nano kit	Agilent Technologies	Ratingen
Agilent Sure Select	Agilent	Waldbronn
BCA protein assay kit	Thermo Scientific	Karlsruhe
Bio Prime Kit	Life Technologies	Darmstadt
Cell proliferation kit I	Roche	Mannheim
Library Column Purification Kit	Applied Biosystems	Darmstadt
LightCycler 480 ProbesMaster	Roche	Mannheim
Plasmid maxi kit	Qiagen	Hilden
Plasmid mini kit	Qiagen	Hilden
Recover All Extraction Kit	Life Technologies	Darmstadt
Repli-g Mini Kit	Qiagen	Hilden
RNeasy mini kit	Qiagen	Hilden
RNeasy mini kit	Qiagen	Hilden
SuperScript VILO cDNA synthesis kit	Life Technologies	Darmstadt
TAE 226 inhibitor	Novartis	Switzerland

5.5 Cell Culture Reagents

Cell culture reagents	Manufacturer	Location
Dimethylsulphoxide (DMSO)	PAN Biotech	Aidenbach
F12 Nutrient Media	Life Technologies	Darmstadt
Fetal calf serum (FCS)	PAA	Cölbe
HEPES	PAN Biotech	Aidenbach
L-Glutamine	PAN Biotech	Aidenbach
Non essential amino acids (NEAA)	Life Technologies	Darmstadt
Penicillin/Streptomycin	PAA	Cölbe
Phosphate buffered saline (PBS)	Life Technologies	Darmstadt
RPMI 1640	Life Technologies	Darmstadt
RPMI 1640+ GLutamax	Life Technologies	Darmstadt
Trypsin-EDTA	Life Technologies	Darmstadt

5.6 Cell Lines

Cell line	Description	Manufacturer
Du-145	Brain metastasis derived from prostate cancer	ATCC
LNCaP	Lymph node metastasis derived from prostate cancer	ATCC
PC-3	Bone metastasis derived from prostate cancer	ATCC
VCaP	Bone metastasis derived from prostate cancer	ATCC

5.7 Antibodies

Antibodies	Manufacturer	Location
14-3-3 ζ (C-16): sc-1019 polyclonal	Santa Cruz	Heidelberg
Goat anti mouse HRP	Sigma Aldrich	Steinheim
Goat anti rabbit HRP	Sigma Aldrich	Steinheim
GOLPH2 Antibody (5B10)	Abnova	Heidelberg
Mouse anti *β-actin*	Sigma Aldrich	Steinheim
p63 Antibody (4A4)	Dako	Belgium
Prostate Specific Antigen Antibody (35H9)	Novocastra	UK
Purified Mouse Anti-FAK monoclonal	BD Transduction Laboratories	Heidelberg
Purified Mouse Anti-Human FAK (pY397) monoclonal	BD Transduction Laboratories	Heidelberg

5.8 Primers

Primers for qPCR	Sequence
β-actin forward	5'GCACCCAGCACAATGAAGA3'
β-actin reverse	5'CGATCCACACGGAGTACTTG3'
YWHAZ forward	5'GATCCCCAATGCTTCACAAG3'
YWHAZ reverse	5'TGCTTGTTGTGACTGATCGAC3'
PTK2 forward	5'TGAGGGAGAAGTATGAGCTTGC3'
PTK2 reverse	5'TTGGCAAATAACGAATTCTCAA3'
GAPDH forward	5'GAGTCAACGGATTTGGTCGT3'
GAPDH reverse	5'TGGGATTTCCATTGATGACA3'
GAPDH probe	5'FAM-CAATGACCCCTTCATTGACC-TAMRA-3'

β-actin forward	5'AGAGCTACGAGCTGCCTGAC3'
β-actin reverse	5'AGTACTTGCGCTCAGGAGGA3'
β-actin probe	5'FAM-CTGTACGCCAACACAGTGCT-TAMRA-3'
TBP forward	5'GCCCGAAACGCCGAATAT3'
TBP reverse	5'CCGTGGTTCGTGGCTCTCT-3'
TBP probe	5'FAM-ATCCCAAGCGGTTTGCTGCGG-TAMRA-3'

Primers for PCR	**Sequence**
TBXAS1 forward	5'GCCCGACATTCTGCAAGTCC3'
TBXAS1 reverse	5'GGTGTTGCCGGGAAGGGTT3'
RAG1 forward	5'TGTTGACTCGATCCACCCCA3'
RAG1 reverse	5'TGAGCTGCAAGTTTGGCTGAA3'
AF4 reverse	5'CCGCAGCAAGCAACGAACC3'
AF4 forward	5'GCTTTCCTCTGGCGGCTCC3'
AF4 reverse	5'GGAGCAGCATTCCATCCAGC3'
AF4 forward	5'CATCCATGGGCCGGACATAA3'
PLZF forward	5'TGCGATGTGGTCATCATGGTG3'
PLZF reverse	5'CGTGTCATTGTCGTCTGAGGC3'

5.9 siRNA

siRNA	**Sequence**
YWHAZ target sequencing	5'AAAGUUCUUGAUCCCCAAUGC3'
Scrambled sequence	5'-CAG-UCGCGUUUGCGACUGG3'
YWHAZ pooled sequencing	5'GCUUGGUAUUCAUUACUUC3' 5'GAAUCAUACCCCAUGGAUA3' 5'UCUGUAUGUUCUAUUGUGC3' 5'UCUUGAUCCCCAAUGCUUC3'

5.10 Buffers and Solutions

Buffers and solutions	
Ripa-lysis buffer	1% Igepal CA 600 0.5% Na-deoxycholate 10%SDS 0.25 M EDTA PBS
TBS-T (pH 7.5)	50 mM Tris-Cl 150 mM NaCl 0.05% Tween 20
Transfer buffer (pH 8.3)	250 mM Tris-Cl 1.92 M Glycine
Running buffer (pH 8.3)	250 mM Tris-Cl 1.92 M Glycine 1% SDS

20x SSC (pH7.0)	3 M NaCl 300 mM Tridsodium citrate
Cot 1 solution	1.5 µg/µl cot-1 in hybridization buffer
1x PBS (pH 7.4)	137 mM NaCl 10 mM Phosphate 2.7 mM KCl
TE (pH 8.0)	10 mM Tris 1 M EDTA
PI/RNase A	50 mg/ml Propidium Iodide 0.5% Glucose in 1x PBS
Stacking Gel buffer (pH 6.8)	125 mM Tris-Cl 0.1% SDS
Separating Gel Buffer (pH 8.8)	375 mM Tris-Cl 0.1% SDS
2 x SSC	0.3 M NaCl 7.5mM Sodium citrate
Hypotonic Potassium Chloride (0.075M)	0.56 g 100 ml dH_20
Hybridization Buffer	10% Formamide 10% Dextran sulphate sodium in 2x SSC

5.11 BAC Clones

BAC clones	Clone	Manufacturer
ERG centromeric	RP11-24A1	Invitrogen
ERG telomeric	RP11-372017	Invitrogen
Centromeric Clones	Chr. 5,8,10,16,X	Invitrogen
PTEN	CTD-2267G16	Invitrogen
cMYC	CTD-3056O22	Invitrogen
AR	RP11-479J1	Invitrogen
NKX3.1	RP11-213G6	Invitrogen
YWHAZ	CTD-2310E8	Invitrogen
PTK2	RP11-188K5	Invitrogen

6. Methods

6.1 Next generation sequencing (SOLiD4)

DNA Extraction

A 3 µm biopsy needle was used to punch three cores from FFPE, HOPE and fresh-frozen tissues for DNA extraction. Extraction was performed using the RecoverAll™ total nucleic acid isolation kit for FFPE and HOPE fixed tissue. Fresh frozen tissue was extracted using the Phenol:Chloroform:Isoamylalcohol (PCI) (25:24:1) method. This method, upon centrifugation at 16200 x g (Multifuge 1L-R, Thermo Scientific, Germany) creates an upper aqueous phase, containing nucleic acids, and a lower organic phase, containing proteins. DNA was obtained in the aqueous phase in the absence of guanidine thiocyanate. Precipitated DNA was resuspended in 50 µl of distilled water and stored at -20°C and used for further applications.

DNA Concentration and Integrity

DNA concentration of the samples was determined using the NanoDrop™. This instrument is capable of providing a 260/280 ratio, and for DNA a ratio of approximately 2 is considered pure. In parallel a 2100 Bioanalyzer was also used for sizing, quality control and quantification of the DNA. This instrument is based on a lab-on-chip technology and is capable of quantifying the samples and checking for its integrity by displaying specific peaks. The Bioanalyzer works on the principle of capillary electrophoresis, where in the presence of high electric fields, fast separation of the sample occurs. Upon separation, the computer generates an electrogram providing provides a precise quantitative analysis of the sample. Only a minute amount of sample (1 µl) is needed for the analysis.

DNA Sample Shearing

Upon qualification and quantification of the samples, they were sheared using the Covaris^{TM} S2 (Life Technologies GmbH, Darmstadt, Germany) to produce fragments of 150-180 bp. For sequencing purposes, a minimum of 1.5 µg of DNA is required. The Covaris instrument uses acoustic energy to shear the DNA samples into small fragments for further amplification and sequencing. Ultrasound is applied to the samples for shearing generating fragments.

The following program was used for the shearing-

Setting	Value
Number of Cycles	6
Bath Temperature	5°C
Bath Temperature Limit	8°C
Mode	Frequency sweeping
Water Quality Testing Function	Off
Duty Cycle	20%
Intensity	5
Cycles per Burst	200
Time	60 seconds

Sample Purification and Amplification

After shearing, the samples were subjected to end repair and purified using the SOLiD Library Column Purification Kit (Applied Biosystems, Darmstadt). The appropriate fragments selected using the Agencourt AMPure XP (Beckman Coulter, Krefeld) beads and amplified. The PCR amplification mix consisted of the following components–

Setting	Value
Adapter ligated library	15 µl
Nuclease free water	15.5 µl
SureSelect AB pre-capture primers	8 µl
5x Herculase II reaction buffer	10 µl
100mM dNTP mix	0.5 µl
Herculase II fusion DNA polymerase	1 µl

The PCR protocol-

Step	Temperature	Time
Step 1	98°C	2 min
Step 2	98°C	30 sec
Step 3	54°C	30 sec
Step 4	72°C	1 min
Step 5		Repeat step 2 through 4 for 6 cycles
Step 6	72°C	10 min
Step 7	4°C	Hold

Hybridization to the Library

The DNA fragments that were hybridized to the AMPure beads and eluted post amplification, were subjected to adaptor ligation to P1 and P2 adaptors. These adaptor ligated were then hybridized to the Agilent SureSelect capture library (Agilent, Waldbronn). The SureSelect Target Enrichment allows capture of all targeted exomes from the DNA sample of interest. This system uses 120-mer baits to capture regions of the exome from the fragmented DNA sample. Targeted regions are selected using streptavidin magnetic beads and quantified using the Agilent Bioanalyzer DNA 100 and high sensitivity DNA chip.

Templated Bead Preparation

After library construction, each library is clonally amplified on P1 DNA beads using oil emulsion PCR known as the EZ Bead system. The random fragments of the sample are placed on the beads in oil phase. This PCR occurs in the oil phase immobilizing the copies for sequencing using the SOLiD4.

Figure 9: SOLiD Sequencing pipeline overview.

6.2 Fixation protocols (Fresh frozen, FFPE and HOPE)

Fresh PCa tissues were cryopreserved by freezing in liquid nitrogen for up to 3 minutes and then storing in -80°C. FFPE fixation was performed by fixing in 10% neutral buffered formalin and embedded in paraffin. For HOPE fixation of tissues, tissue samples were dipped in HOPE® I solution at 0-4°C for 12-72 hours. This was following by the removal of the HOPE® I solution and the addition of the ice cold

HOPE® II and acetone solution for two hours. These steps were repeated twice. Low melting paraffin was then melted onto the tissue in a block cassette an stored at 4°C.

6.3 Fluorescent *In Situ* Hybridization

Tissue Microarray Construction

Tissue microarray slides were constructed from FFPE PCa samples. The tissue microarrays contained samples of a total of 137 localized PCa cases, 105 primary PCa with 71 corresponding lymph node metastasis, and 39 cases of CRPC. Each case was represented in triplicates and each core was 0.6 mm in diameter.

FISH Assays

A fluorescence *in-situ* hybridization (FISH) assay was used to detect the genes that were amplified/deleted or rearranged at the chromosomal level. FISH uses a technique to identify the presence or absence of specific DNA sequences on the chromosomes. Fluorescently labeled probes that are complementary to the regions of interest were used to detect chromosomal alterations (**Figure 10**). The fluorescent signals were then detected using a fluorescence microscope (Zeiss, Jena, Germany) to detect the emitted fluorescence of the gene of interest.

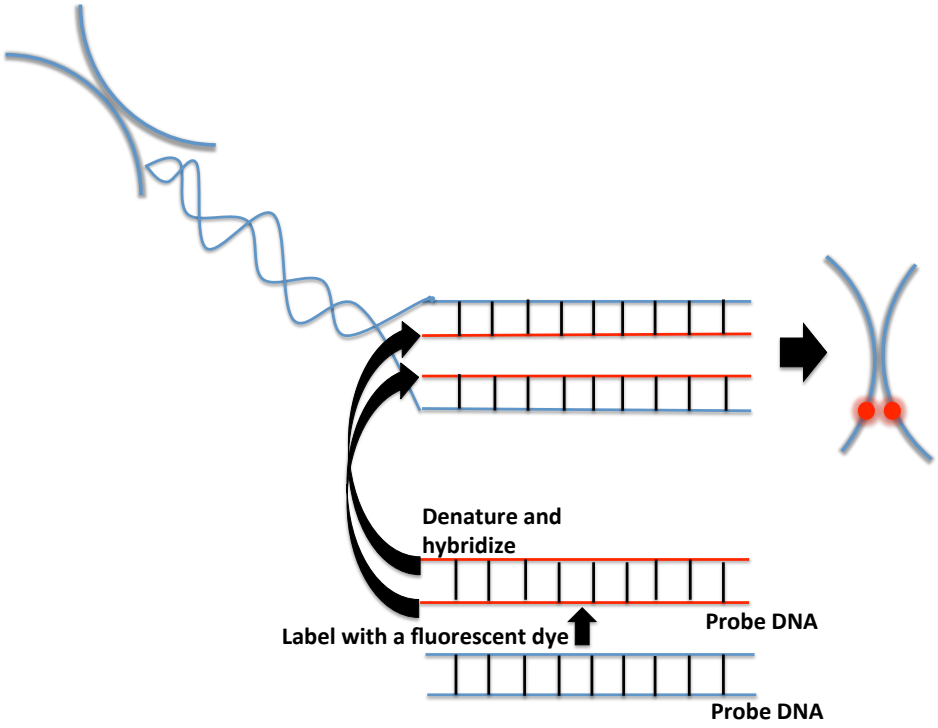

Figure 10: Fluorescent *In Situ* Hybridization (FISH).
Fluorescently labeled DNA probes, complimentary to the gene of interest, hybridize to single stranded DNA. The fluorescence is then detected using a fluorescence microscope. This method is used to detect regions of chromosomal amplification, deletion or rearrangement (87).

Deparaffinized sections were pre-treated with a 100 mM Tris and 50 mM EDTA solution at 92.8C° for 15 min. and digested with Digest-All III (dilution 1:2) at 37°C for 14 min.; FISH probes were denatured at 73°C for 5 min. and immediately placed on ice. Subsequently, the tissue sections and FISH probes were co-denatured at 94°C for 3 min. and hybridized overnight at 37°C. Post hybridization washing was done with 2x SSC at 75°C for 5 min, and the fluorescence detection was carried out using streptavidin-Alexa-594 conjugates (1:200 in hybridization buffer) and anti-digoxigenin-FITC (dilution 1:200 in hybridization buffer). Slides were then counterstained with 4',6-Diamidin-2' phenylindoldihydrochloride (DAPI) and mounted.

The samples were analyzed under a 63x oil immersion objective using a fluorescence microscope (Eclipse 80i, Nikon, Germany) equipped with appropriate DAPI, FITC,

TRITC and Alexa 594 Flour filters, a charge-coupled device camera and the FISH imaging and capturing software Metafer 4 (Metasystems, Altlussheim, Germany). Three experienced evaluators did the evaluation of the tests independently. At least 100 nuclei per case were evaluated.

Preparation of Metaphase Spreads for Adherent Cells

In order to assess the specificity of the FISH probes, the probes were tested on metaphase spreads. 5 ml of heparinized human blood was cultured in the incubator (BBD 6220 CO_2 Incubator, Thermo Scientific**,** Germany) at 37°C for three days and were then treated with colcemid (0.1 μg/ml) for 4 h. Colcemid disrupts the spindle apparatus and the cells are maintained in the metaphase. The cells were then lysed using a hypotonic potassium chloride solution (0.075 M). The cells were washed three times with ice cold methanol:acetic acid solution (2:1).

6.4 Cell Culture

Cell Lines

LNCaP, VCaP, PC-3 and DU-145, immortalized PCa cell lines, obtained from the American Type Culture Collection (ATCC) were cultured according to the ATCC, USA online instructions. LNCaP and DU-145 cells were cultured in RPMI-1640 media with L-glutamine and without Phenol Red (Gibco, UK), supplemented with 1% penicillin/streptomycin, 10% FBS and 25 mM HEPES. PC-3 cells were grown in F12K nutrient mixture containing L-glutamine (Gibco, UK), supplemented with 1% penicillin/streptomycin and 10% FBS. VCaP cells were grown in DMEM-F12 nutrient mixture (Gibco, UK) supplemented with 1% penicillin/streptomycin, 10% FBS and 1% L-glutamine.

Cell Culture Conditions

All cells were split and fed under a sterile laminar hood (Sterile Mars Safety Class 2, Scanlaf, Denmark) The cells were grown incubated in an incubator in humidified environment at 37°C with 5% CO_2 (BBD 6220 CO_2 Incubator, Thermo Scientific**,** Germany).

Cell Passaging

All cell lines were passaged upon achieving 80% confluency. The T-75 cell culture flasks were trypsinized using 1.5 ml (0.25% Trysin-EDTA) and incubated for 3 min at 37°C (BBD 6220 CO_2 Incubator, Thermo Scientific**,** Germany). The cells were then collected and centrifuged at 3200 x g for 5 min (Multifuge 1L-R, Thermo Scientific, Germany). The cell pellet was resuspended in PBS and the centrifugation was repeated. The supernatant was aspirated and new media was introduced, the cells were then seeded into new tissue culture flasks.

Cell Counting

The cells were trypsinized as described above. The pellet was then dissolved in a given volume of media. 10 µl of cells were added to 90 µl of Trypan blue solution (0.4% sterile filtered prepared in 0.81% sodium chloride and 0.06% potassium phosphate) (Sigma Aldrich, Germany). The cells were then counted using a Neubauer counting chamber. The average of four squares was taken to determine the concentration of cells.

Concentration= Number of cells x 10,000/ Number of squares x dilution

Freezing and Thawing Cells

Cells were trypsinized as described above. The cells were then centrifuged (Multifuge 1L-R, Thermo Scientific, Germany) at 3200 x g for 5 min and the supernatant discarded. Freezing medium consisting of 10% DMSO and 10% FBS was added to the cells in cryo vials. Each vial had an end volume of 1ml. The vials were placed in -80°C overnight and then in liquid nitrogen for long-term storage.

For thawing, cells were slowly allowed to thaw in a 37°C water bath until the sides are thawed but the center remains frozen. Then the cells were diluted by adding 1ml of media to the vial. Cells were centrifuged at 3200 x g for 5 min and washed with PBS. New medium was added and the cells were seeded.

6.5 Protein Analysis

Protein Isolation

Cells were trypsinized and washed with PBS. The pellet was then suspended in solution containing 100µl of RIPA-buffer, protease inhibitor, PMSF and phosphatase inhibitor (1:100). The cells were allowed to lyse on ice for 2 hours, after which they were centrifuged (1L-R, Thermo Scientific, Germany) at 13800 x g for 20 min at 4°C. The supernatant was transferred to a new tube 1.5 ml Eppendorf tube and stored at -20°C.

Protein Concentration

Protein concentration of the sample was determined using the BCA protein assay kit according to manufacturers' protocol. The principle of this kit is based on the formation of a Cu^{+2} protein complex under alkaline conditions. This is followed by

the reduction of Cu^{+2} to Cu^{+1}. The extent of reduction is based on the amount of protein present. BCA forms a purple color in the presence of Cu^{+1} in alkaline solutions. Its absorbance is read at 562 nm. A standard curve was also prepared using protein concentrations ranging from 0-1.2 mg/ml.

SDS-PAGE and Western Blot

Protein lysates, varying from 20 µg – 50 µg were used for Western blot analysis. Proteins were separated based on molecular weight using a 12% SDS-polyacrylamide gel for approximately 1.5 hours at 150 V (200 mA).

The proteins were transferred to a nitrocellulose/PVDF membrane using the semi-dry procedure (1 h, 16 V). After the transfer, a Ponceau S staining was performed to detect protein loading and washed with TBS-T, the membrane was then blocked with TBST 5% skim milk powder, diluted in TBS-T. Incubation with the respective primary antibody and its recommended dilution was done overnight at 4°C.

The following day, the membranes were incubated with the corresponding secondary antibody, conjugated to horseradish peroxidase for 1 h at room temperature. Visualization of the protein bands was carried out with the enhanced chemiluminescence (ECL plus) detection system (GE Healthcare, Munich). The ECL reagent contains luminol substrate and peroxide solution. The ECL is based on the emission of light during the horseradish peroxides and hydrogen peroxide catalyzed oxidation of luminol. Signal intensities for the Western blots were measured using the Scion Image software (Scion Corp., MD, USA). Protein yield was calculated using the AxioVision Rel 4.8 (Carl Zeiss Imaging Solutions GmbH, Göttingen, Germany). The protein yield was calculated using the following formula-

Total protein amount/(area ∗ section thickness ∗ number of sections) = Xµg/mm3

6.6 Functional Assays

RNA Extraction

The RNA extraction on the cells lines was performed using the RNeasy kit (Qiagen, Hilden) according to the manufacturers protocol. The cells were lysed in an appropriate volume of the lysis buffer RLT containing 1% β-mercaptoethanol. RNA was then eluted using distilled water. The RNA concentration was measured by calculating its optical density which was measured with a photometer at λ=260 nm. It is known that RNA with an OD_{260} of 1 corresponds to a concentration of 40 µg/ml. The Agilent Bioanalyzer was also used to assess the integrity of the RNA. The quality of the RNA was verified by the identification of the ribosomal RNA (18S and 28S).

Synthesis of cDNA

RNA is converted to cDNA to detect the amount of mRNA in the samples. After extraction of total RNA, reverse transcription was performed by using the Super Script Vilo cDNA synthesis Kit (Life Technologies, Germany) according to the manufacturers protocol. The amount of RNA was adjusted to 200 ng per reaction (total volume: 20 µl). The reaction occurred under the following profile: 25°C/10 min; 42°C/60 min; 85°C/5 min.

Semi quantitative Real-Time PCR

Each sample was tested in triplicates. The PCR was performed in the Roche LC480 Light Cycler (Roche, Basel) under the following conditions: 95°C for 10 min, 57°C for 30 sec, 72°C for 1 sec and 40°C for 30 sec. The threshold cycle (Ct) values were normalized using the housekeeping gene *β-actin.* Water was taken as a negative control.

The principle behind the Light Cycler assay is the measurement of fluorescence. A C_T value is determined, this value denotes the first detection of fluorescence after crossing the threshold that has been set by the user. The normalized C_T values, also called ΔC_T, are calculated the following way:

Formula 1:

$$\Delta C_{T=} C_{T\ (target\ gene)} - C_{T\ (housekeeping\ gene)}$$

The lower the C_T value the higher the mRNA expression, because less cycles are needed to reach the specific threshold in the intensity of the fluorescence. The difference of one C_T value between two samples corresponds to double of the amount of RNA (cDNA), when the efficiency of the primers is assumed to be 100%. Since the primer efficiency was assumed to be 100%, the following calculation was carried out to calculate the gene expression:

Formula 2:

$$Gene\ Expression = 2^{-\Delta CT}$$

Mutational Analysis

Mutational analysis was performed by Sanger sequencing. Briefly, DNA extraction was performed using the phenol-chloroform method, as mentioned above. Mutational analysis was performed by Sanger sequencing using specific primers or the genes of interest. DNA was denatured in to single strands allowing the primers to anneal to the template strand. Upon attaching of the primer, strand elongation takes place in the presence of fluorescently labeled nucleotides (ddNTPs) and normal nucleotides

(dNTPs). The sequencing is run in four different sequencing reactions. When the fluorescently labeled ddNTP is incorporated, strand elongation is terminated, and a light is emitted. This emitted fluorescence was then recorded on a chromatogram with fluorescent peaks.

Gene Knockdown

PC-3 cells were transfected using Lipofectamine RNAiMAX (Invitrogen, USA) according to the instructions of the manufacturer. The siRNAs were added at a concentration of 100 nmol/L. Western Blots were performed as described above to detect the efficiency of the knockdown using antibodies specific to the protein. Similarly, β-actin was used as a control for protein loading.

Inhibition Assay

PC-3 cells were treated with TAE-226, a pharmacological PTK2 (Protein Tyrosine Kinase 2) inhibitor (Novartis, Switzerland) at various concentrations. The inhibitor was dissolved in dimethyl sulfoxide (DMSO) and stored at 4-8°C. Western Blot was performed using specific antibodies to detect the targeted proteins, in parallel, β-actin was used as a control.

Proliferation Assay

Cell proliferation assays were performed on the PC-3 cells treated with the pharmacological TAE226 inhibitor or after *YWHAZ* knockdown experiments using a cell proliferation MTT Kit (Roche, Switzerland) according to the manufacturers protocol. A total of 5000 cells were seeded in a 96 well plate, followed by treatment with inhibitor/siRNA. Cell proliferation was determined after 24, 48 and 72 hrs of

incubation. This calorimetric assay is based on the reduction of 3-(4,5-dimethythiazol-2-yl)-2,5-diphenyl tetrazolium bromide (MTT) by mitochondrial succinate dehydrogenase. Viable cells produce formazan as a product. The formazan is then solubilized with an organic solvent and released. The absorbance was read at 595 nm.

Cell Migration Assay

Boyden Chamber migration assays were performed using the 24-well Matrigel invasion chambers with 8 μm polycarbonate filters that are coated with Matrigel (BD Bioscience, USA). $1x10^5$ cells were placed in the Matrigel pre-coated upper chamber insert (BD Biosciences, USA) with media containing 2% FBS. The lower chamber was filled with media containing 10% FBS. The principle is the movement of cells moving from the upper chamber to the lower chamber as cells are attracted to media containing 10% FBS. The cells were incubated for 24 hrs, after which the membrane was removed from the insert and stained with hematoxylin (Fulda, Germany). The invading and migrating cells were counted in three different fields and the two-sided unpaired T-test was used to determine statistical significance.

Apoptosis Assays

Cells were grown for 24, 48 and 72 hours with the pharmacological TAE226 inhibitor (Novartis, Switzerland) and stained with Hoechst 33342 and YO-PRO-1, as described by the manufacturers protocol. YO-PRO-1 enters the apoptotic cells and stains them. Hoechst 33342 brightly stains the condensed chromatic of apoptotic cells and dimly stains the normal living cells. Cell treated with Doxorubicin (Sigma Aldrich, Germany) at a 10 μM concentration was used as a positive control, and untreated cells were used as a negative control. Data acquisition was performed on an LSR II flow

cytometer (BD Biosciences, Germany). FlowJo software was used to perform further data analysis (TreeStar, US).

Cell Cycle Arrest

Cells treated with the pharmacological TAE226 inhibitor were fixed in 70% ethanol and stained with PI/RNase A solution (50 µg/ml of RNase A (Sigma, USA), 50 mg/ml of propidium iodide (Sigma, Germany)) dissolved in sample buffer containing 0.5% glucose in 1x PBS. The FACS analysis was performed using a Becton Dickinson FACSCalibur to determine DNA content. The data analysis software FlowJo (TreeStar, US) was used for further analysis.

7. Results

7.1 Objective I: Determining the DNA, RNA and protein integrity of fresh-frozen, FFPE and HOPE fixed tissue to identify the optimal tissue for sequencing and functional studies.

PCa tissue is commonly available in three forms: fresh frozen, FFPE and HOPE fixed respectively. For sequencing and molecular based studies, it is necessary to determine the DNA, RNA and protein integrity of each fixation protocol for downstream applications.

This study was performed on prostatectomy samples obtained from 10 patients who had undergone a radical prostatectomy at the University Hospital of Tuebingen. An in-depth histological examination was performed on all specimens prior to DNA and RNA extraction. This histological examination involved a hematoxylin and eosin staining (HE staining) performed on the frozen tissue to identify regions of tumor for DNA/RNA/protein analysis. Upon identification and isolation of the cancer region, the frozen sample was cut into three equal sizes and subsequently fixed using the conventional FFPE protocol, HOPE-fixation and cryo conservation methods.

A. Histological and Morphological Analysis

Upon the FFPE, HOPE and cryopreservation of each sample, they were all subjected to a histological and morphological analysis. The histological and morphological analysis for each sample was performed by HE staining, immunohistochemistry (IHC) analysis and FISH analysis.

The samples were firstly, subjected to an HE staining. HE staining detects the nuclei of the cells and stains them blue due to the hemalum dye and stains the eosinophilic structure (such as proteins) in shades of red and orange using the eosin dye. This

method was used to distinctly identify the cell membranes and nuclei in each fixation protocol. With reference to histomorphology, HOPE specimens often displayed a FFPE like morphology (**Figure 11 A**) where the nucleus and the cells were distinctly stained with no interference and no or little background. The tumor regions were clearly identified in both FFPE and HOPE fixed specimens. Fresh frozen specimen, on the other hand, exhibited typical freeze related artefacts, which included a distorted morphology and interfering background.

The samples were then subjected to IHC staining using the p63 antibody. The p63 is a homolog of the tumor suppressor p53. The antibody is known to stain the basal cells of the prostate gland. A variation in the manufacturer's protocol was required for the IHC staining of HOPE samples, which required no epitope retrieval and a brief proteinase treatment for better signal quality. Both the FFPE and fresh frozen samples possessed benign and infiltrating PCa glands while the HOPE specimen depicted tumor glands and an intraductal spread of PCa (**Figure 11 B**). The p63 antibody stained the basal cells of the FFPE and frozen specimen, and in the HOPE specimen, the antibody stained both the basal cells with intraductal spread. The antibody binding specificity and signal strength were comparable in all three fixation protocols. Unfortunately, the histomorphologic quality was inferior in the fresh frozen samples with interfering background due to freezing (**Figure 11 B**).

Thirdly, a FISH analysis was performed using probes specific for the *TMPRSS2-ERG* rearrangement. While performing a FISH analysis, the nucleus of the cell is distinctly visible due to DAPI and similarly, depending on the extent of degradation of the DNA, the FISH probes attach to the targeted regions of interest. The fresh frozen specimen exhibited specific signals but a typical freeze related clumping of cells was observed. The nuclei of the cells did not possess a clear morphology. On the other

hand, the FISH, using probes specific for the *TMPRSS2:ERG* gene fusion, on both FFPE and HOPE fixed PCa tissue showed distinctly specific signals and clear nuclear morphology (**Figure 11 C**).

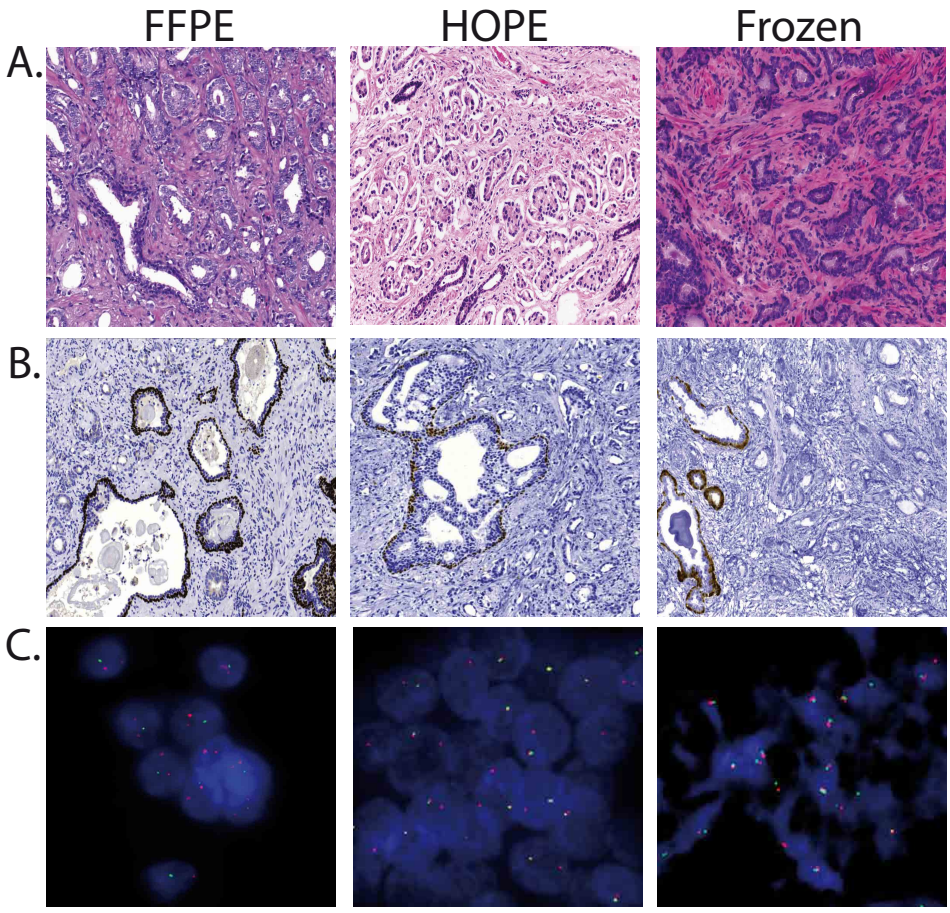

Figure 11: Morphological quality comparison between FFPE, HOPE, and fresh-frozen specimens.
(A) Representative HE stained sections of FFPE, HOPE, and fresh frozen material.
(B) Representative p63 antibody IHC of FFPE, HOPE, and fresh frozen material.
(C) Representative Fluorescence in-situ hybridization of ERG rearrangement on FFPE, fresh frozen and HOPE tissue sections (Braun and Menon *et al*., 2011). (88)

B. DNA Integrity Analysis

DNA extraction was performed from the FFPE, HOPE-fixed and fresh frozen specimen from six patient samples. To assess the DNA integrity, a PCR analysis was performed using a set of five primers yielding five different amplicons. Genes of varying amplicon sizes were chosen to determine the extent of DNA fragmentation

induced by the fixation protocols. The genes included human thromboxane synthase gene- 100bp (*TBXAS1*, exon 9; Chr7q34-35), human recombination activating gene- 200bp (*RAG1*, exon 2; Chr11p13), human promyelocytic leukemia zinc-finger gene- 300bp (*PLZF*, exon 1; Chr11q23.1), and human *AF4* gene- 400 and 600bp (exon 3; and exon 11; Chr5q31). 100 ng/µl of DNA was introduced into each reaction for the analysis. All six samples showed distinct bands ranging from 100-400bp. The 600bp band was absent or hardly visible in the FFPE samples (**Figure 12**).

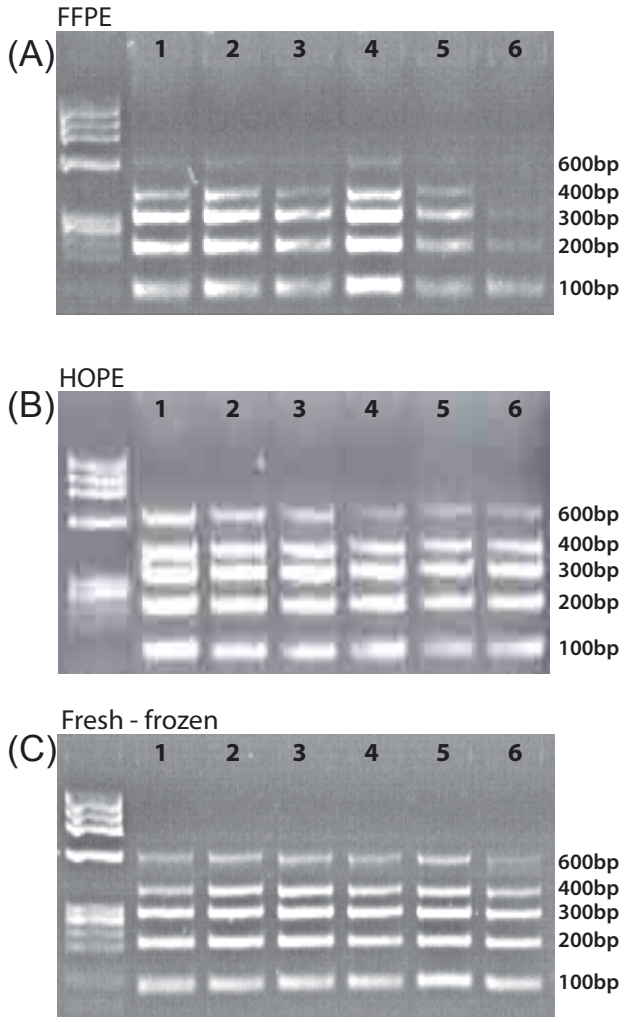

Figure 12: DNA integrity of FFPE, HOPE, and fresh-frozen tissues.
(A-C) Agarose gels showing PCR products ranging from 100-600bp from six FFPE, HOPE and fresh frozen patient samples (Braun and Menon *et al*., 2011). (88)

C. RNA Integrity Analysis

RNA extraction was performed on the FFPE, HOPE fixed, and fresh frozen samples from six patients, followed by a real time RT-PCR. The RNA was then reverse transcribed to produce cDNA, which was then used to determine the Ct value for comparison. The real time RT-PCR was performed using three housekeeping genes, *TBP* (73bp), *GAPDH* (201bp) and *ß-actin* (300bp) namely. The amplicons of all three house-keeping genes were of varying sizes in order to determine the degree of RNA fragmentation induced by the fixation protocols. The results of the RNA integrity analysis showed that the fresh frozen specimen had the lowest average Ct value (**Figure 13**). This is primarily due to the lack of fixative interference in these tissues.

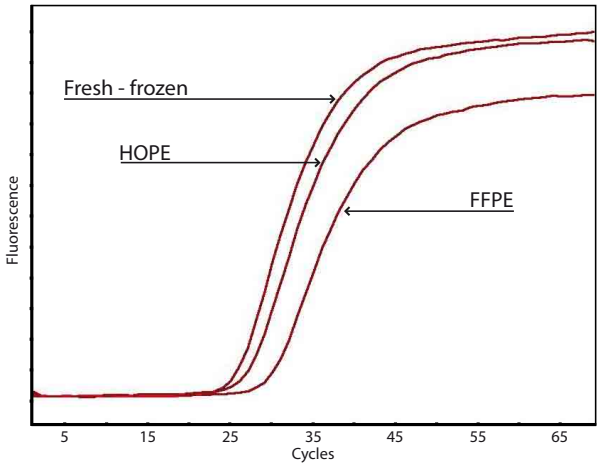

Figure 13: Representative real-time RT-PCR targeting TATA-binding-protein (TBP, 73bp) in FFPE, HOPE, and fresh-frozen tissues.
The threshold value of HOPE fixed specimens was comparable to that of the fresh-frozen specimen (Braun and Menon *et al*., 2011). (88)

The average C_t threshold HOPE values for *TBP, GAPDH* and *ß-actin* were 29.2, 27.8, and 27.6 respectively. The average C_t threshold FFPE values for *TBP, GAPDH* and *ß-actin* were 33.2, 34.5, and 35.5, respectively. The average C_t threshold of fresh-frozen specimens values for *TBP, GAPDH* and *ß-actin* were 27.1, 26.4, 25.8 respectively (**Table 1**). Each experiment was performed in triplicates and repeated three times. The differences in the average C_t values were statistically significant.

Ct values for TBP mRNA expression

FFPE	HOPE	Native
29.9	27.15	25.5
31.89	29.18	27.2
34.8	29.8	28.1
33.6	29.7	27.5
33.1	29.9	26.3
35.86	29.6	28.2

Ct values for GAPDH mRNA expression

FFPE	HOPE	Native
29.4	25.5	25.1
35.8	29.7	27.4
37.7	27.9	25.6
31.7	28	27.3
36.2	27.9	25.7
35.9	27.8	27.1

Ct values for β-actin mRNA expression

FFPE	HOPE	Native
36.9	28.2	26.7
38.7	25.6	24.1
31.8	31.1	25.8
34.2	26	25.5
33.2	29.3	28.1
38.12	25.7	24.8

Table 1: Mean cycle threshold values for the housekeeping genes TBP, GAPDH and ß-actin from the corresponding FFPE, HOPE, and fresh-frozen samples from three independent experiments (Braun and Menon *et al*., 2011). (88)

D. Protein Analysis

To assess for protein quantity and quality, proteins were extracted from FFPE, HOPE fixed and fresh frozen specimen and Western blots were then performed. For the FFPE and HOPE fixed samples, 3-8x10 µm sections were used and for fresh frozen samples 10-15x20 µm sections were transferred to a reaction tube for protein

extraction. 18 µg of protein was loaded into the gel for each sample. PSA and GOLPH2 were estimated, as both proteins are abundantly found in PCa (89). Western blots were performed using antibodies against PSA (**Figure 14 A**) and GOLPH2 (**Figure 14 B**). Bands were observed at approximately 45-50 kDa and 34 kDa. The bands obtained for the HOPE fixed tissues were comparable to the intensity of the bands obtained from the fresh frozen tissue samples (**Figure 14**).

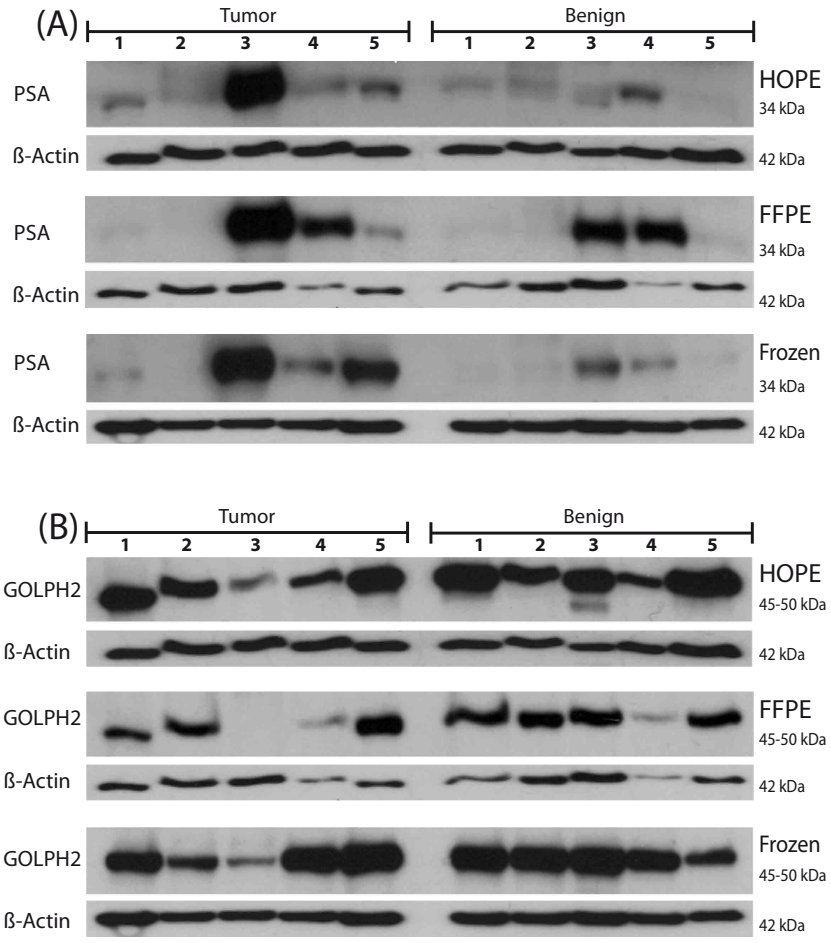

Figure 14: Western Blot analysis of HOPE, FFPE, and fresh-frozen samples
(A) PSA (34 kDa) antibody and ß-actin (42 kDa) antibody as a control
(B) GOLPH2 (45-50 kDa) antibody, and ß-actin (42 kDa) antibody as a control (Braun and Menon *et al*., 2011). (88)

Furthermore, the signal intensities of the Western blots were quantified using the Scion Image software (Scion Corp., MD, USA). Upon normalization of the PSA and GOLPH2 antibodies' signal intensities with that of β-actin, the analysis revealed that

all three fixation protocols had comparable signal intensities (**Figure 15 A and B**). Also, the protein yield from each fixation protocol was determined using the AxioVision Rel 4.8 (Carl Zeiss Imaging Solutions GmbH, Göttingen, Germany) by measuring the area of the section used for protein extraction. The protein yields for FFPE, HOPE and fresh frozen samples were also comparable and in some cases the HOPE and FFPE fixed specimen yielded higher proteins than the fresh frozen samples (**Figure 15 C**).

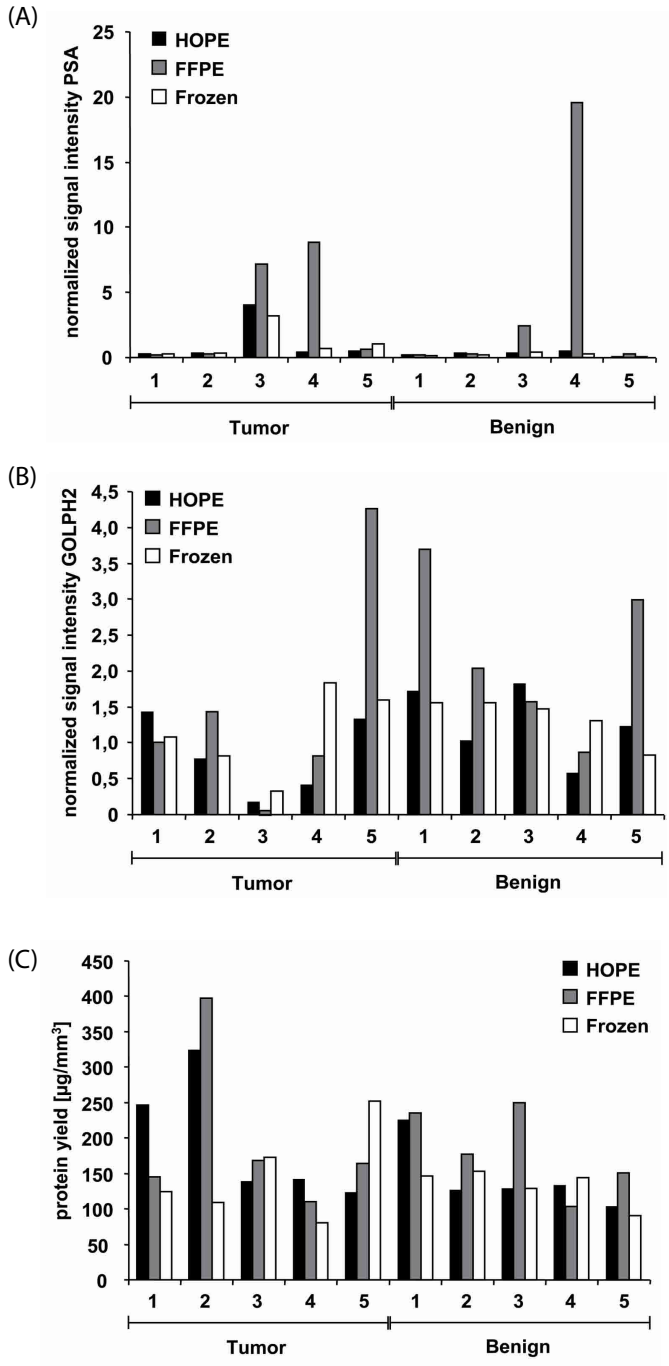

Figure 15: Quantification of the Western blot.
Western Blot for the (A) PSA antibody and (B) GOLPH2 antibody. (C) Measurement of protein yield for HOPE, FFPE and fresh frozen specimen (Braun and Menon *et al.,* 2011). (88)

The results of Objective I have been published in *BMC Cancer* titled, 'The HOPE fixation technique- a promising alternative to common prostate cancer biobanking approaches.' (Braun and Menon *et al.,* 2011) (88).

7.2 Objective II: Determining the sequencing efficiency of FFPE tissue, in comparison to fresh-frozen tissue, both obtained from the same patient, using the SOLiD4 sequencing platform.

Fresh frozen tissue of CRPC is very rare. This is due to the fact that patients suffering from the advanced form of PCa initially develop bone metastasis. If there are other treatment options available, patients are reluctant to undergo tissue biopsies (90). Furthermore, the limited available CRPC material is present in a FFPE fixed form and not as HOPE fixed material. The previous study analysed the efficiency of FFPE tissue to study DNA, RNA and protein. Based on the previous results, the second aim of the study was to examine the usability of FFPE tissue for sequencing. This was performed by obtaining a fresh frozen prostatectomy sample from a patient and dividing fresh it into two, and subjecting one half to FFPE fixation and fresh freezing the second half. Both halves were exome sequenced and data analysis was performed to determine the overlap between both. For normalization purposes, normal prostatic tissue from the same patient was used.

A. Bioinformatic Analysis

All three samples (FFPE non-tumor, FFPE tumor, and fresh frozen PCa tissues) were sequenced and the sequencing output from the SOLiD4 sequences results in many fragments that are 50 bp in length. The principle behind using 50 bp length fragments for sequencing is beneficial when using FFPE tissue as the tissue is degraded, damaged or in small quantities due to the formalin fixation protocol. These 50 bp fragments are randomly arranged and need to be aligned to the human reference genome. Previous groups have sequenced the human genome, which is approximately 3 Gb (giga bases) in size. This reference genome is referred to as hg19. The 50 bp sequenced data was aligned with the human reference genome, hg19, in order to

identify single nucleotide variations (SNVs), insertions, deletions and amplifications within the patient sample. This alignment was performed using a software tool called BLAST-like fast accurate search tool (BFAST), which aligns the sequencing output character by character to the reference genome.

A SNV can be denoted as a single nucleotide variation that occurs in the DNA of a genome in comparison to the genome of the biological species. Similarly, an insertion/deletion (Indel) refers to the incorporation/removal of a few base pairs in the DNA with reference to the DNA of the biological species (**Figure 16**). A mutation was denoted as a SNV/Indel where it was read more than 25 times in the sequence during the alignment step. The aligned sequence was given a scored called a PHRED score. The PHRED score is used to determine the quality and accuracy of the called base . The score is determined by evaluating the peak resolution and peak shape of the corresponding base. A score is then assigned by comparing the preexisting PHRED score tables for the correct base call (91, 92).

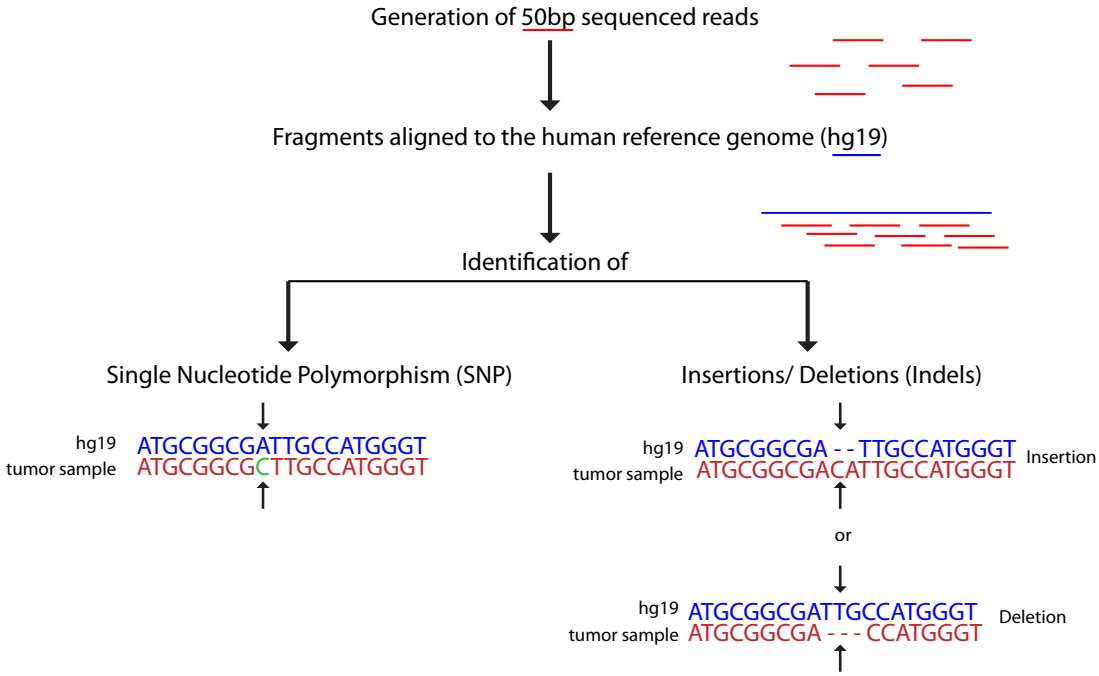

Figure 16: Data analysis pipeline identifying SNVs and Indels from a sequenced CRPC tumor sample.

Similarly a copy number variation (CNV) analysis was performed. A CNV refers to an abnormal number of copies of a DNA sequence in a cell. As all sequenced samples were human cancer tissues, a diploid copy number was expected. When the CNV analysis yielded more than two copies of a DNA sequence, it was referred to as amplification. Similarly, a CNV analysis yielding less than two copies of a DNA sequences was referred to as a deletion. Normalization was performed using the non-tumor DNA from the same patient.

Exome Sequencing of FFPE and Fresh Frozen PCa Tissue

All three sequenced samples (FFPE non-tumor, FFPE tumor, and fresh frozen PCa tissues) yielded approximately 99 to 113 million reads. Uniquely mapped reads, or reads that uniquely aligned to the reference human genome (hg19), were 43.9 million for FFPE normal PCa, 42.5 million for FFPE tumor tissue and 51.0 million reads for the fresh frozen tumor tissue. From the unique reads, the percentage of reads that aligned were 81.9% for FFPE normal, 78.47% for FFPE tumor and 84.44% for fresh frozen tumor tissue. With reference to all the on-target reads, the percentage of targeted exons for each sample was 98.19% for FFPE normal prostatic, 98.32% for FFPE tumor and 98.52% for fresh frozen tumor (**Table 2**).

Parameters	FFPE Normal prostatic tissue	FFPE Tumor	Fresh-frozen Tumor
Reads	**100,675,212**	**99,910,447**	**113,195,686**
Rejected reads	9,011,246	10,280,465	7,809,343
Valid reads	91,663,966	89,629,982	105,386,343
Non-uniquely mapped reads	47,691,531	47,113,995	54,345,991
Uniquely placed reads	**43,972,435**	**42,515,987**	**51,040,352**
On target reads (within +-150bp)	36,016,954	33,363,890	42,077,913
On target reads in %	**81.91%**	**78.47%**	**82.44%**
All Intervals/Exons	165,481	165,481	165,481
Targeted exons	162,490	162,699	163,027
Targeted exons in %	**98.19%**	**98.32%**	**98.52%**
Non- targeted exons	2,991	2,782	2454
Total number of SNVs	**11,300**	**8843**	**12,183**

Table 2: Comparison of exome sequence read data between FFPE normal prostatic, FFPE tumor and fresh-frozen tumor tissues (Menon *et al*., 2012). (93)

B. Single Nucleotide Variation (SNV) Analysis

SNVs were analyzed to draw a parallel between the sequenced FFPE tumor and fresh frozen PCa tissue. Of interest were the SNVs that were specific to the tumor tissues. A total of 11300 SNVs were identified for FFPE normal prostatic tissue, 8843 SNVs for FFPE tumor and 12184 SNVs for fresh frozen tumor tissue (**Figure 17**). The overlap of SNVs between the FFPE tumor and the fresh frozen tumor were 5873. 66.4% of the SNVs identified in the FFPE tumor sample were common to the fresh frozen tumor sample (**Figure 17 A**). The tumor specific SNVs were identified after normalization with normal prostatic tissue. There were a total of 2884 SNVs identified from the DNA obtained from FFPE tissue and 4837 SNVs identified for DNA obtained from fresh frozen tissue. There was a 41.9% overlap between the FFPE tumor and FFPE normal prostatic tissue (**Figure 17 B**). Similarly, there was a 45.4% overlap between the fresh frozen tumor and FFPE normal prostatic tissue (**Figure 17 C**). A 66% between the DNA obtained from the FFPE tumor and the fresh frozen tumor suggests that FFPE tissue, could be a good alternative to fresh frozen tissue for sequencing.

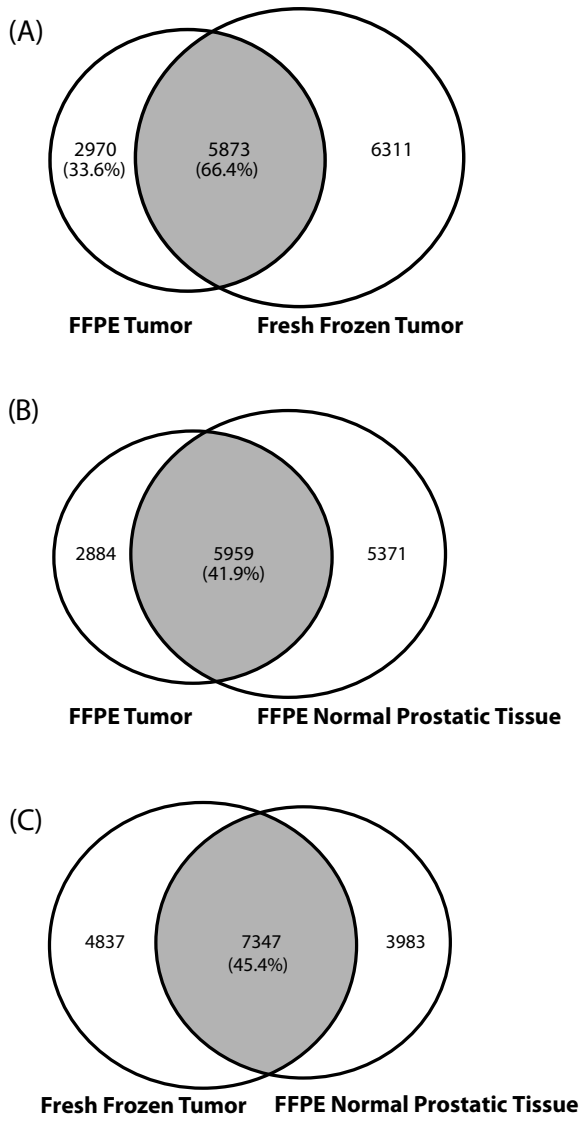

Figure 17: Venn diagrams representing SNV profiles
(A) FFPE tumor vs. fresh frozen tumor tissue, (B) Fresh-frozen tumor vs. FFPE Normal prostatic tissue and (C) FFPE tumor vs. FFPE Normal prostatic tissue samples (Menon *et al*., 2012). (93)

C. Copy Number Variation (CNV)

A CNV analysis was performed between the FFPE tumor sample and the fresh frozen tumor sample. All samples were obtained from the same patient. In order to study the CNV, normalization was performed using normal prostatic tissue from the same patient. The CNV analysis was then plotted. Similarity was observed between the FFPE tumor and fresh frozen tumor tissue. For each chromosome, the ratio between normal and tumor tissue was calculated. Furthermore, the log2 was applied to the

ratios. The genomic position is represented on the x-axis. The log2 ratios of the fragments are represented on the y-axis and the average is depicted by the red line. Chromosomes 17, 21 and 22 showed the best overlap for CNV analysis between both tissue types (**Figure 18**). These results show that there was an overlap between the copy number variation between the DNA obtained from the FFPE tumor and fresh frozen tumor tissues for a few chromosomes. The limitation in this study was the low sequencing coverage of the FFPE fixed tissues, therefore, a higher sequencing coverage would have generated an even more distinct overlap.

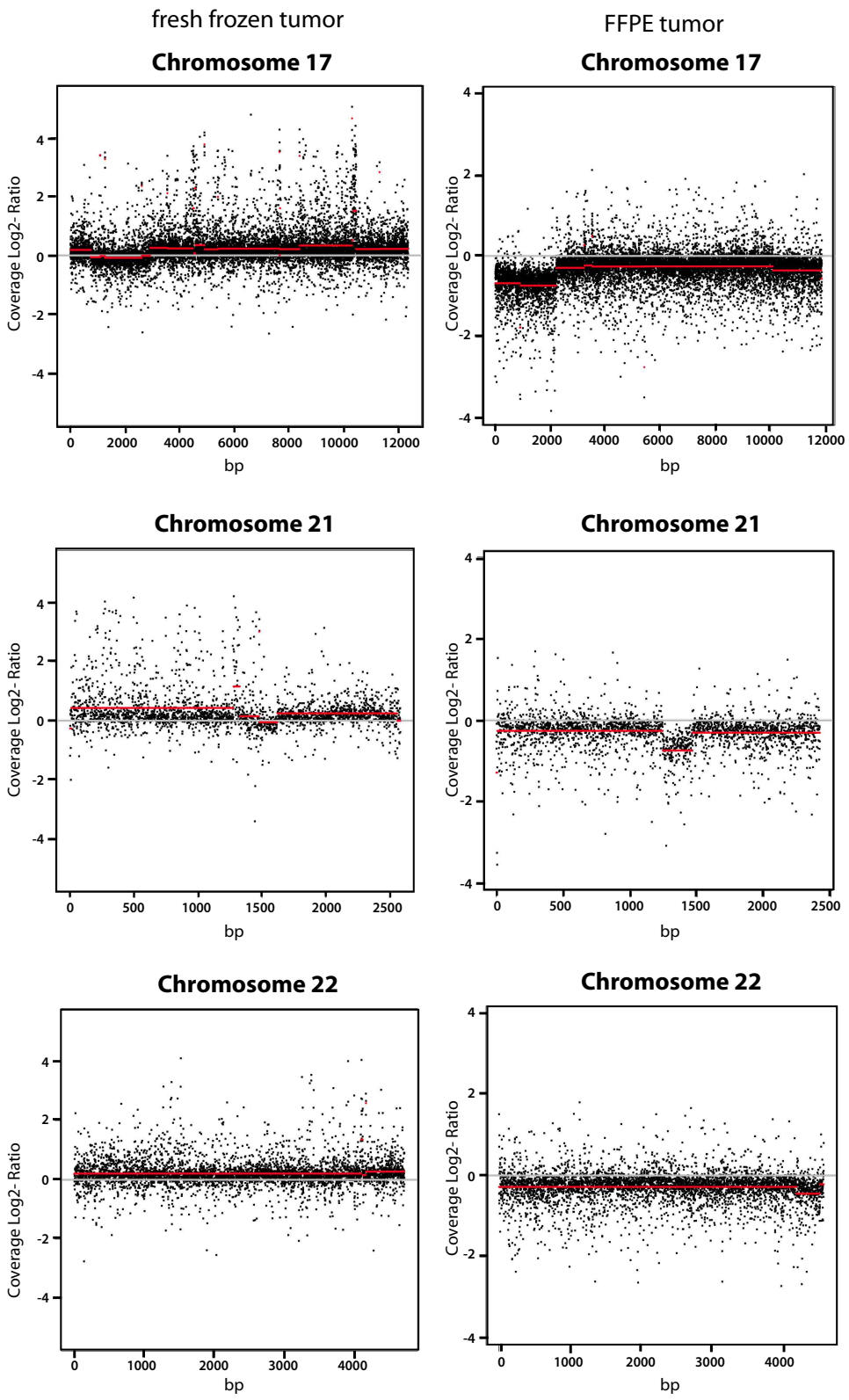

Figure 18: Representative copy number variation analysis (Chr. 17, 21 and 22) of exome sequenced fresh frozen tumor and FFPE tumor after normalization with FFPE normal prostatic tissue (Menon *et al.*, 2011). (93)

The bioinformatic analysis was carried out by Mario Deng, the bioinformatician in the lab.

The results of Objective II have been published in *International Journal of Molecular Sciences* titled, 'Exome enrichment and SOLiD sequencing of formalin fixed paraffin embedded (FFPE) prostate cancer tissue' (Menon *et al*., 2012) (93).

7.3 Objective III: Identification of novel therapeutic targets for castration resistant prostate cancer by whole exome sequencing, and functional validation of the identified targets.

Having confirmed the usability of FFPE tissue for whole exome sequencing (Objective II), the central aim of the project was to perform exome sequencing on CRPC patient samples to detect mutations/deletions/insertions which encode for genes that could be potential therapeutic targets. The exome sequencing cohort consisted of five CRPC patient samples. The organs of metastasis included lung, rectum, stomach and kidney. For each patient sample, there was corresponding non-tumor tissue for normalization purposes to identify somatic copy number alterations and SNVs specific to the tumor. The organ sites for the non-tumor tissue included lung, kidney and liver. All samples were obtained from the University Hospital of Tuebingen, Germany with the approval of the Institutional Review Board (395/2008BO1). The five sequenced patients had undergone hormonal therapy for CRPC and were negative for the *TMPRSS2-ERG* gene fusion.

A. Exome Sequencing Using the SOLiD4 platform

The average coverage for the five CRPC and their corresponding non-tumor samples that were exome sequenced was >50x and the average read length was 50bp. The five sequenced samples were aligned to the reference genome (hg19) and bioinformatically analyzed using the bioinformatic pipeline mentioned in Objective II. All the tumor CRPC samples were normalized using corresponding non tumor tissue from the same patients to identify amplifications and deletions. The aligned files were

viewed using the Integrative Genome Viewer 2.2 (Massachusetts, USA). Regions of amplification in three or more samples included 1q23.2-q32.2, 8q12.1-q24.21, 16p13.3-11.2, 17q24.2-25.3 and Xp22.2-p22.11. Regions of deletion included chromosome 8p22-p22.2, 11q22.3-23.3, 16q12.2-24.2, 17p13.2-12, 18q12.2-23, 19q13.11-13.3 and 22q12.2-13.32 (**Figure 19**). Furthermore, to validate the sequenced data, well-known amplifications (*cMYC, AR*) and deletions (*PTEN, NKX3.1*) in PCa were also identified in the in the DNA of the CRPC patients (**Figure 19**).

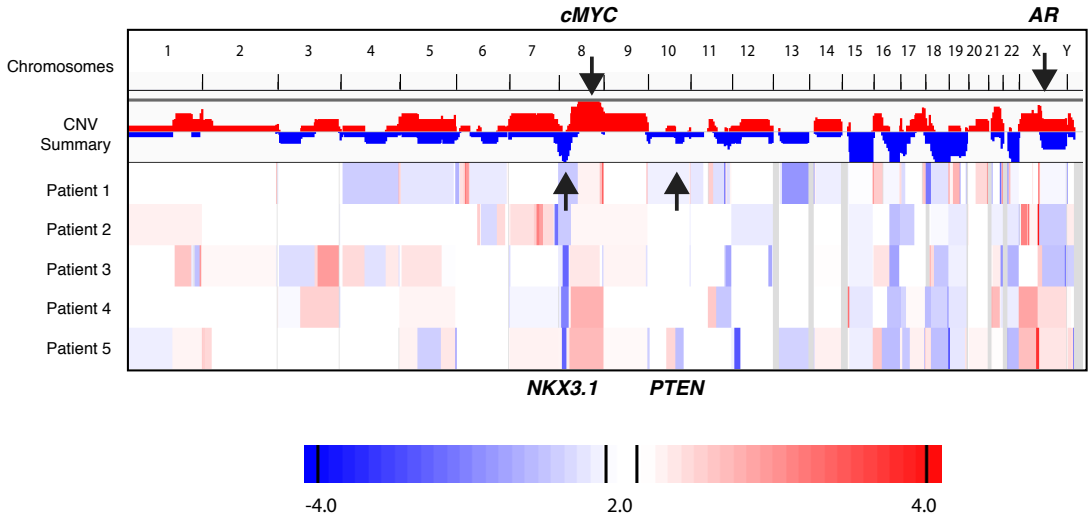

Figure 19: Somatic copy number alternations and validation of the five sequenced CRPC samples.
Regions of amplification were depicted in red, regions of deletion were depicted in blue and copy number neutral regions were depicted in white. Exemplary genes (*cMYC, NKX3.1, PTEN, AR*) previously known to be amplified/deleted in CRPC were also identified in our discovery cohort. (**Menon *et al*., *Manuscript in preparation***).

B. Cross Validation of Somatic Copy Number Gains and Losses by Data Mining

We identified certain regions of amplification and deletions in our CRPC cohort. The amplifications that were observed included the *AR* co-activator gene *NCOA2 (SRC-2)* (nuclear receptor coactivator 2), a cluster of amplifications on chromosome 8 comprising of *TERF1* (telomeric repeat binding factor), *RPL7* (ribosomal protein L7),

STAU2 (staufen, RNA binding protein, homolog2), *UBE2W* (ubiquitin-conjugating enzyme E2W), *COX6C* (cytochrome c oxidase subunit VIc), *and GRHL2* (grainyhead-like 2). Furthermore, there were deletions of the tumor suppressor genes *LATS2* (large tumor suppressor, homolog2), *PLAG1* (pleiomorphic adenoma gene 1), *RB1* (retinoblastoma 1), *HSD17B2* (hydroxysteroid (17-beta) dehydrogenase 2), and *HSDL1* (hydroxysteroid dehydrogenase like 1), *BIN3* (bridging integrator 3), *RHOBTB2* (Rho-related BTB domain containing 2), *CHMP7* (charged multivesicular body protein 7), *LOXL2* (lysyl oxidase-like 2), and *FUT10* (fucosyltransferase 10). Our data regarding the amplifications and deletions from the exome sequenced CRPC cases is consistent with the recent finding reported in sequencing performed on fresh frozen CRPC samples (82). Moreover, we found an amplification of *PIK3CA* (phosphatidylinositol-4,5-bisphosphate 3-kinase, catalytic subunit alpha), *HOXA3* (homeobox A3), *AR*, and deletions of *CHD1* (chromodomain helicase DNA binding protein 1), *NT5E* (5'-nucleotidase), *PTEN, RB1* and *TP53,* also described in another recent sequencing study on fresh frozen CRPC samples (85).

C. Validation of Somatic Copy Number Gains and Losses by FISH and *SPOP* Mutational Analysis

The commonly found alterations found in all PCa patients include the *NKX3.1* deletion, *AR* amplification and *cMYC* amplification. On the other hand, *PTEN* deletion was observed only in one of the patient samples. Furthermore, FISH assays were performed on the above mentioned commonly found alterations in PCa (*ERG, PTEN, cMYC, AR, NKX3.1*) on a PCa progression cohort to identify the frequency of a PCa stage specific deletion/amplification. This cohort consisted of clinically localized PCa, LN metastasized PCa and CRPC. BAC clones were used for the FISH

assays and were identified using the Ensembl genome browser online tool. A split signal (**Figure 4**) was used to identify the *TMPRSS2-ERG* gene fusion by FISH. Similarly, for the potentially amplified or deleted genes, a reference probe spanning the centromere of the corresponding probe was used. The target probes were labeled with biotin to produce a red signal.

NKX3.1 was deleted in 32% of the localized PCa, 88% in LN metastasized PCa and 91% in CRPC. Similarly, *PTEN* deletion was observed in 1% of the localized PCa, 26% of the LN metastasis samples and in 23% of the CRPC. The frequency of patients harboring the deletion of these tumor suppressor genes was lowest in localized PCa and highest in CRPC. Well know oncogenes, such as *cMYC,* were amplified in 1% of localized PCa, 8% of LN metastasized samples and 16% of the CRPC. Similarly, *AR*, known to be amplified in advanced PCa, also exhibited the same trend (83). *AR* amplifications were only seen in the CRPC samples at a frequency of 40%. On the other hand, the frequency of the *ERG* rearrangement was highest in localized PCa at a frequency of 49%, 46% in lymph node metastasized cases and lowest in CRPC with a frequency of 28% (**Figure 20**) (94). These results indicate that the data obtained from the sequencing performed on the CRPC patients showed representative genes expected to be amplified or deleted based on the stage of disease. For example, the AR amplification frequency was highest in CRPC of the progression cohort, similarly all five of the sequenced patients also harbored the amplification. Similarly, the tumor suppressor gene *NKX3.1*, was deleted at a high frequency in CRPC of the progression cohort, was also deleted in all the five CRPC sequenced patients possibly due to the advanced stage of disease.

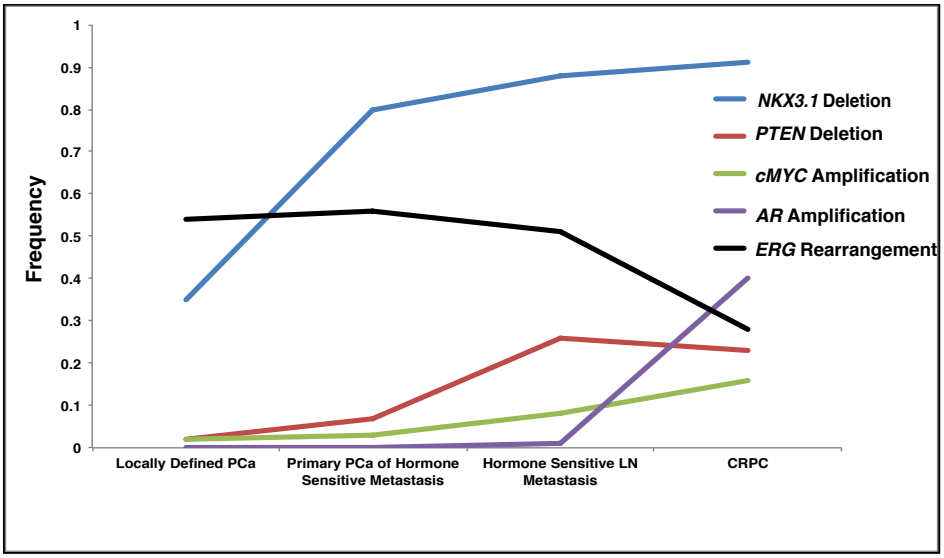

Figure 20: FISH validation of genes known to be amplified/deleted/rearranged in PCa.
The frequency of genetic alterations was determined with regards to the tumor stage from primary PCa to CRPC (**Menon *et al., Manuscript in preparation***).

Furthermore, all five sequenced CRPC patients were negative for the *TMPRSS2-ERG* gene fusion. A recent study reported that patients negative for the gene fusion were positive for mutations in the *SPOP* gene, thereby creating a new molecular subtype for PCa (86). The five CRPC patient DNA was also subjected to resequencing for *SPOP* mutations, but no mutations were identified. *SPOP* mutations are seen in up to 6-15% of all prostate tumors (86). Our sequencing cohort was very small and therefore may be the reason due to which the mutation was not detected.

D. Identification of Novel Therapeutic Drug Targets for CRPC

After having validated the CRPC exome sequencing data by identifying amplified/deleted/mutated genes through FISH and resequencing, the next aim was to identify novel alterations in genes that could serve as potential therapeutic targets in CRPC.

The sequencing coverage of the five CRPC patients was an average of 50x. This coverage was too low to distinguish between actual SNVs and false positives induced due to FFPE fixation. However, the mutational analysis did identify a few mutations commonly found in PCa, which included amongst others: rs198977 (*KLK2*), rs2233324 (*NDRG1*), rs422471 (*TMPRSS2*), rs1337076 (*AR*). The rs numbers refer to the reference number of the SNV that has been previously recorded in the mutation database and has been detected in PCa.

Due to the low coverage, it was difficult to identify SNVs that could serve as therapeutic targets. Therefore, the data analysis was focused on the copy number variation analysis. Focusing on the copy number variation analysis, amplified genes were identified that could serve as potential therapeutic target for CRPC.

Regions of amplification and deletion were identified throughout the exome. A total of 928 genes were amplified and a total of 647 genes were deleted (Appendix I and II).

Amongst all the regions of amplification, the 8q region has been previously described in prostate cancer and it also harbors the amplification of the oncogene *cMYC* (95). In the sequenced data, this 8q amplicon was present in all five sequenced samples. Therefore, this 8q region was studied in further detail to identify genes having oncogenic potential and therapeutic significance in CRPC. In the 8q region, firstly, genes known to play a role in cancer were identified. Secondly, the search was further narrowed by identifying genes with commercially available inhibitors. Lastly, from this list, the focus was centered on genes studied to a limit extent in PCa. Amongst all the genes in the 8q amplicon, two genes that were amplified at a higher frequency than *cMYC* were *YWHAZ* and *PTK2*. *YWHAZ* is present on 8q22.3 and *PTK2* is present on 8q24.3. These two genes were amplified in the CRPC sequenced cases.

These two genes were further validated on the PCa progression cohort and the somatic copy number variation was analyzed by FISH (**Figure 21 and 22)**. The amplification status of the two genes in the five sequenced patient samples was also further confirmed by FISH. A case was amplified when 80-100% of the cells in the case harbored the amplification.

Regarding *YWHAZ*, 3.7% of the cases were 1mplified in localized PCa, 25.4% in LN metastasis and 48.4% in CRPC (**Figure 21 B**). The frequency between all three subsets was significantly different.

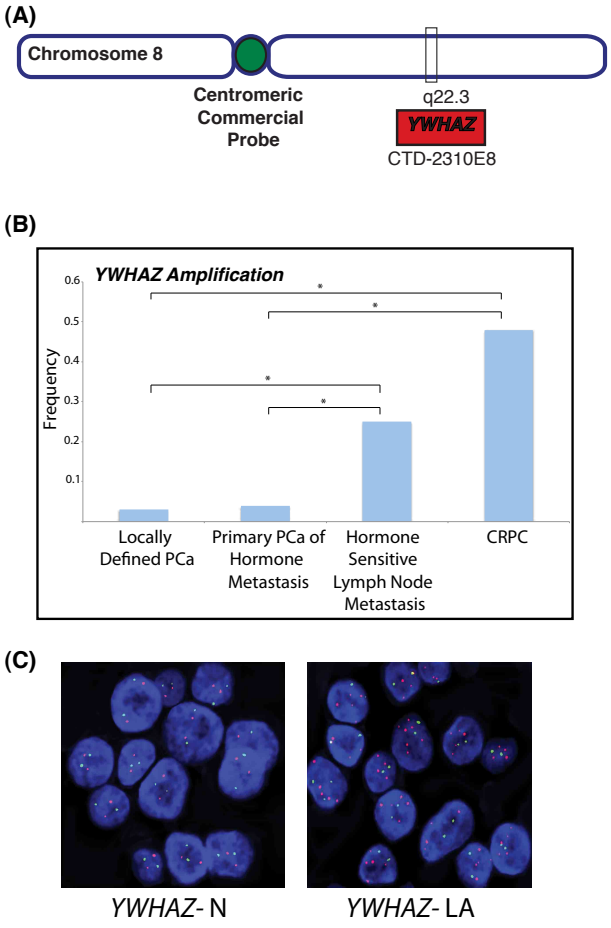

Figure 21: *YWHAZ* amplification in the PCa progression cohort.
A. Schematic representation of the BAC clones spanning the *YWHAZ* gene at chr.8q22.3.
B. Frequency of *YWHAZ* amplification determined in the PCa progression cohort using FISH.
(* Indicates a significant effect ($p<0.05$)
C. Representative nuclei of the patient samples analyzed by FISH. The amplification can be observed as copy number>2 red target signals in comparison to green reference signals. Non-amplified nuclei (N) are represented in a diploid state with two red and two green signals.
(**Menon *et al.*, *Manuscript in preparation***).

For *PTK2,* we found 1.8% of the cases to be amplified in localized PCa and 32.8% in LN metastasis and 35.5% in CRPC. The amplification frequency between the primary PCa and LN metastasized PCa, and CRPC was highly significant (**Figure 22 B**).

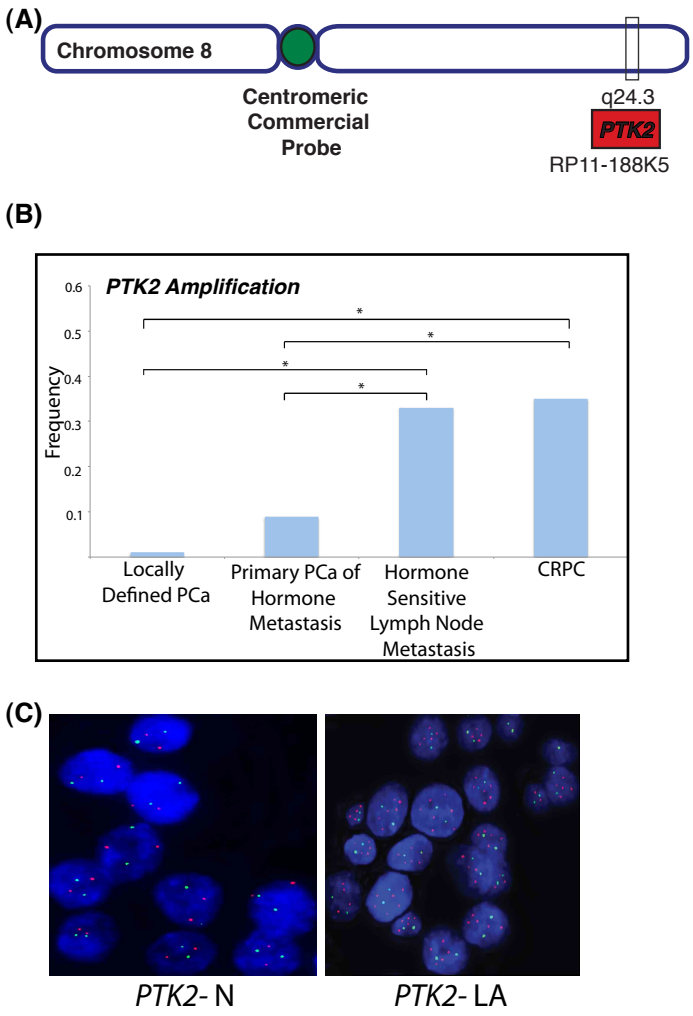

Figure 22: *PTK2* amplification in the PCa progression cohort.
A. Schematic representation of the BAC clones spanning the PTK2 gene at chr.8q24.3.
B. Frequency of *PTK*2 amplification determined in the PCa progression cohort using FISH. (* Indicates a significant effect ($p<0.05$)
C. Representative nuclei of the patient samples analyzed by FISH. The amplification can be observed as copy number >2 red target signals in comparison to green reference signals. Non-amplified nuclei (N) are represented in a diploid state with two red and two green signals.
(**Menon *et al*., *Manuscript in preparation***).

Furthermore, the amplification status of the genes were correlated with their protein expression in the PCa progression cohort. The protein expression was digitally quantified using an image analysis software (Tissue Studio v.2.1, Definiens AG, Munich, Germany) to assign a number to each case depending on the average staining intensities. The IHC stained slides were scanned and the tumor cells were circled in each case. The software then detected the staining intensity for each patient sample and assigned a number based on the intensity. For both YWHAZ and PTK2, the amplified cases had a significantly higher protein expression in comparison to the non-amplified cases (**Figure 23 B and 24 B**). For PTK2, the phosphorylated antibody (pPTK2) was used to determine the protein expression. The phosphorylated form is the active form of PTK2.

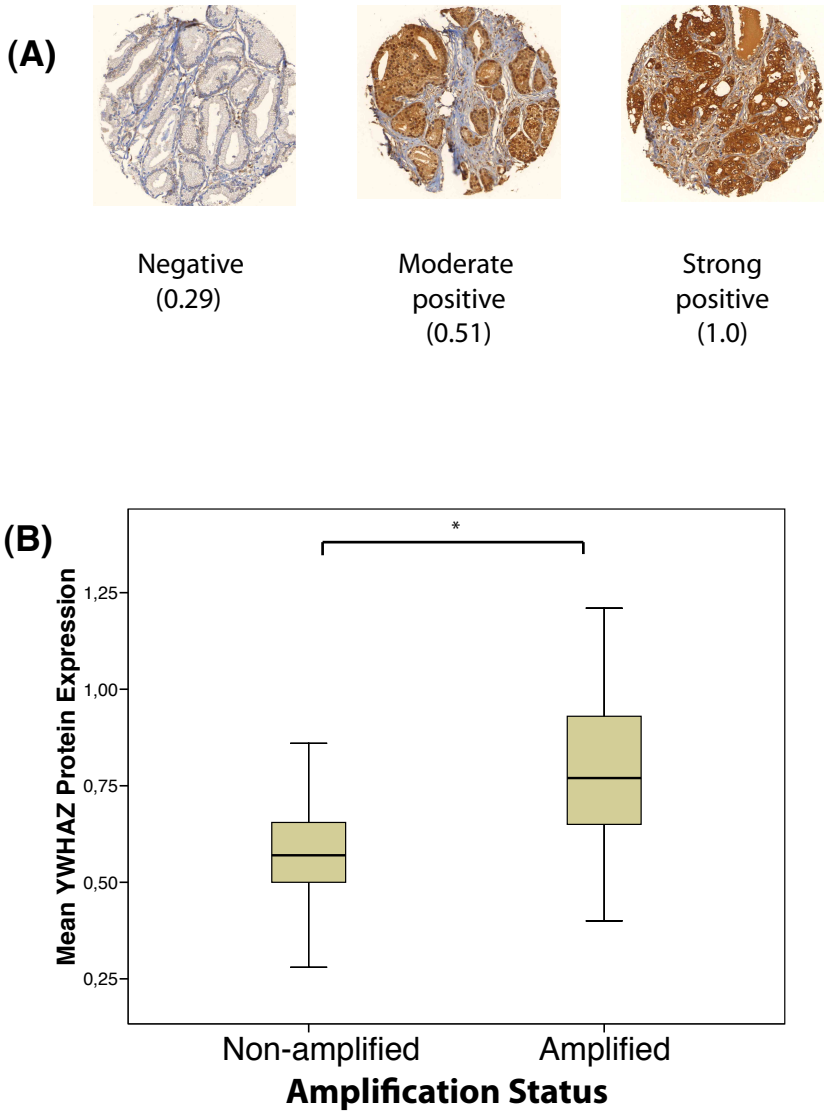

Figure 23: YWHAZ protein expression in the PCa Progression cohort assessed by immunohistochemistry. (* Indicates a significant effect (p<0.05))

A. YWHAZ expression in representative prostate cancer tissue samples indicating a strong cytoplasmic and nuclear expression. The strong positively stained case is assigned a number 1.0 based on its staining intensity whereas the negative case is assigned a 0.29 based on a weak staining.

B. A graph showing the Definiens assigned mean YWHAZ protein expression values (Y axis) in *YWHAZ* amplified and non-amplified PCa cases (X axis). The protein expression is significantly higher in the *YWHAZ* amplified samples.

(**Menon *et al. Manuscript in preparation***).

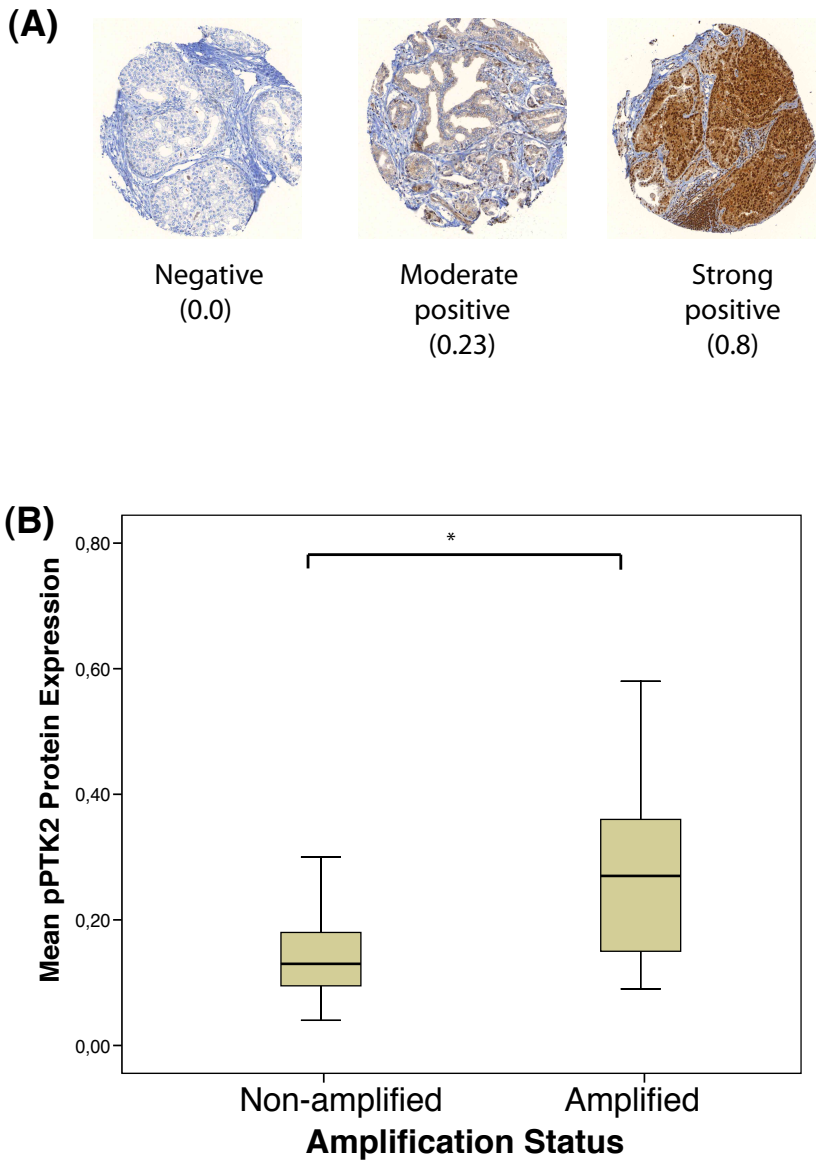

Figure 24: pPTK2 protein expression in the PCa Progression cohort assessed by immunohistochemistry. (* Indicates a significant effect (p<0.05))
A. pPTK2 expression in representative prostate cancer tissue samples indicating a strong cytoplasmic expression. The strong positively stained case is assigned a number 0.8 based on its staining intensity whereas the negative case is assigned a 0.0.
B. A graph showing the Definiens assigned mean pPTK2 protein expression values (Y axis) in *PTK2* amplified and non-amplified PCa cases (X axis). The protein expression is significantly higher in the *PTK2* amplified samples.
(**Menon *et al.*, *Manuscript in preparation***).

These results indicate that the frequency of both *PTK2* and *YWHAZ* amplifications is highest in CRPC patients. Furthermore, there is a positive correlation between genomic amplification and protein expression.

E. The Amplification and Expression of *YWHAZ* and *PTK2* in PC-3 cells

In order to determine the functional role of *YWHAZ* and *PTK2* amplifications in PCa, we identified a cell line harboring both gene amplifications. The PC-3 cell line is an androgen independent cell line derived from bone metastasis. These cells revealed a high level amplification, for both, *YWHAZ* and *PTK2* when assessed by FISH (**Figure 25 A and C**). Western Blots were performed to detect protein expression within the cell line. (**Figure 25 B and D**).

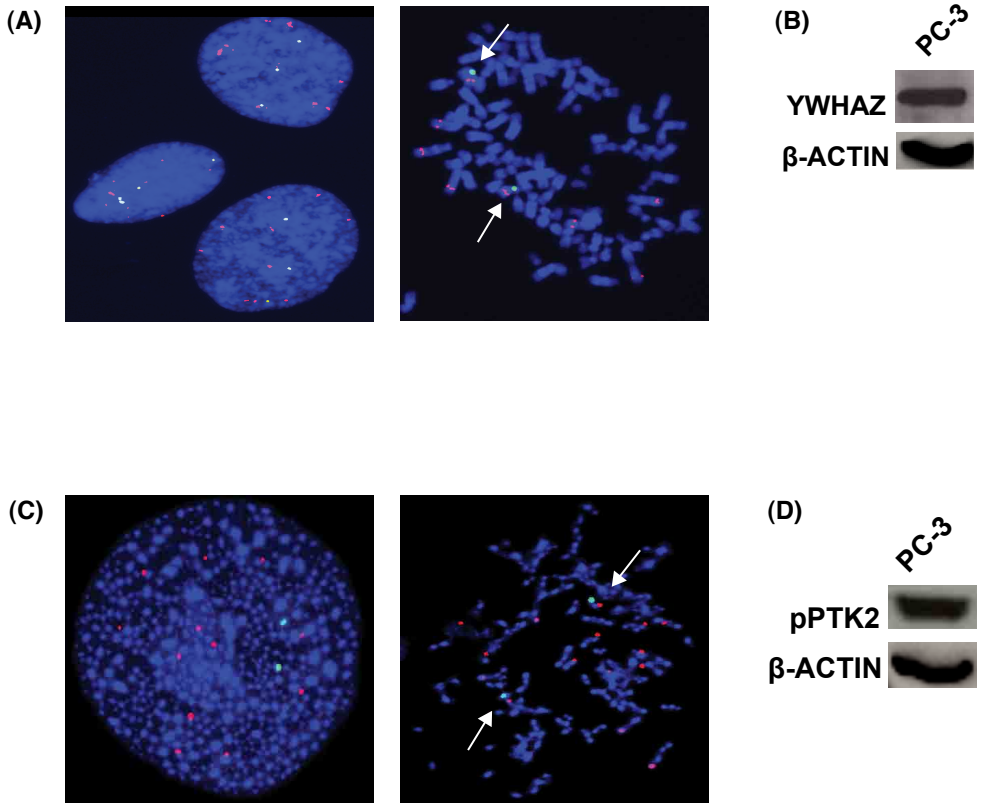

Figure 25: *YWHAZ* and *PTK2* amplification and protein expression in the PC-3 cells
A. *YWHAZ* amplification, determined by FISH, in the PC-3 cells in the interphase and the metaphase.
B. *YWHAZ* protein expression determined by Western Blot in the same cell line.
C. *PTK2* amplification, determined by FISH, in the PC-3 cells the interphase and the metaphase.
D. *PTK2* protein expression by Western Blot in the same cell line
(**Menon *et al*., *Manuscript in preparation***).

F. Effect of *YWHAZ* Knockdown on Proliferation and Migration/Invasion in the PC -3 cells

To evaluate the role of YWHAZ in cancer progression, studies were performed to see what effect the *YWHAZ* knockdown would have on proliferation and migration/invasion. As shown above, *YWHAZ* is expressed in the PC-3 cell line. The endogenous protein expression was reduced by performing a knockdown using siRNA specific to the gene. The siRNA used for the knockdown included duplexes specific for *YWHAZ* and a four siRNA pooled oligonucleotide sequence targeting *YWHAZ*. In parallel, a non-targeting scrambled siRNA was used as a control. Upon adding siRNAs the YWHAZ knockdown was evident after 72 hrs of treatment (**Figure 26).** After the knockdown, its effect on migration and proliferation was measured.

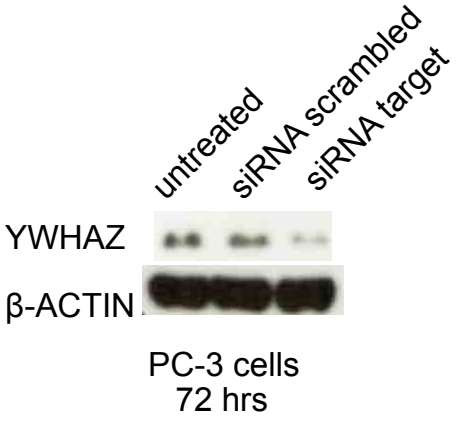

Figure 26: Representative YWHAZ expression by Western Blot 72 hrs after knockdown in the PC-3 cells.
YWHAZ protein expression was significantly reduced after 72 hrs of treatment with siRNA.
(**Menon *et al. Manuscript in preparation***).

The effect of the knockdown on proliferation was assessed after 24, 48 and 72 hrs by performing an MTT assay. At the 72 hr time point, the proliferation of the cells

treated with targeting siRNA, was significantly lower than the control group (**Figure 27**).

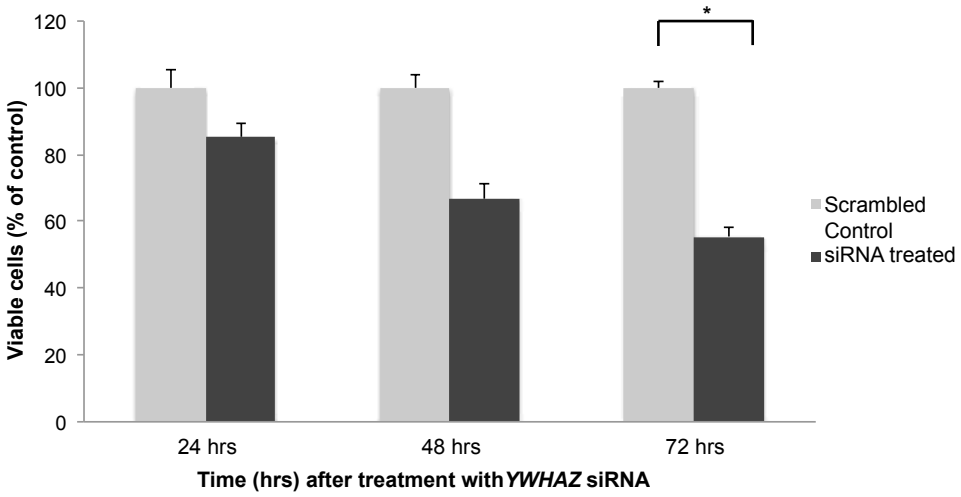

Figure 27: Measurement of cell proliferation using the MTT assay on the *YHWAZ* knocked down PC-3 cells after 24 hrs, 48 hrs and 72 hrs.
Percentage of viable cells was calculated by using the mean of three independent experiments. There was a significant decrease in proliferation between the control group and the knocked down cells (* Indicates a significant effect ($p<0.05$))
(Menon *et al.*, *Manuscript in preparation*).

To test for the effect of the knockdown on migration, a Boyden Chamber migration/invasion chamber was performed. The targeted siRNA treated cells had significantly lower migration ability compared to the control group. There was a 55% decrease in migration in comparison to the control-scrambled siRNA. The difference between the control group, treated with scrambled siRNA, and cells with *YWHAZ* knocked down was highly significant (**Figure 28**).

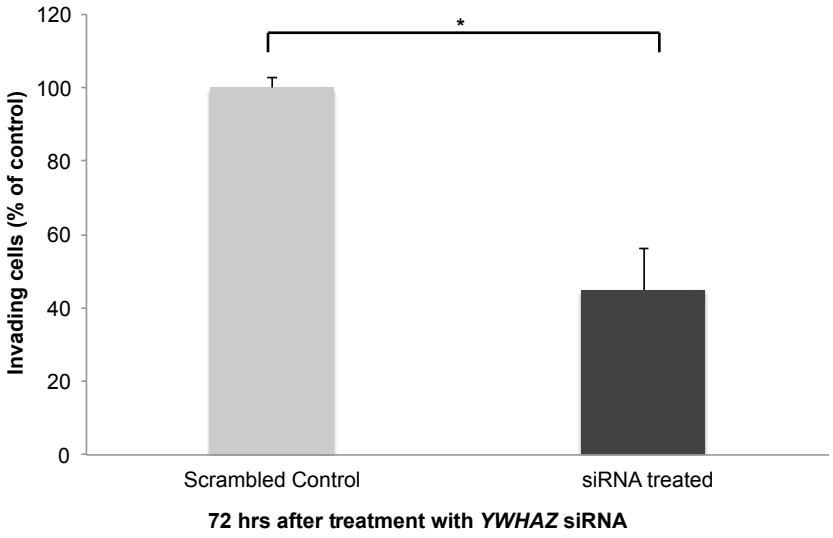

Figure 28: Migration/invasion assay for the PC-3 cells harboring the *YWHAZ* knockdown. Percentage of invading cells was calculated by using the mean of three independent experiments There was a 55% decrease in migration in the knocked down cells when compared to the control (* Indicates a significant effect ($p<0.05$)) (**Menon *et al.*, *Manuscript in preparation***).

These results indicate that the YWHAZ knockdown did affect cell proliferation and migration. Therefore, blocking YWHAZ could potentially reduce PCa progression.

G. Effect of the pharmacological PTK2 inhibitor, TAE226, on PC-3 cells

Similarly, the effect of pPTK2 suppression on the PC-3 cell line was determined by treating the cell line with the commercially available pharmacological TAE226 inhibitor. The cell line was treated with a gradient of the TAE226 inhibitor (0-10 μM). Similarly, the effect of the inhibitor was tested on cell proliferation and migration. A Western Blot was performed to analyze the reduction in protein expression at each time point (**Figure 29**). DMSO treated cells were used as a control.

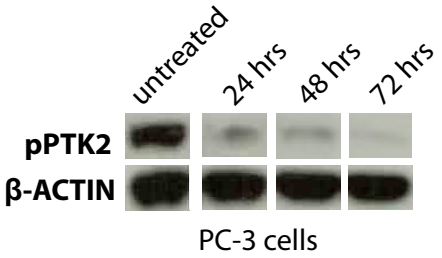

Figure 29: Representative phospho PTK2 expression by Western Blot after treatment with the 10 µM TAE226 pharmacological inhibitor after 24, 48 and 72 hrs.
There was a time dependent gradual decrease in protein expression after treatment with the inhibitor (**Menon *et al. Manuscript in preparation***).

There was a significant reduction in pPTK2 expression at a concentration of 10 µM of the inhibitor. After 72 hrs of exposure to the inhibitor, a significant decrease in cell proliferation was observed at the same concentration (**Figure 30**).

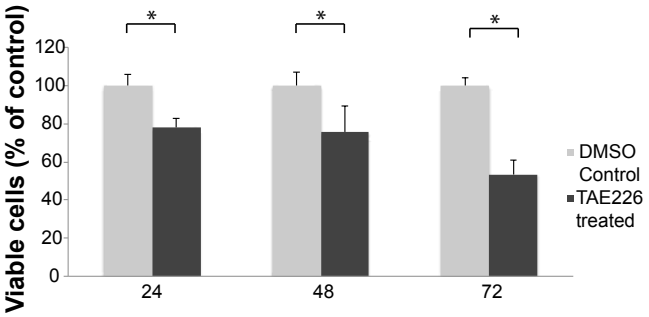

Figure 30: Measurement of cell proliferation using the MTT assay on the PC-3 cells treated with 10 µM TAE226 pharmacological inhibitor after 24, 48 and 72 hrs.
Percentage of viable cells was calculated by using the mean of three independent experiments The least number of viable cells were observed after 72 hrs of treatment with the inhibitor
(* Indicates a significant effect $p<0.05$) (**Menon *et al.*, *Manuscript in preparation***).

The data suggests that the inhibitor had a significant effect on cell proliferation. As a control, the cells were treated with a 10 µM concentration of DMSO.

Next a cell cycle analysis was performed to see the stage at which the cells are arrested when exposed to the inhibitor. The cells were subjected to a PI staining assessed by flow cytometry. PI intercalates in the deep groove of double stranded DNA.

As shown in **Figure 31**, after 24 hours of treatment with the inhibitor, the majority of the cells were arrested at the G_1 phase. After 48 hours of treatment with the inhibitor, a majority of the cells were arrested in the G_2 phase. Eventually, 72 hrs of treatment with the inhibitor majority of cells were arrested at the G_1 phase, followed by the G_2 phase. There was a decrease in the number of cells in the S-phase after all three time points (**Figure 31**). As a control, the cells were treated with a 10 µM concentration of DMSO.

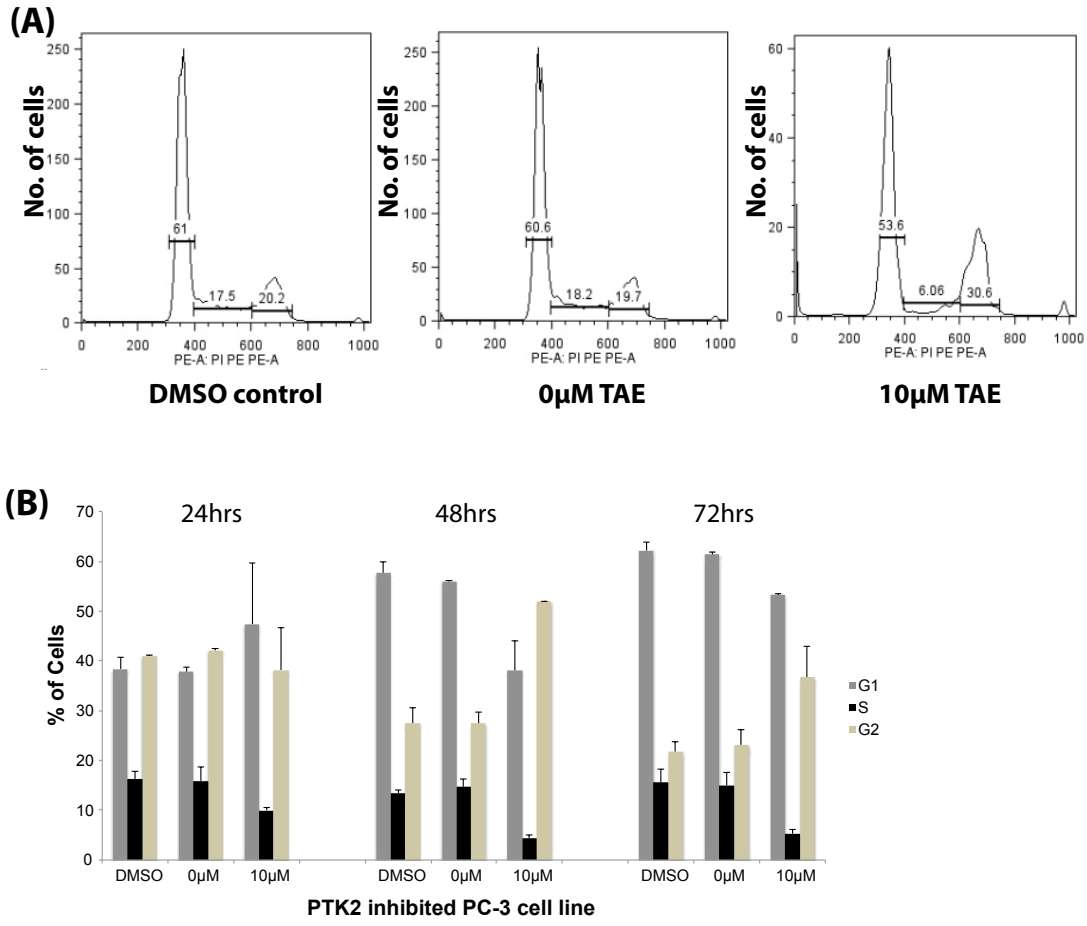

Figure 31: PI staining cell cycle arrest assay for PC-3 cells treated with pharmacological TAE226 inhibitor.
A. Representative cell cycle analysis of PC-3 cells treated with DMSO and pharmacological TAE226 inhibitor.
B. Percentage of viable cells was calculated by using the mean of three independent experiments. At a 10 µM concentration, the cells are arrested at the G_1 and G_2/M phase. There was a decrease in the number of cells in the S-phase. (* Indicates a significant effect $p<0.05$) (**Menon *et al.*, *Manuscript in preparation***).

Next, the effect of the inhibitor in inducing apoptosis was tested. This was done by performing a Hoechst 33342/Yo Pro-1 apoptosis assay with the inhibitor at a 10 μM concentration. The inhibitor is dissolved in DMSO. Therefore, as a control, the cells were treated with a 10 μM concentration of DMSO to test for apoptosis. Hoechst 33342 stains the condensed chromatin of apoptotic cells and dimly the chromatin of live cells. Yo Pro-1 enters the apoptotic cells. The FACS staining showed cells in four different quadrants. Apoptotic cells are Yo Pro-1+ and Hoechst 33342- and +, while viable cells are Yo Pro-1 and Hoechst 33342-. shown in the left upper quadrant while viable cells are in the lower left quadrant. Doxorubicin was used as a positive control and at a concentration of 10 μM, it induced apoptosis in 99% of the cells. On the other hand, only 4% of the untreated cells underwent apoptosis. After 72 hrs of treatment with the inhibitor, a negligible amount of cells were apoptotic (12%). Therefore, the results of this assay showed that the inhibitor at high concentrations of 10 μM did not induce apoptosis in the cells (**Figure 32**).

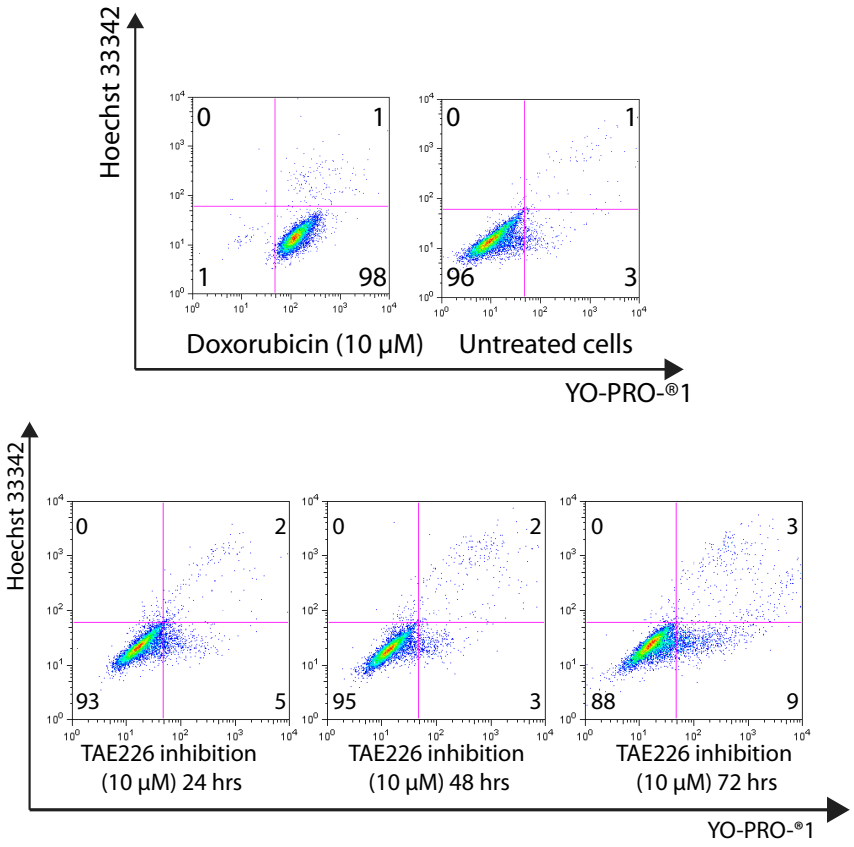

Figure 32: Representative FACS analysis data to determine apoptosis in the TAE226 treated PC-3 cells by staining with YO-PRO-1 (X axis) and Hoechst 33342 (Y axis).
The positive control, Doxorubicin, at a 10 µM concentration induced apoptosis in the cells. Negligible amount of cells were apoptotic at the highest inhibitor concentration of 10 µM. In this figure the colors designate the density of the cell population where blue is the least dense and red is the most dense (**Menon *et al*. *Manuscript in preparation***).

Furthermore, the PTK2 inhibited cells were subjected to migration/invasion *in vitro*. The pharmacological TAE226 inhibitor treated cells had a significant decrease in migration compared to the untreated PC-3 cells. The difference in invasion capacity of the control group versus the PTK2 inhibited cells was highly significant (**Figure 33**).

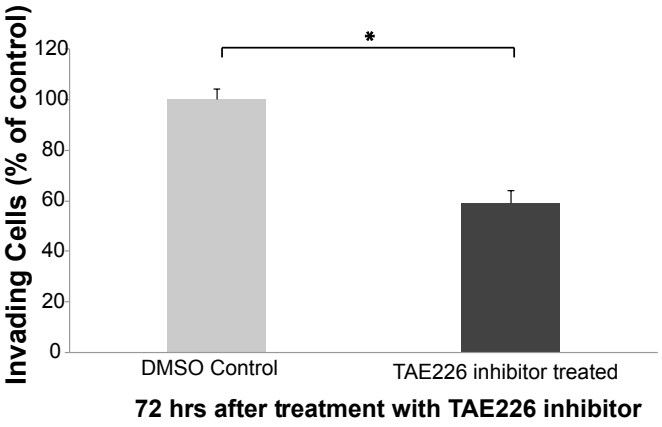

Figure 33: Migration/invasion assay for PC-3 cells treated with the pharmacological inhibitor at a concentration of 10 µM.
Percentage of invading cells was calculated by using the mean of three independent experiments. There was a 40% decrease in migration compared to the control group.
(**Menon et al.,*Manuscript in preparation***).

These results indicate that the *PTK2* inhibited PC-3 cell line did show a significant decrease in proliferation and migration. Furthermore, upon treatment with the pharmacological TAE226 inhibitor, the cells were arrested at the G_1 and G_2 phase. Therefore, the *PTK2* gene could potentially serve as a therapeutic target for CRPC patients.

The results of Objective III are presented in a manuscript which is under preparation., 'Somatic copy number alterations by whole exome sequencing implicates *YWHAZ* and *PTK2* in castration resistant prostate cancer' (Menon *et al*., 2013 *Manuscript in preparation*).

The bioinformatic analysis was carried out by Mario Deng, the bioinformatician in the lab.

8. Discussion

PCa translational research requires the availability of well-annotated human prostate tissue samples (96-99). However, for clinical practices, hospitals require all prostatic tissue to be available for diagnostic purposes. Due to this requirement, the availability of fresh frozen tissue for research purposes in very limited. It has been previously shown that FFPE tissue is easy to handle and store (100). Most of the material available in the pathology archives is present in FFPE form. Therefore, there is a need to assess the quality of FFPE fixed tissue for research purposes, in particular next generation sequencing.

8.1 Validation of FFPE and HOPE fixed tissue for DNA, RNA and protein analysis

A comparative study was performed using HOPE fixed, FFPE fixed and fresh frozen tissue to analyze DNA, RNA and protein integrity. HOPE fixed specimen yielded far better results than the FFPE fixed specimen (**Figure 11,12,13,14**). HOPE fixation did not present nucleic acid degradation and methylene cross-linking, they displayed superior morphology and also required no antigen retrieval for IHC analysis. For the FISH analysis, the HOPE samples required enzymatic pretreatment for better signals. DNA extracted from all three fixation methods yielded good results, appropriate for molecular downstream applications (**Figure 12**). Unfortunately, due to fixation, RNA obtained from FFPE specimens were fragmented (**Figure 13**). On the other hand, FFPE samples could be successfully used for amplification of shorter fragments of up to 400bp in length.

Our study was the first to extensively analyse the efficiency of the HOPE fixation protocol for research purposes. In a pathology setting, the most commonly used

fixation protocol is FFPE as these samples are cheap and easy to handle. DNA extraction from FFPE tissues have previously been studied by various groups (101-103). Our study yielded better results for DNA extracted from the HOPE specimen in comparison to the FFPE specimen. Similar to our results, a study performed by Gupta *et al*., noticed a 100 fold enhanced sensitivity for the HOPE fixed material, in comparison to the formalin fixed material (104). Furthermore, another study by Wiedorn *et al*., supports our study. They claim that high molecular weight nucleic acids are preserved when specimen are HOPE fixed (105).

With regards to RNA extraction and integrity, a similar study conducted by Arzt *et al.*, compared the RNA extraction protocols for HOPE and FFPE fixed specimen. They found that they had a higher yield of RNA in the FFPE extracted samples when compared to the HOPE samples (106). Also, they reported that the RNA integrity was the same for both fixative techniques. On the contrary, in our study, FFPE specimen fared better than the HOPE specimen. A reason for the difference in RNA based results may be due to the modifications introduced by the authors in the RNA extraction protocol. The authors used two different kits for RNA extraction, and an addition purification step (106). A major limitation in our study was the lack of Bioanalyzer data to determine RNA integrity. A Bioanalyzer analysis in addition to the qRT-PCR analysis would have strengthened our study. Furthermore an optimized RNA extraction protocol could also drastically increase the RNA yield from the fixed specimen.

With regards to protein extraction, a study conducted by Uhlig *et al*., showed the efficiency of HOPE fixed specimen in western blot analysis (107). They compared specimen that were fixed 2-4 year ago, and noticed that in the HOPE fixed specimen, the antigens on the cell surfaces were intact. In our study, we studied prostate cancer

tissue that was HOPE, FFPE and cryofixed a few days prior to the experiments. Therefore, we did not take into consideration the prolonged effect of fixation on the specimen, which is a limitation of our study. The impact of the fixation on RNA , DNA and protein, over a prolonged period of time was not taken into consideration. Therefore, a study assessing this effect of fixation on DNA, RNA and protein would help in identifying the ideal fixation protocol for sequencing based studies.

All in all, this was the first paper to compare HOPE, FFPE and fresh frozen tissue for RNA, DNA and protein analysis.

8.2 Validation of exome sequencing efficiency of FFPE tissue

The study of genomic and transcriptomic alterations in cancer has been made possible by the emergence of next generation sequencing technologies (108). These technologies have enabled the detection of mutations, substitutions, insertions, deletions, and copy number alterations. Fresh frozen tissue is the most commonly used tissue type for sequencing due to its high DNA and RNA integrity. Due to the scarcity of fresh frozen CRPC, a pilot study was conducting using FFPE tissue for sequencing. The abundant availability of FFPE tissue in the pathology archives would facilitate the use of FFPE material for sequencing would provide an in-depth analysis of the functional biology of cancer, cancer progression and drug therapy. Unfortunately, the use of FFPE material for RNA sequencing is limited. Due to the fixation and instability of RNA, it is very difficult to extract high integrity RNA. Therefore, transcriptome sequencing still remains a challenge as FFPE material is only suitable for DNA based sequencing protocols.

To test for the exome sequencing efficiency of FFPE material, a pilot study was performed to compare the sequencing results obtained from both fresh frozen and

FFPE fixed PCa tissue from a single patient. The results of this study showed that 66% of the SNVs detected in FFPE tissue were also seen in the fresh frozen tissue (**Figure 17**). These positive results lead to the next objective. A major limitation of our study was the low sequencing coverage. Several studies have shown that a high sequencing coverage of 100x or more drastically decreases the detection of false positives SNVs and is sufficient for a reliable CNV analysis (109, 110).

8.3 Identification of genes, by whole exome sequencing, that could serve as druggable targets for CRPC

With regards to PCa, in particular, treatment options for patients suffering from CRPC still remains a significant challenge. There is an urgent to identify therapeutic targets for CRPC using tools such as next generation sequencing techniques. The objective of this study was also to identify relevant genes that could serve as druggable targets for CRPC by performing exome sequencing on five CRPC/normal paired samples. Due to the scarcity of CRPC fresh frozen material, FFPE material was used for exome sequencing.

Our exome sequencing data identified many areas of amplification and deletions in the CRPC samples (**Figure 19**). Recent sequencing studies on CRPC fresh frozen material identified several clusters of amplification on chromosome 8 and other chromosomes (82, 85). These clusters were also identified in our sequencing data. The genes that were amplified on chromosome 8 included *TERF1, RPl7, STAU2, UBE2W, COX6C,* and *GRHL2.*

Among the amplicons in our exome sequenced data, the 8q region was amplified in all five sequenced patients. The 8q amplicon also harbors the proto-oncogene *cMYC*(111, 112). Two more genes residing on chromosome 8, namely *YWHAZ* and

PTK2, were also amplified in all five patients. Furthermore, the latter two genes were amplified at a much higher frequency than the well known proto-oncogene *cMYC* (95). Of note, the amplification frequency of *YWHAZ* was 3.7% in the localized PCa cases and 48.4% in CRPC patients. Similarly the amplification frequency of *PTK2* increased from 3.7% in localized PCa to 48.4% in CRPC. This shows that the amplification frequency for both genes was the highest in CRPC patients (**Figure 21 and 22**).

YWHAZ, a 14-3-3 family protein, is overexpressed and up-regulated in various cancers and is also a drug target in head and neck cancers and breast cancer (113-115). This gene is involved in many cellular processes such as metabolism, protein trafficking, signal transduction, apoptosis and cell cycle regulation. In head and neck tumors, the amplification of the gene resulted in neoplastic transformation. Furthermore, the cells were resistant to apoptosis and had accelerated cell growth (116). In breast cancer, *YWHAZ* induced chemotherapy resistance, and played a vital role in the partial transformation of human mammary epithelial cells (HMECs) (117). There are commercially available inhibitors for the 14-3-3 family of proteins, namely Difopein and R18. Unfortunately, they do not target the *YWHAZ* but the whole family of genes. Therefore, to specifically target *YWHAZ,* siRNAs specific to the gene were used. These siRNAs were previously also used for the study of *YWHAZ* and its role in breast cancer (115). Results obtained by the studies performed on the head and neck cell lines and breast cancer cell lines showed that *YWHAZ* knockdown enhanced anchorage independent growth and made cells more sensitive to stress induced apoptosis (113, 116). In our functional studies, the knockdown resulted in decreased proliferation and migration (**Figure 27 and 28**). Based on the results of this study, there is a necessity to develop drugs specifically targeting *YWHAZ*. One limitation to

this experiment involves the off target effects of the siRNA. siRNAs are known to introduce off targets effects such as multiple site cleavage or a translational block due to imperfect match of the 3' UTR (118). Creating a PC-3 cell line harboring a stable knockdown of the gene could eliminate these off-target effects.

Furthermore, a recent publication elucidated the role of *YWHAZ* in prostate cancer LNCaP cells, which is an androgen responsive cell line (119). This group showed that upon treatment with DHT, LNCaP cells showed and increased expression of *YWHAZ* and also promoted proliferation and motility. Upon immunoprecipitation, it was shown that *YWHAZ* associated with the androgen receptor. The gene increased *AR* transcriptional activity by binding to the receptor in the nucleus. These studies support the role that *YWHAZ* has in patients harboring an *AR* amplification. It is known that 10-30% of the CRPC patients harbor and *AR* amplification (120). Therefore, a cocktail of antiandrogen drugs in combination with drugs specifically targeting *YWHAZ* could cumulatively have an effect in halting PCa progression.

YWHAZ has been described be involved in various cell processes but there is limited information on the biological function of the gene. *YWHAZ* has three sites that are phosphorylated by PBK/Akt phosphorylation. This induces the dimerization and activation of the gene (121). Furthermore, another interaction partner of *YWHAZ* is beta-catenin. The gene has been shown to activate beta-catenin through survival kinase Akt. And beta-catenin in turn activates the Wnt responsive genes in the Wnt signaling pathway. All these pathways play a role in furthering tumorigenesis (122). Also, *YWHAZ* studies have shown that knockdown results in decreased MAPK and AKT activity. In turn MAPK and AKT are associated with apoptotic molecules such as Bcl2 and Bax, which act complementary to each other (123). As *YWHAZ* is known to interact with various signaling pathways, it is important identify its biological and

functional role. To further understand the activation and pathways the gene interacts with, it would be interesting to perform a knockdown/overexpression of *YWHAZ* in a PCa cell line followed by an expression chip analysis. This would give an overview of the genes that are up or down regulated in the cell line harboring the overexpression or knockdown. Furthermore, the up or down regulated genes would also provide a brief overview regarding the signaling pathways involved. Another experiment that could be conducted is coimmunoprecipitation to assess for the binding partners of *YWHAZ*. As this gene has not been extensively studied in literature, much remains to be done to understand its biological relevance.

Similarly, *PTK2* is another gene, known to play a role in decreased cell adhesion and increased cell survival in ovarian, gastric and breast cancers (124-126). For *PTK2*, the phosphorylation of the amino acid Y397, induces the formation of the *PTK2-Src* complex and activates it (127-129). The Src family kinases play a major role in integrin signaling. Upon phosphorylation of the Y397 and formation f the *PTK2-Src* complex various signal transduction pathways are triggered (130). The *PTK2-Src* complex, in breast cancer, is involved in ERK activation through the ERK-MAPK pathway to maintain tumor growth and migration (126). Studies using the *PTK2* specific inhibitor have been shown to decrease migration, invasion and proliferation in cancers (127, 131, 132). The pharmacological TAE226 inhibitor, a *PTK2* specific inhibitor, reduces levels of phosphorylated *PTK2* by inhibiting both the Y397 and Y861 phosphorylation (127, 133). In ovarian cancer, the inhibitor has shown to be effective in both chemotherapy sensitive and resistant ovarian cancer models (127). When our CRPC PC-3 cells were treated with inhibitor, they exhibited a significant decrease in both migration and proliferation (**Figure 30 and 33**). Furthermore, the flow cytometry analysis of the PI staining showed cells arrested in the G_1 and G_2/M

phases. Therefore, similar to *YWHAZ, PTK2* could also serve as a potential therapeutic target for CRPC and the pharmacological TAE226 inhibitor could be provided to patients in combination with other cancer drugs to treat PCa.

PTK2 is also known as focal adhesion kinase (FAK). It is a part of the non receptor tyrosine protein kinase and is required for many normal cellular functions such as cell proliferation, differentiation, migration, adhesion (134). *PTK2* is up regulated in gliomas and breast cancers. The TAE226 inhibitor has been tested in gliomas and breast cancer. It inhibited the phosphorylation of Y397 and insulin like growth factor I. Furthermore, it also inhibited downstream targets genes such as Akt (135). As the inhibitor has provided successful results in glioma and breast cancer xenograft models (131), the next step would be to test the inhibitor on prostate xenograft models. This would essentially bring us closer to determining the role of *PTK2* as a therapeutic target in CRPC.

An extension to the *YWHAZ* experiments would involve using the DU-145 PCa cell line, not harboring the *YWHAZ* amplification, to stably overexpress the gene. The effect that the stable transfection has on migration and proliferation would be assessed. Furthermore, these cells could be introduced in mice to see whether it leads to an increase in tumor growth and cell migration. In parallel, the PC-3 cell line could be used to create a stable knockdown for *YWHAZ*, followed by assessing the migration and proliferation characteristics of the cells. Based on the results obtained, they could also be introduced into mice. The creation of stable cells lines would help in erasing the off target effects caused by siRNA.

Similarly for *PTK2*, an extension to the project could involve injecting mice with the PC-3 cells, harboring the *PTK2* amplification, and treating the mice with the TAE226 inhibitor to notice shrinkage in tumor or a decrease in metastasis.

Conclusion

In conclusion, this study was able to illustrate that FFPE specimen can also be used for next generation sequencing protocols. FFPE tissue is a promising alternative to fresh frozen material for prostate cancer storage and could be a reliable source of material for comprehensive research in routine diagnostics.

Through the exome sequencing study on CRPC patient samples, two amplified genes, *YWHAZ* and *PTK2* both residing on chromosome 8, were identified as potential therapeutic targets. Both genes, when inhibited, showed an effect in proliferation and invasion in the PC-3 cells.

Much still remains to be done in the field of CRPC treatment options for patient care, but the evolution of next generation sequencing technologies has made it possible to study the genetic basis of cancer. In the future, these studies will eventually lead to the development of personalized medicine to improve patient care.

References

1. Jemal A, Bray F, Center MM, Ferlay J, Ward E, Forman D. Global cancer statistics. CA Cancer J Clin. 2011;61:69-90.
2. Taichman RS, Loberg RD, Mehra R, Pienta KJ. The evolving biology and treatment of prostate cancer. J Clin Invest. 2007;117:2351-61.
3. Boyd LK, Mao X, Lu YJ. The complexity of prostate cancer: genomic alterations and heterogeneity. Nat Rev Urol. 2012;9:652-64.
4. Ferlay J SH, Bray F, et al. GLOBOSCAN 2008. Cancer incidence and mortality worldwide
. 2010.
5. Gerard J. Tortora BD. Principles of Anatomy and Physiology: John Wiley and Sons, Inc.; 2006.
6. Timms BG. Prostate development: a historical perspective. Differentiation. 2008;76:565-77.
7. Shen MM, Abate-Shen C. Molecular genetics of prostate cancer: new prospects for old challenges. Genes Dev. 2010;24:1967-2000.
8. Pham H, Ziboh VA. 5 alpha-reductase-catalyzed conversion of testosterone to dihydrotestosterone is increased in prostatic adenocarcinoma cells: suppression by 15-lipoxygenase metabolites of gamma-linolenic and eicosapentaenoic acids. J Steroid Biochem Mol Biol. 2002;82:393-400.
9. Chen W, Tsai SJ, Liao CY, Tsai RY, Chen YJ, Pan BJ, et al. Higher levels of steroidogenic acute regulatory protein and type I 3beta-hydroxysteroid dehydrogenase in the scalp of men with androgenetic alopecia. J Invest Dermatol. 2006;126:2332-5.
10. Gulley JL. Prostate Cancer: Demos Medical Publishing LLC; 2011.
11. Braun M M, R, Nikolov P, Perner S. ERG rearrangment as a Clonal Expansion Marker for Prostate Cancer. The Open Prostate Cancer Journal. 2010;3:63-8.
12. Lucas JN. Prostate Cancer: Nova Biomedical Books; 2004.
13. Dong JT. Chromosomal deletions and tumor suppressor genes in prostate cancer. Cancer Metastasis Rev. 2001;20:173-93.
14. Ouyang X, DeWeese TL, Nelson WG, Abate-Shen C. Loss-of-function of Nkx3.1 promotes increased oxidative damage in prostate carcinogenesis. Cancer Res. 2005;65:6773-9.
15. Dang CV. c-Myc target genes involved in cell growth, apoptosis, and metabolism. Mol Cell Biol. 1999;19:1-11.
16. Sato K, Qian J, Slezak JM, Lieber MM, Bostwick DG, Bergstralh EJ, et al. Clinical significance of alterations of chromosome 8 in high-grade, advanced, nonmetastatic prostate carcinoma. J Natl Cancer Inst. 1999;91:1574-80.
17. Gil J, Kerai P, Lleonart M, Bernard D, Cigudosa JC, Peters G, et al. Immortalization of primary human prostate epithelial cells by c-Myc. Cancer Res. 2005;65:2179-85.

18. Whang YE, Wu X, Suzuki H, Reiter RE, Tran C, Vessella RL, et al. Inactivation of the tumor suppressor PTEN/MMAC1 in advanced human prostate cancer through loss of expression. Proc Natl Acad Sci U S A. 1998;95:5246-50.
19. Wang S, Gao J, Lei Q, Rozengurt N, Pritchard C, Jiao J, et al. Prostate-specific deletion of the murine Pten tumor suppressor gene leads to metastatic prostate cancer. Cancer Cell. 2003;4:209-21.
20. Wang SI, Parsons R, Ittmann M. Homozygous deletion of the PTEN tumor suppressor gene in a subset of prostate adenocarcinomas. Clin Cancer Res. 1998;4:811-5.
21. Mulholland DJ, Dedhar S, Wu H, Nelson CC. PTEN and GSK3beta: key regulators of progression to androgen-independent prostate cancer. Oncogene. 2006;25:329-37.
22. Varambally S, Dhanasekaran SM, Zhou M, Barrette TR, Kumar-Sinha C, Sanda MG, et al. The polycomb group protein EZH2 is involved in progression of prostate cancer. Nature. 2002;419:624-9.
23. Min J, Zaslavsky A, Fedele G, McLaughlin SK, Reczek EE, De Raedt T, et al. An oncogene-tumor suppressor cascade drives metastatic prostate cancer by coordinately activating Ras and nuclear factor-kappaB. Nat Med. 2010;16:286-94.
24. Pardal R, Clarke MF, Morrison SJ. Applying the principles of stem-cell biology to cancer. Nat Rev Cancer. 2003;3:895-902.
25. Dittmer J, Nordheim A. Ets transcription factors and human disease. Biochim Biophys Acta. 1998;1377:F1-11.
26. Tomlins SA, Rhodes DR, Perner S, Dhanasekaran SM, Mehra R, Sun XW, et al. Recurrent fusion of TMPRSS2 and ETS transcription factor genes in prostate cancer. Science. 2005;310:644-8.
27. Braun M, Scheble VJ, Menon R, Scharf G, Wilbertz T, Petersen K, et al. Relevance of cohort design for studying the frequency of the ERG rearrangement in prostate cancer. Histopathology. 2011;58:1028-36.
28. Mehra R, Tomlins SA, Shen R, Nadeem O, Wang L, Wei JT, et al. Comprehensive assessment of TMPRSS2 and ETS family gene aberrations in clinically localized prostate cancer. Mod Pathol. 2007;20:538-44.
29. Helgeson BE, Tomlins SA, Shah N, Laxman B, Cao Q, Prensner JR, et al. Characterization of TMPRSS2:ETV5 and SLC45A3:ETV5 gene fusions in prostate cancer. Cancer Res. 2008;68:73-80.
30. Wang J, Cai Y, Yu W, Ren C, Spencer DM, Ittmann M. Pleiotropic biological activities of alternatively spliced TMPRSS2/ERG fusion gene transcripts. Cancer Res. 2008;68:8516-24.
31. Donald J Tindall PTS. Recent Advances in Prostate Cancer: World Scientific Publishing Co.; 2011.
32. She QB, Solit DB, Ye Q, O'Reilly KE, Lobo J, Rosen N. The BAD protein integrates survival signaling by EGFR/MAPK and PI3K/Akt kinase pathways in PTEN-deficient tumor cells. Cancer Cell. 2005;8:287-97.
33. Wu C, Huang J. Phosphatidylinositol 3-kinase-AKT-mammalian target of rapamycin pathway is essential for neuroendocrine differentiation of prostate cancer. J Biol Chem. 2007;282:3571-83.
34. Kinkade CW, Castillo-Martin M, Puzio-Kuter A, Yan J, Foster TH, Gao H, et al. Targeting AKT/mTOR and ERK MAPK signaling inhibits hormone-refractory prostate cancer in a preclinical mouse model. J Clin Invest. 2008;118:3051-64.

35. Begley L, Monteleon C, Shah RB, Macdonald JW, Macoska JA. CXCL12 overexpression and secretion by aging fibroblasts enhance human prostate epithelial proliferation in vitro. Aging Cell. 2005;4:291-8.
36. Bethel CR, Chaudhary J, Anway MD, Brown TR. Gene expression changes are age-dependent and lobe-specific in the brown Norway rat model of prostatic hyperplasia. Prostate. 2009;69:838-50.
37. Blum DL, Koyama T, M'Koma AE, Iturregui JM, Martinez-Ferrer M, Uwamariya C, et al. Chemokine markers predict biochemical recurrence of prostate cancer following prostatectomy. Clin Cancer Res. 2008;14:7790-7.
38. De Marzo AM, Marchi VL, Epstein JI, Nelson WG. Proliferative inflammatory atrophy of the prostate: implications for prostatic carcinogenesis. Am J Pathol. 1999;155:1985-92.
39. Kelley MR, Cheng L, Foster R, Tritt R, Jiang J, Broshears J, et al. Elevated and altered expression of the multifunctional DNA base excision repair and redox enzyme Ape1/ref-1 in prostate cancer. Clin Cancer Res. 2001;7:824-30.
40. Fordyce CA, Heaphy CM, Joste NE, Smith AY, Hunt WC, Griffith JK. Association between cancer-free survival and telomere DNA content in prostate tumors. J Urol. 2005;173:610-4.
41. Zhang Z, Rosen DG, Yao JL, Huang J, Liu J. Expression of p14ARF, p15INK4b, p16INK4a, and DCR2 increases during prostate cancer progression. Mod Pathol. 2006;19:1339-43.
42. Dehm SM, Tindall DJ. Regulation of androgen receptor signaling in prostate cancer. Expert Rev Anticancer Ther. 2005;5:63-74.
43. Lonergan PE, Tindall DJ. Androgen receptor signaling in prostate cancer development and progression. J Carcinog. 2011;10:20.
44. Yeh S, Lin HK, Kang HY, Thin TH, Lin MF, Chang C. From HER2/Neu signal cascade to androgen receptor and its coactivators: a novel pathway by induction of androgen target genes through MAP kinase in prostate cancer cells. Proc Natl Acad Sci U S A. 1999;96:5458-63.
45. Kim J, Coetzee GA. Prostate specific antigen gene regulation by androgen receptor. J Cell Biochem. 2004;93:233-41.
46. Lu S, Liu M, Epner DE, Tsai SY, Tsai MJ. Androgen regulation of the cyclin-dependent kinase inhibitor p21 gene through an androgen response element in the proximal promoter. Mol Endocrinol. 1999;13:376-84.
47. Chuan YC, Pang ST, Cedazo-Minguez A, Norstedt G, Pousette A, Flores-Morales A. Androgen induction of prostate cancer cell invasion is mediated by ezrin. J Biol Chem. 2006;281:29938-48.
48. Li BY, Liao XB, Fujito A, Thrasher JB, Shen FY, Xu PY. Dual androgen-response elements mediate androgen regulation of MMP-2 expression in prostate cancer cells. Asian J Androl. 2007;9:41-50.
49. Heemers H, Verrijdt G, Organe S, Claessens F, Heyns W, Verhoeven G, et al. Identification of an androgen response element in intron 8 of the sterol regulatory element-binding protein cleavage-activating protein gene allowing direct regulation by the androgen receptor. J Biol Chem. 2004;279:30880-7.
50. Petre CE, Wetherill YB, Danielsen M, Knudsen KE. Cyclin D1: mechanism and consequence of androgen receptor co-repressor activity. J Biol Chem. 2002;277:2207-15.

51. Wu Y, Kawate H, Ohnaka K, Nawata H, Takayanagi R. Nuclear compartmentalization of N-CoR and its interactions with steroid receptors. Mol Cell Biol. 2006;26:6633-55.
52. Prescott J, Coetzee GA. Molecular chaperones throughout the life cycle of the androgen receptor. Cancer Lett. 2006;231:12-9.
53. Kaarbo M, Klokk TI, Saatcioglu F. Androgen signaling and its interactions with other signaling pathways in prostate cancer. Bioessays. 2007;29:1227-38.
54. Lin HK, Wang L, Hu YC, Altuwaijri S, Chang C. Phosphorylation-dependent ubiquitylation and degradation of androgen receptor by Akt require Mdm2 E3 ligase. Embo J. 2002;21:4037-48.
55. Gregory CW, Johnson RT, Jr., Presnell SC, Mohler JL, French FS. Androgen receptor regulation of G1 cyclin and cyclin-dependent kinase function in the CWR22 human prostate cancer xenograft. J Androl. 2001;22:537-48.
56. Ronnett BM, Carmichael MJ, Carter HB, Epstein JI. Does high grade prostatic intraepithelial neoplasia result in elevated serum prostate specific antigen levels? J Urol. 1993;150:386-9.
57. Leland W.K. Chung WBI, Jonathan W. Simons. Prostate Cancer- Biology, Genetics, and the New Therapeutics: Humana Press Inc.; 2007.
58. Chi KN, Bjartell A, Dearnaley D, Saad F, Schroder FH, Sternberg C, et al. Castration-resistant prostate cancer: from new pathophysiology to new treatment targets. Eur Urol. 2009;56:594-605.
59. Amaral TM, Macedo D, Fernandes I, Costa L. Castration-resistant prostate cancer: mechanisms, targets, and treatment. Prostate Cancer. 2012;2012:327253.
60. Pezaro CJ, Mukherji D, De Bono JS. Abiraterone acetate: redefining hormone treatment for advanced prostate cancer. Drug Discov Today. 2012;17:221-6.
61. Omlin A, de Bono JS. Therapeutic options for advanced prostate cancer: 2011 update. Curr Urol Rep. 2012;13:170-8.
62. Richards J, Lim AC, Hay CW, Taylor AE, Wingate A, Nowakowska K, et al. Interactions of abiraterone, eplerenone, and prednisolone with wild-type and mutant androgen receptor: a rationale for increasing abiraterone exposure or combining with MDV3100. Cancer Res. 2012;72:2176-82.
63. Visakorpi T, Hyytinen E, Koivisto P, Tanner M, Keinanen R, Palmberg C, et al. In vivo amplification of the androgen receptor gene and progression of human prostate cancer. Nat Genet. 1995;9:401-6.
64. Dehm SM, Schmidt LJ, Heemers HV, Vessella RL, Tindall DJ. Splicing of a novel androgen receptor exon generates a constitutively active androgen receptor that mediates prostate cancer therapy resistance. Cancer Res. 2008;68:5469-77.
65. Schafer SC, Pfnur M, Yerly S, Fandel TM, Jichlinski P, Lehr HA. Cryopreservation of prostate cancer tissue during routine processing of fresh unfixed prostatectomy specimen: demonstration and validation of a new technique. Prostate. 2009;69:191-7.
66. Coombs NJ, Gough AC, Primrose JN. Optimisation of DNA and RNA extraction from archival formalin-fixed tissue. Nucleic Acids Res. 1999;27:e12.
67. Desciak EB, Maloney ME. Artifacts in frozen section preparation. Dermatol Surg. 2000;26:500-4.

68. Shi SR, Cote RJ, Wu L, Liu C, Datar R, Shi Y, et al. DNA extraction from archival formalin-fixed, paraffin-embedded tissue sections based on the antigen retrieval principle: heating under the influence of pH. J Histochem Cytochem. 2002;50:1005-11.
69. Beltran H, Yelensky R, Frampton GM, Park K, Downing SR, Macdonald TY, et al. Targeted Next-generation Sequencing of Advanced Prostate Cancer Identifies Potential Therapeutic Targets and Disease Heterogeneity. Eur Urol. 2012.
70. Wisniewski JR, Dus K, Mann M. Proteomic workflow for analysis of archival formalin fixed and paraffin embedded clinical samples to a depth of 10,000 proteins. Proteomics Clin Appl. 2012.
71. Olert J, Wiedorn KH, Goldmann T, Kuhl H, Mehraein Y, Scherthan H, et al. HOPE fixation: a novel fixing method and paraffin-embedding technique for human soft tissues. Pathol Res Pract. 2001;197:823-6.
72. Goldmann T, Dromann D, Marzouki M, Schimmel U, Debel K, Branscheid D, et al. Tissue microarrays from HOPE-fixed specimens allow for enhanced high throughput molecular analyses in paraffin-embedded material. Pathol Res Pract. 2005;201:599-602.
73. Wiedorn KH, Olert J, Stacy RA, Goldmann T, Kuhl H, Matthus J, et al. HOPE--a new fixing technique enables preservation and extraction of high molecular weight DNA and RNA of > 20 kb from paraffin-embedded tissues. Hepes-Glutamic acid buffer mediated Organic solvent Protection Effect. Pathol Res Pract. 2002;198:735-40.
74. Zhou X, Ren L, Meng Q, Li Y, Yu Y, Yu J. The next-generation sequencing technology and application. Protein Cell. 2010;1:520-36.
75. Shendure J, Ji H. Next-generation DNA sequencing. Nat Biotechnol. 2008;26:1135-45.
76. Chaw YF, Crane LE, Lange P, Shapiro R. Isolation and identification of cross-links from formaldehyde-treated nucleic acids. Biochemistry. 1980;19:5525-31.
77. Gullapalli RR, Desai KV, Santana-Santos L, Kant JA, Becich MJ. Next generation sequencing in clinical medicine: Challenges and lessons for pathology and biomedical informatics. J Pathol Inform. 2012;3:40.
78. Choi M, Scholl UI, Ji W, Liu T, Tikhonova IR, Zumbo P, et al. Genetic diagnosis by whole exome capture and massively parallel DNA sequencing. Proc Natl Acad Sci U S A. 2009;106:19096-101.
79. Ng SB, Turner EH, Robertson PD, Flygare SD, Bigham AW, Lee C, et al. Targeted capture and massively parallel sequencing of 12 human exomes. Nature. 2009;461:272-6.
80. Hudson TJ, Anderson W, Artez A, Barker AD, Bell C, Bernabe RR, et al. International network of cancer genome projects. Nature. 2010;464:993-8.
81. The Cancer Genome Atlas.
82. Friedlander TW, Roy R, Tomlins SA, Ngo VT, Kobayashi Y, Azameera A, et al. Common structural and epigenetic changes in the genome of castration-resistant prostate cancer. Cancer Res. 2012;72:616-25.
83. Berger MF, Lawrence MS, Demichelis F, Drier Y, Cibulskis K, Sivachenko AY, et al. The genomic complexity of primary human prostate cancer. Nature. 2011;470:214-20.

84. Kumar A, White TA, MacKenzie AP, Clegg N, Lee C, Dumpit RF, et al. Exome sequencing identifies a spectrum of mutation frequencies in advanced and lethal prostate cancers. Proc Natl Acad Sci U S A. 2011;108:17087-92.
85. Grasso CS, Wu YM, Robinson DR, Cao X, Dhanasekaran SM, Khan AP, et al. The mutational landscape of lethal castration-resistant prostate cancer. Nature. 2012.
86. Barbieri CE, Baca SC, Lawrence MS, Demichelis F, Blattner M, Theurillat JP, et al. Exome sequencing identifies recurrent SPOP, FOXA1 and MED12 mutations in prostate cancer. Nat Genet. 2012;44:685-9.
87. National Institute of Health NHGRI. "Talking Glossary of Genetic Terms".
88. Braun M, Menon R, Nikolov P, Kirsten R, Petersen K, Schilling D, et al. The HOPE fixation technique--a promising alternative to common prostate cancer biobanking approaches. BMC Cancer. 2011;11:511.
89. Kristiansen G, Fritzsche FR, Wassermann K, Jager C, Tolls A, Lein M, et al. GOLPH2 protein expression as a novel tissue biomarker for prostate cancer: implications for tissue-based diagnostics. Br J Cancer. 2008;99:939-48.
90. Lin J, Yang H, Kelly WK. Prostate cancer biomarker: a key field to explore. Asian J Androl. 2013.
91. Ewing B, Hillier L, Wendl MC, Green P. Base-calling of automated sequencer traces using phred. I. Accuracy assessment. Genome Res. 1998;8:175-85.
92. Ewing B, Green P. Base-calling of automated sequencer traces using phred. II. Error probabilities. Genome Res. 1998;8:186-94.
93. Menon R, Deng M, Boehm D, Braun M, Fend F, Biskup S, et al. Exome Enrichment and SOLiD Sequencing of Formalin Fixed Paraffin Embedded (FFPE) Prostate Cancer Tissue. Int J Mol Sci. 2012;13:8933-42.
94. Scheble VJ, Scharf G, Braun M, Ruiz C, Sturm S, Petersen K, et al. ERG rearrangement in local recurrences compared to distant metastases of castration-resistant prostate cancer. Virchows Arch. 2012.
95. Bubendorf L, Kononen J, Koivisto P, Schraml P, Moch H, Gasser TC, et al. Survey of gene amplifications during prostate cancer progression by high-throughout fluorescence in situ hybridization on tissue microarrays. Cancer Res. 1999;59:803-6.
96. Troyer D. Biorepository standards and protocols for collecting, processing, and storing human tissues. Methods Mol Biol. 2008;441:193-220.
97. Riegman PHJ, Dinjens WNM, Oosterhuis JW. Biobanking for interdisciplinary clinical research. Pathobiology. 2007;74:239-44.
98. Oosterhuis JW, Coebergh JW, van Veen EB. Tumour banks: well-guarded treasures in the interest of patients. Nat Rev Cancer. 2003;3:73-7.
99. Knox K, Kerr DJ. Establishing a national tissue bank for surgically harvested cancer tissue. Brit J Surg. 2004;91:134-6.
100. Hewitt SM, Lewis FA, Cao Y, Conrad RC, Cronin M, Danenberg KD, et al. Tissue handling and specimen preparation in surgical pathology: issues concerning the recovery of nucleic acids from formalin-fixed, paraffin-embedded tissue. Arch Pathol Lab Med. 2008;132:1929-35.
101. Ivarsson M, Carlson J. Extraction, quantitation, and evaluation of function DNA from various sample types. Methods Mol Biol. 2011;675:261-77.
102. Huijsmans CJ, Damen J, van der Linden JC, Savelkoul PH, Hermans MH. Comparative analysis of four methods to extract DNA from paraffin-embedded

tissues: effect on downstream molecular applications. BMC Res Notes. 2010;3:239.
103. Huang WY, Sheehy TM, Moore LE, Hsing AW, Purdue MP. Simultaneous recovery of DNA and RNA from formalin-fixed paraffin-embedded tissue and application in epidemiologic studies. Cancer Epidemiol Biomarkers Prev. 2010;19:973-7.
104. Sen Gupta R, Hillemann D, Kubica T, Zissel G, Muller-Quernheim J, Galle J, et al. HOPE-fixation enables improved PCR-based detection and differentiation of Mycobacterium tuberculosis complex in paraffin-embedded tissues. Pathol Res Pract. 2003;199:619-23.
105. Wiedorn KH OJ, Stacy R, Goldmann T, Kuhl H, Matthus J, Vollmer E, Bosse A. Preservation of high molecular weight nucleic acids by application of the novel HOPE fixative. Pathol Res Pract. 2002;198:735-40.
106. Arzt L, Kothmaier H, Quehenberger F, Halbwedl I, Wagner K, Maierhofer T, et al. Evaluation of formalin-free tissue fixation for RNA and microRNA studies. Exp Mol Pathol. 2011;91:490-5.
107. Uhlig U, Uhlig S, Branscheid D, Zabel P, Vollmer E, Goldmann T. HOPE technique enables Western blot analysis from paraffin-embedded tissues. Pathol Res Pract. 2004;200:469-72.
108. Meyerson M, Gabriel S, Getz G. Advances in understanding cancer genomes through second-generation sequencing. Nat Rev Genet. 2010;11:685-96.
109. Schweiger MR, Kerick M, Timmermann B, Albrecht MW, Borodina T, Parkhomchuk D, et al. Genome-wide massively parallel sequencing of formaldehyde fixed-paraffin embedded (FFPE) tumor tissues for copy-number- and mutation-analysis. PLoS One. 2009;4:e5548.
110. Kerick M, Isau M, Timmermann B, Sultmann H, Herwig R, Krobitsch S, et al. Targeted high throughput sequencing in clinical cancer settings: formaldehyde fixed-paraffin embedded (FFPE) tumor tissues, input amount and tumor heterogeneity. BMC Med Genomics. 2011;4:68.
111. Beroukhim R, Mermel CH, Porter D, Wei G, Raychaudhuri S, Donovan J, et al. The landscape of somatic copy-number alteration across human cancers. Nature. 2010;463:899-905.
112. Jenkins RB, Qian J, Lieber MM, Bostwick DG. Detection of c-myc oncogene amplification and chromosomal anomalies in metastatic prostatic carcinoma by fluorescence in situ hybridization. Cancer Res. 1997;57:524-31.
113. Neal CL, Yu D. 14-3-3zeta as a prognostic marker and therapeutic target for cancer. Expert Opin Ther Targets. 2010;14:1343-54.
114. Macha MA, Matta A, Chauhan S, Siu KM, Ralhan R. 14-3-3 zeta is a molecular target in guggulsterone induced apoptosis in head and neck cancer cells. BMC Cancer. 2010;10:655.
115. Neal CL, Yao J, Yang W, Zhou X, Nguyen NT, Lu J, et al. 14-3-3zeta overexpression defines high risk for breast cancer recurrence and promotes cancer cell survival. Cancer Res. 2009;69:3425-32.
116. Lin M, Morrison CD, Jones S, Mohamed N, Bacher J, Plass C. Copy number gain and oncogenic activity of YWHAZ/14-3-3zeta in head and neck squamous cell carcinoma. Int J Cancer. 2009;125:603-11.

117. Li Y, Zou L, Li Q, Haibe-Kains B, Tian R, Desmedt C, et al. Amplification of LAPTM4B and YWHAZ contributes to chemotherapy resistance and recurrence of breast cancer. Nat Med. 2010;16:214-8.
118. Jackson AL, Linsley PS. Recognizing and avoiding siRNA off-target effects for target identification and therapeutic application. Nat Rev Drug Discov. 2010;9:57-67.
119. Murata T, Takayama K, Urano T, Fujimura T, Ashikari D, Obinata D, et al. 14-3-3zeta, a novel androgen-responsive gene, is upregulated in prostate cancer and promotes prostate cancer cell proliferation and survival. Clin Cancer Res. 2012;18:5617-27.
120. Waltering KK, Urbanucci A, Visakorpi T. Androgen receptor (AR) aberrations in castration-resistant prostate cancer. Mol Cell Endocrinol. 2012;360:38-43.
121. Powell DW, Rane MJ, Chen Q, Singh S, McLeish KR. Identification of 14-3-3zeta as a protein kinase B/Akt substrate. J Biol Chem. 2002;277:21639-42.
122. Tian Q, Feetham MC, Tao WA, He XC, Li L, Aebersold R, et al. Proteomic analysis identifies that 14-3-3zeta interacts with beta-catenin and facilitates its activation by Akt. Proc Natl Acad Sci U S A. 2004;101:15370-5.
123. Min S, Liang X, Zhang M, Zhang Y, Mei S, Liu J, et al. Multiple Tumor-Associated MicroRNAs Modulate the Survival and Longevity of Dendritic Cells by Targeting YWHAZ and Bcl2 Signaling Pathways. J Immunol. 2013;190:2437-46.
124. Park JH, Lee BL, Yoon J, Kim J, Kim MA, Yang HK, et al. Focal adhesion kinase (FAK) gene amplification and its clinical implications in gastric cancer. Hum Pathol. 2010;41:1664-73.
125. Emmanuel C, Gava N, Kennedy C, Balleine RL, Sharma R, Wain G, et al. Comparison of expression profiles in ovarian epithelium in vivo and ovarian cancer identifies novel candidate genes involved in disease pathogenesis. PLoS One. 2011;6:e17617.
126. Luo M, Guan JL. Focal adhesion kinase: a prominent determinant in breast cancer initiation, progression and metastasis. Cancer Lett. 2010;289:127-39.
127. Halder J, Lin YG, Merritt WM, Spannuth WA, Nick AM, Honda T, et al. Therapeutic efficacy of a novel focal adhesion kinase inhibitor TAE226 in ovarian carcinoma. Cancer Res. 2007;67:10976-83.
128. Recher C, Ysebaert L, Beyne-Rauzy O, Mansat-De Mas V, Ruidavets JB, Cariven P, et al. Expression of focal adhesion kinase in acute myeloid leukemia is associated with enhanced blast migration, increased cellularity, and poor prognosis. Cancer Res. 2004;64:3191-7.
129. Aronsohn MS, Brown HM, Hauptman G, Kornberg LJ. Expression of focal adhesion kinase and phosphorylated focal adhesion kinase in squamous cell carcinoma of the larynx. Laryngoscope. 2003;113:1944-8.
130. Toutant M, Costa A, Studler JM, Kadare G, Carnaud M, Girault JA. Alternative splicing controls the mechanisms of FAK autophosphorylation. Mol Cell Biol. 2002;22:7731-43.
131. Liu TJ, LaFortune T, Honda T, Ohmori O, Hatakeyama S, Meyer T, et al. Inhibition of both focal adhesion kinase and insulin-like growth factor-I receptor kinase suppresses glioma proliferation in vitro and in vivo. Mol Cancer Ther. 2007;6:1357-67.

132. Kurio N, Shimo T, Fukazawa T, Takaoka M, Okui T, Hassan NM, et al. Anti-tumor effect in human breast cancer by TAE226, a dual inhibitor for FAK and IGF-IR in vitro and in vivo. Exp Cell Res. 2011;317:1134-46.
133. Sood AK, Coffin JE, Schneider GB, Fletcher MS, DeYoung BR, Gruman LM, et al. Biological significance of focal adhesion kinase in ovarian cancer: role in migration and invasion. Am J Pathol. 2004;165:1087-95.
134. Parsons JT. Focal adhesion kinase: the first ten years. J Cell Sci. 2003;116:1409-16.
135. Shi Q, Hjelmeland AB, Keir ST, Song L, Wickman S, Jackson D, et al. A novel low-molecular weight inhibitor of focal adhesion kinase, TAE226, inhibits glioma growth. Mol Carcinog. 2007;46:488-96.

Appendix I

List of Amplfied Genes

Chromsome 1

KIFAP3	GAS5	NCF2	IVNS1ABP	TNNT2
GORAB	ZBTB37	RGL1	RGS1	PHLDA3
PPPRX1	RC3H1	GLT25D2	TROV2	CSRP1
FMO3	GPR52	TSEN15	GLRX2	PTPN7
BAT2D1	CACYBP	STX6	KCNT2	PTPN7
METTL13	MRPS14	MR1	CFH	KLHL12
DNM3	TNN	QSOX1	CFHR3	PPF1A4
PIGC	TNR	XPR1 (?)	ASPM	CHI3L1
FASLG	RFWD2	CACNA1E	CRB1	ZC3H11A
TNFSF4	PAPPA2	DHX9 (?)	LHX9	SYT2
SLC9A11	ASTN1	SMG7	PTPRC	KDM5B
KLHL20	RASAL2	RGS (?)	NR5A2	ADORA1
FMO1	ANGPTL1	NPL	KIF14	CHIT1
XTP2	ABL2	GLUL	PKP1	PRELP
MYOC	SOAT1	SMG7	HNTN1	ATP2B4
VAMP4	nphs2	EDEM3	LAD1	ETNK2
SNORD79	TDRD5	TRP	NAV1	NFASC
RABGAP1L	CEP350	PDC	RNPEP	RBBP5
FASLG	LAMC1	RFN2	ELF3	DSTYK
CENPL	NMNAT2	PRG4	TMEM9	PVRL4
TMCC2	CD46	VASH2	CD1E	NIT1
KLHDC8A	CD55	PROX1	CD1C	DEDD
PCTK3	DAF	PTPN14	PYHIN1	USP21
LAX1	CR2	KCNK2	IFI16	PPOX
SOX13	CAMK1G	KCTD3	CADM3	SDHC
MDM4	LAMB3	ESRRG	DARC	FCRLA
LRRN2	IRF6	GPATCH2	CRP	RGS4
NFASC	SYT14	SPATA17	DUSP23	NUF2
TMCC2	HHAT	MEF2D	NESG1	PBX1
LEMD1	RCOR3	IQGAP3	IGSF8	LMX1A
ELK4	TRAF5	APOA1BP	SLAMF9	TMCO1
SRGAP2	RD3	AIBP	PEX19	MGST3
RASSF5	NEK2	GPATCH4	NCSTN	TADA1
DYRK3	ANGEL2	HAPLN2	KCNJ9	POU2F1
IL19	RPS6KC1	BCAN	COPA	RCSD
FAIM3	DTL	HDGF	CD84	DCAFNME7
PIGR	NENF	SH2D2A	LY9	BLZF1
FCAMR	ATF3	NTRK1	F119	SELP
PFKFB2	NSL1	FCRL5	TSTD1	SELL
C4BPB	TATDN3	KIRREL	F11R	TOMM40L
NR1I3	FCGR3A	DUSP12		

Chromosome 3

IGSF11	MBD4	GYG1	PLXND1	TNIK
UPK1B	TMCC1	HLTF	ACRP1	PLD1
B4GALT4	ATP2C1	HPS3	EIF2A	GHSR
MDSRP	NPHP3	CP	CLRN1	NCEH1
CD80	ASTE1	PFN2	MED12L	ECT2
ADPRH	NEK11	RNF13	IGSF10	NLGN1
PLA1A	CPNE4	IFT122	MBNL1	TBL1XR1
POPDC2	CCRL1	CCDC14	SGEF	KCNMB2
AAT1	UBA5	HIFOO	DHX36	ZMAT3
NR1I2	CDV3	PLXND1	MME	MFN1
GSK3B	TF	ACRP1	PLCH1	ACTL6A
FSTL1	RAB6A	EIF2A	GMPS	MRPL47
HGD	AMOTL2	CLRN1	KCNAB1	NDUFB5
POLQ	CEP63	MED12L	SSR3	USP13
HCLS1	KY	IGSF10	LEKR1	PEX5L
GOLB1	EPHB1	MBNL1	CCNL1	FXR1
IQCB1	PCCB	SGEF	SHOX2	VWA5B2
EAF2	MSL2	DHX36	RSRC1	ALG3
ILDR1	STAG2	MME	MFSD1	ECE2
CD86	TMEN22	PLCH1	SCHIP1	TTC14
CASR	CLDN18	GMPS	VEPH1	FXR1
KPNA1	DZIP1L	KCNAB1	MFL1	SOX2
PARP9	ARMC8	SSR3	IQCJ	ATP11B
SEMA5B	MRAS	LEKR1	PPM1L	MCCC1
PDIA5	CEP70	CCNL1	SMC4	MCF2L2
ADCY5	PRR23A	SHOX2	NMD3	B3GNT5
MYLK	COPB2	RSRC1	ZBBX	KLHL6
KALRN	RBP1	MFSD1	SERPINI2	ABCC5
UMPS	BDR1	SCHIP1	WDR49	HTR3D
SLC41A3	FAIM	VEPH1	GOLIM4	AP2M1
SNX4	SPSB4	GYG1	MECOM	THPO
ROPN1B	ACPL2	HLTF	EVI1	TRA2B
MCM2	ZBTB38	HPS3	MYNN	VPS8
ABTB1	RASA2	CP	SAMD7	PARL
ACAD9	RNF7	PFN2	CLDN11	LIPH
TRPA1	ATR	RNF13	SLC2A2	ETB5
ZDXC	PLOD2	IFT122	FNDC3B	DGKG
GATA2	PLSCR4	CCDC14	TNFSF10	CRYGS
RAB7A	ZIC4	HIFOO	PHC3	AHSG
ISY1	AGTR1	PLXND1	SKIL	FETUB
RFC4	PIGX	RNF13	SLC2A2	ETB5
MASP1	SENP5	TEMEM44	TNK2	LRCH3
BCL6	LPP	DLG1	NCBP2	EIF4G1
TP63	IL1RAP	IQCG	MF12	CLCN2
OPA1	FGF12	APOD	BDH1	CHRD
MAP3K13	ZDHHC19	RAD54B	ST6GAL1	LMLN
IGF2BP2	PCYT1A	UBXN7	TBCCD1	

Chromosome 8

RLBP1L1	IMPA1	UQCRB	EIF3H	FAM49B
ASPH	AZFAND1	PTDSS1	MED30	HHLA1
YTHDF3	SNX16	SDC2	SAMD12	SLA
MYBL1	REX01L1	MATN2	COL14A1	MYC
COPS5	ESRP1	POP1	ATAD2	ASAP1
CSPP1	E2F5	RGS22	WDYHV1	ADCY8
CPA6	MMP16	OSR2	FBOX32	TG
SULF1	RIPK2	GRHL2	ANXA13	SLA
TRAM1	OSGIN2	NCALD	TATDN1	ZFAT
LACTB2	SLC26A7	RRM2B	ENPP2	TRAPPC9
XKR9	PDP1	UBR5	DERL1	EIF2C2
STAU2	CDH17	BAALC	WDR67	PTK2
UBE2W	NBN	RIMS2	ZHX1	ESRP1
TCEB1	DECR1	DPYS	MTSS1	PABPC1
GDAP1	RUNX1T1	ANGPT1	MTBP	YWHAZ
ZFHX4	INTS8	GOLSYN	TRPS1	KLF10
PKIA	VPS13B	OXR1	MYC	AZIN1
IL7	FBX043	RSPO2	TMEM71	TATDN1
STMN2	SNX31	NUDCD1	PHF20L1	NDUFB9
HEY1	PABPC1	ENY2	WISP1	NSMCE2
MRPS28	YWHAZ	KCNV1	NDRG1	KHDRBS3
JPH1	NCALD	TRPS1	ST3GAL1	FAM49B
PI15	GEM	CSMD3	KHDRBS3	HHLA1
SLA	ASAP1	TG	ZFAT	EIF2C2
MYC	ADCY8	SLA	TRAPPC9	PTK2
ESRP1	KLF10	NDUFB9	KHDRBS3	HHLA1
PABPC1	AZIN1	NSMCE2	KHDRBS3	TATDN1
YWHAZ	TATDN1			

Chromosome 11

LPXN	WDR74	CAPN1	MRPL21	CTTN
ZFP91	SNHG1	MEN1	LRP5	DHCR7
GLYAT	SNORD22	EHD1	TPCN2	IL18BP
GATFC	SLC3A2	TM7SF2	PFFIA1	NUMA1
FAM111A	NXF1	SYVN1	SHANK2	LRTOMT
DTX4	UST6	POLA2	ORAOV1	FOLR1
PATL1	HRASLS5	DPF2	MYEOV	PDE2A
STX3	LGALS12	FRMD8	ANO1	CLPB
GIF	RTN3	LTBP3	CTTN	ARAP1
MS4A3	NUDT22	RELA	DHCR7	P2RY6
CD6	DNAJC4	CFL1	IL18BP	PLEKHB1
CYBASC3	GPR137	FIBP	NUMA1	PAAF1
DDB1	KCNK4	CTSW	LRTOMT	CHRDL2
ZP1	ESRRA	KLC2	FOLR1	GDPD5
VWCE	PRDX5	RIN1	PDE2A	NEU3
DAK	MARK2	PELI3	CLPB	PPME1
SYT7	O2UB1	DPP3	ARAP1	UVRAG
FADS1	TRPT1	BBS1	P2RY6	APHC
VMD2	VEGFB	PC	PLEKHB1	INTS4
BEST1	FKBP2	POLD4	PAAF1	MOGAT2
ASRGL1	PLCB3	PPP1CA	CHRDL2	CAPN5
EEF1G	BAD	CORO1B	MRPL21	MYO7A
MTA2	PYGM	DOC1R	LRP5 (?)	APHC
EML3	FAU	CABP2	TPCN2	LRRC32
GANAB	SF1	GSTP1	PFFIA1	WNT1
UBXN1	STIP1	NDUFV1	SHANK2	CAPN5
BSCL2	ATL3	TCIRG1	ORAOV1	POLD3
TAF6L	NRXN2	CHKA	MYEOV	OVOL1
STX5	ZFPL1	SAPAS3	ANO1	SNX32
EFEMP2	SART1	MRPL11	ATG18L2	RPS6KA4
CFL1	EIF1AD	TMEM134	FCHSD2	RASGRP2
FIBP	BANF1	SUV420H1	SNHG1	SLC3A2
FOSL1	SF3B2	STARD10		

Chromosome 16

HN1L	IL32	PARN	M6PR	TNRC6A
NME3	NAT15	BFAR	NOMO2	SLC5A11
EME2	TRAP1	DNASE1L2	RPS15A	JMJD5
SPSB3	CREBBP	RNPS1	SMG1	IL4R
NUBP2	ADCY9	ABCA3	TMC7	IL21R
IGFALS	NMRAL1	TBC1D24	SYT17	GSG1L
HAGH	HMOX2	PGP	TMC5	XPO6
FAHD1	MGRN1	E4F1	IQCK	EIF3CL
RPS2	ANKS3	DCI	GPRC5B	CLN3
TBL3	GLYR1	AMDHD2	ACSM2A	SULT1A1
NOXO1	UBN1	PDPK1	THUMPD1	ATXN2L
GFER	NAGPA	PRSS27	ERI2	SH2B1
PKD1	A2BP1	HCFC1R1	LYRM1	ATP2AI
MLST8	ABAT	CCDC64B	TMEM159	RABEP2
CCNF	PMM2	ZSCAN10	ZP2	CD19
PDPK1	USP7	ZNF434	CRYM	CLDN9
SRRM2	GRIN2A	UNQ2771	IMAA	THOC6
PRSS33	NUBP1	CLUAP1	IGSF6	SNX29
FLYCH2	CIITA	PDXDC1	OTOA	MKL2
KREMEN2	LITAF	NTAN1	NPIPL3	NDE1
PAQR4	RSL1D1	RRN3	VWA3A	ABCC1
PKMYT1	GSPT1	NPIP	EEF2K	PRKCB
RBBP6				

Chromosome 17

MRPL27	VEZF1	CSH2	ACOX1	PCYT2
EME1	MKS1	CYB561	SRP68	SIRT7
ACSF2	LPO	KCNH6	LGICZ	MAFG
CHAD	BZRAP1	MAP3K3	EXOC7	HEXDC
RSAD1	RNF43	LIMD2	SPHK1	NARF
EPN3	Sep-04	STRADA	PHBDF2	ICAM2
SPATA20	TEX14	DDX42	CYGC	DDX5
CACNA1G	RAD51C	PSMC5	PRCD	TEX2
ABCC3	TRIM37	CSHL1	JMJD6	SMURF2
TOB1	PRR11	GNA13	MFSD11	ARMC7
SPAG9	DHX40	RGS9	TMC6	HN1
MBTD1	TMEM49	AXIN2	AFMID	SUMO2
CA10	HEATR6	HELZ	BIRC5	GGA3
KIF2B	CLTC	BPTF	PGS1	MIF4GD
TOM1L1	TUBD1	WIPI1	DNEL2	TSEN54
COX11	RNFT1	AMZ2	USP36	SEC14L1
STXBP4	PPM1D	KCNJ16	CANT1	ARHGDIA
HLF	BCAS3	KIF19	CARD14	ANAPC11
PCTP	TBX4	CD300A	GAA	PYCR1
NOG	BRIP1	FDXR	SGSH	STRA13
DGKE	INTS2	SLC16A5	ACTG1	GPS1
TRIM25	TLK2	RAB37	AZI1	DUS1L
AKAP1	ACE	LLGL2	GCGR	CSNK1D
CUEDC1	DCP1	ITGB4	P4HB	

Chromosome X

NLGN4X	PIR	ZFX	PCTK1	CCNB3
HDHD1A	BMX	PDK3	ZNF41	FAM156A
STS	ASB11	PCYT1B	ARAF	RIBC1
PINPL4	ACE2	POLA1	TIMP1	PHF8
FAM9B	CTPS2	MAGEB6	ELK1	TRO
SHROOM2	RBBP7	GK	UXT	KLF8 (?)
MID1	REPS2	DMD	ZNF182	USP51
ARHGAP6	NHS	BCOR	SSX4B	SPIN3
AMELX	SCML1	CYBB	FTSJ1	ASB12
WWC3	RAI2	SYTL5	PORCN	LAS1L
TBL1X	BEND2	SRPX	DATL1	VSIG4
HCCS	SCML2	RPGR	OATL1	AR
PRPS2	CDKL5	MID1IP1	WDR13	OPHN1
MSL3	PPEF1	DDX3X	SUV39H1 (?)	STARD8
EGFL6	PHKA2	CASK	PQBP1	EDA2R
TCEANC	GPR64	NYX	OTUD5	VSIG4
TRAPPC2	PDHA1	MAOB	EBP	WDR13
GMP6B	YY2	KDM6A	HDAC6 (?)	TIMM17B
GLRA2	CNKSR2	ZFN673	MAGIX	PQBP1
FANCB	MBTPS2	SLC9A7	CCDC22	WDR45
MOSPD2	SMS	RGN	FOXP3	RBM10
PIGA	PHEX	UBA1	JM4	SAT1
OFD1	ACOT9	PHF16	AKAP4	ASB9

Appendix II

List of Deleted Genes

Chromosome 8

LONRF1	MTMR7	NPM2	NKX3-1	ESCO2
DLC1	MTUS1	FGF17	ADAM28	PBK
SGCZ	FGF20	EPB49	GNRH1	ELP3
DM004805	ZDHHC2	FAM160B2	KCTD9	RC74
MSR1	VPS37A	NUDT18	CDCA2	INTS9
MTUS1	MTMR7	REEP4	NEFM	DUSP4
SH2D4A	SLC7A2	LG13	DOCK5	RBPMS
HT-15	PDGFRL	SFTPC	GNRH1	GSR
NEFM	FGL1	BMP1	BNIP3L	UBXN8
EBF2	PCM1	PHYHIP	DPYSL2	PURG
RB3	ASAH1	POLR3D	PTK2B	WRN
FZD3	CSGALNACT1	PIWIL2	ADRA1A	NRG1
THEM66	PSD3	SLC39A14	EPHX2	FUT10
WRN	SH2D4A	PPP3CC	SCARA2	BIN3
NAT1	INTS10	SORBS3	CCDC25	EGR3
STMN4	SLC18A1	PDLIM2	FBXO16	RHOBTB2
TUSC3	GFRA2	CHMP7	PNMA2	CLU
HRF2	DOK2	LOXL2	STMN4	ENTPD4
CNOT7	XPO7			

Chromosome 11

ME3	MRE11A	CASP4	DDX10	DRD2
PRSS23	SESN3	PDGFD	ZC3H12C	ZBTB16
FZD4 (?)	CEP57	CASP5	RDX	ZW10
CTSC	MTMR2	CASP1	BTG4	USP28
GRM5	CNTN5	GRIA4	LAZN	HTR3B
TYR	PGR	CWF19L2	PPP2R1B	RBM7
NOX4	PR	ABH8	ALG9	CADM1
NAALAD2	YAP1	ELMOD1	DIXDC1	BCO2
CHORDC1	DYNC2H1	GUCY1A2	PIH1D2	NCAM1
FAT3	DD1	RAB39	ALG9	TMPRSS5
CCDC67	CASP12	CUL5	DLAT	TTC12
TAFD1	CASP4	ACAT1	IL18	EXPH5
MED17	PDGFD	NPAT	PTS	CASP1
HEPHLI	CASP5	ATM	NCAM1	PANX1

Chromosome 16

CDH11	SLC12A4	HYDIN	NUDT7	SCL9A5
CDH5	DUS2L	AP1G1	MAF	PLEKHG4
TK2	ACD	CALB2	CENPN	RORBP70
CKLF	CENPT	DODH	ATMIN	NFATC3
CMTM1	EDC4	HP	PKD1L2	PMFBP1
CDH16	KCC1	RFWD3	BCDO	MMP2
CES2	CDH1	MLKL	CDH13	AMFR
TRADD	HAS3	WDR59	TAF1C	MT2A
HSF4	NFAT5	ZNRF1	ATP2C2	NLRC5
NOL3	DOX19B	BCAR1	COTL1	RSPRY1
ELMOS3	NQ01	CFDP1	USP10	CETP
FHHOD1	WWP2	KARS	IRF8	CPBE2
TPPP3	PDPR	CNTNAP4	TRADD	COQ9
RLTPR	FUK	MON1B	EXOCL3	DOK4
RANBP10	COG4	WWOX	LRRC29	GPR56
KIFC3	KLKBL4	NDRG4	CDH8	CDH1

Chromosome 17

XAF1	MPDU1	CHD3	PMP22	TOP3A
FBXO39	FXR2	RANGRF	CDRT1	SHMT1
TEKT1	TP53	NDEL1	ZSWIM7	SHBG
ALOX12E	CHD3	MYH10	NCOR1	WRAP53
BCL6B	RANGRF	WDR16	TTC19	DNAH2
ASGR2	NDEL1	USP43	MPRIP	CNTROB
DLG4	MYH10	GAS7	PEMT	DLG4
ACADVL	WDR16	MYH13	SREBF1	ACADVL
PHF23	USP43	MAP2K4	ATPAF2	PHF23
DULLARD	GAS7	SHISA6	DRG2	CLDN7
CLDN7	MYH13	MYOCD	FLII	EIF5A
EIF5A	MPDU1	RICH2	SMCR7	PLSCR3
NEURL4	FXR2	ELAC2	TOM1L2	DVL2
SENP3	TP53	COX10	LRRC48	GPS2
TNK1	FGF11	CHRNB1	POLR2A	TNFSF13
EIF4A1	ALOXE3			

Chromosome 18

NOL4	ZBTB7C	NEDD4L
DTNA	DYM	CCBE1
MAPRE2	RPL17	GRP
ZNF24	MYO5B	VPS4B
GALNT1	MBD1	PIGN
ELP2	CXXC1	CDH7
PIK3C3	MAPK4	TMX3
SETBP1	MRO	SOCS6
SLC14A1	DCC	CBLN2
RNF165	MBD2	NET01
LOXHD1	POLI	CTDP1
PIAS2	TCF4	NFATC1
HDHD2	NEDD4L	BRUNOL4
HDHD2	TXNL1	FHOD3
SMAD2	FECH	

Chromosome 19

GP1	SHKBP1	POU2F2	DMWD	HNRNPUL1
GRAMD1A	LTBP4	CEACAM1	KLC3	(E)GNL2
HPN	ATP5SL	FBL	ERCC2	CLPTM1
LSR	POU2F2	AKT2	HIF3A	SNRPD2
USF2	CEACAM1	PLD3	DAT3	SYMPK
DMKN	FBL	DEDD2	PRKD2	PSG11
ETV2	AKT2	ADCK4	STRN4	CLPTM1
SNX26	PLD3	TMEM91	DHX34	QPCTL
APLP1	DEDD2	ARGHEF1	MEIS3	RSHL1
ALKBH6	ADCK4	ERF	SAE1	FOSB
CAPNS1	TMEM91	PSG11	NAPA	RTN2
HCST	ARGHEF1	ETHE1	ALKBH6	EML2
RASGRP4	ERF	PLAUR	CAPNS1	RBM42
SIRT2	PSG11	GEMIN7	RASGRP4	KIRREL2
KFKBIB	ETHE1	FOSB	SARS2	DMPK
HKR1	PLAUR	RTN2	MRPS12	ATP5SL
SPRED3	SHKBP1	VASP	LTBP4	PAK4
HNRNPL	LTBP4	EML2	NUMBL	

Chromosome 22

TUBA8	AIFM3	CRKL	MAPK1	XBP1
USP18	LZTR1	BCR	TOP3B	EMID1
GGTP3	SEC14L2	GGT2	ZNF280B	EWSR1
PRODH	HP2XM	PI4KA	PRAME	GAS2L1
SLC25A1	SLC7A4	HIC2	MTMR3	AP1B1
CLTCL1	THAP7	UBE2L3	GATSL3	THOC5
GSC2	CRKL	PPIL2	PIK31P1	NF2
HIRA	BCR	YPEL1	CARD10	SMTN
UFD1	GGT2	PPM1F	SH3BP1	SF11
CLDN5	PI4KA	MAPK1	TRIPBP	YWHAH
TBX1	HIC2	TOP3B	PLA2G6	RFPL2
5SELPT	UBE2L3	ZNF280B	WBP2NL	BPIL2
GNB1L	PPIL2	PRAME	2D7P1	FBXO7
TRXR2A	YPEL1	MTMR3	POLDIP3	TOM1
COMT	PPM1F	GATSL3	A4GALT	MMC5
ARVCF	MAPK1	PIK31P1	ARFGAP3	RASD2
RANBP1	TOP3B	CARD10	PACSIN2	MB
ZDHHC8	ZNF280B	SH3BP1	MIOX	RBM9
DGCR8	PRAME	TRIPBP	LMF2	MYH9
TRMT2A	MTMR3	PLA2G6	NCAPH2	RABL2B
RTN4R	GATSL3	CRKL	SCO2	CHEK2
DGCR6L	PIK31P1	BCR	TYMP	YPEL1
RIMBP3	CARD10	GGT2	ODF3B	PPM1F
USP41	AIFM3	PI4KA	CPT1B	SLC7A4
ZHF74	LZTR1	HIC2	CHKB	THAP7
SCARF2	SEC14L2	UBE2L3	ARSA	MED15
KLHL22	HP2XM	PPIL2	SHANK3	PI4KA

13. List of Publications

1. Somatic copy number alterations by whole exome sequencing implicates *YWHAZ* and *PTK2* in castration resistant prostate cancer
   Menon R[*], Deng M[*], Rüenauver K[*], Kunze F, Boehm D, Vogel W, Scheble V, Fend F, Kristiansen G, Wernert N, Oberbeckmann N, Biskup S, Rubin M, Shaikhibrahim Z, Perner S
   Manuscript in preparation.

2. Exome Enrichment and SOLiD Sequencing of Formalin Fixed Paraffin Embedded (FFPE) Prostate Cancer Tissue.
   Menon R, Deng M, Boehm D, Braun M, Fend F, Boehm D, Biskup S, Perner S.
   Int J Mol Sci. 2012;13(7):8933-42. doi: 10.3390/ijms13078933. Epub 2012 Jul 17.

3. The HOPE fixation technique--a promising alternative to common prostate cancer biobanking approaches.
   Braun M*, **Menon R***, Nikolov P, Kirsten R, Petersen K, Schilling D, Schott C, Gündisch S, Fend F, Becker KF, Perner S.
   BMC Cancer. 2011 Dec 7;11:511. doi: 10.1186/1471-2407-11-511.

Abteilung für Prostatakarzinom-Forschung
Sigmund-Freud-Str. 25
53127 Bonn

E-mail: mroopika@gmail.com

Education

Doctoral student

Since August 2009 — Department of Prostate Cancer Research, Bonn, Germany

European Erasmus Mundus M.Sc. in Animal Breeding and Genetics

06/2007-07/2009 — Christian Albrechts Universität zu Kiel, Kiel, Germany

Agro Paris Tech, Paris, France

M.Sc. in Biotechnology

06/2005-05/2007 — Jain University, Bangalore, India

B.Sc. in Biotechnology

08/2002-05/2005 — Bangalore University, Bangalore, India

Research Experience

01/2009 – 07/2009 — INRA — Paris, France

Master's Thesis

- *Genetic Analysis of Immune Response in Experimental Lines of Chicken: Identification and validation of signature of selection.*

05/2006 – 05/2007 — Bangalore University — Bangalore, India

Master's Thesis

- *Homology Modeling of Enoyl-ACP Reductase Domain of Mycobacterium tuberculosis H37Rv and Docking of Herbal Ligands.*

05/2003 – 05/2005 — Seribiotech Research Lab — Bangalore, India

Bachelor's Thesis

- *Integration of Densonucleosis Virus Genome Fragments in Bombyx mori Genome: A PCR Analysis*.

Publications

1. The proto-oncogene ERG is a target of microRNA miR-145 in prostate cancer.
   Martin Hart, Sven Wach, Elke Nolte, Jaroslaw Szczyrba, **Roopika Menon**, Helge Taubert, Arndt Hartmann, Robert Stoehr, Wolf Wieland, Friedrich A. Grässer, Bernd Wullich.
   FEBS J. 2013;

2. Exome Enrichment and SOLiD Sequencing of Formalin Fixed Paraffin Embedded (FFPE) Prostate Cancer Tissue.
   Roopika Menon, Mario Deng, Diana Boehm, Martin Braun, Falko Fend, Detlef Boehm, Saskia Biskup, Sven Perner.
   Int J Mol Sci. 2012;13(7):8933-42.

3. Integrative genomic analyses of somatic mutations identifies key drivers of small cell lung cancer
   Martin Peifer, Lynnette Fernández-Cuesta, Martin L Sos, Julie George, Danila Seidel, Lawryn H Kasper, Dennis Plenker, Frauke Leenders, Ruping Sun, Thomas Zander, **Roopika Menon**, Mirjam Koker, Ilona Dahmen, Christian Müller, Vincenzo Di Cerbo, Hans-Ulrich Schildhaus, Janine Altmüller, Ingelore Baessmann, Christian Becker, Bram de Wilde, Jo Vandesompele, Diana Böhm, Sascha Ansén, Franziska Gabler, Ines Wilkening, Stefanie Heynck, Johannes M Heuckmann, Xin Lu, Kristian Cibulskis, Shantanu Banerji, Gad Getz, Kwon-Sik Park, Daniel Rauh, Christian Grütter ,Matthias Fischer, Laura Pasqualucci, Gavin Wright, Zoe Wainer, Prudence Russell, Iver Petersen, Yuan Chen, Erich Stoelben, Corinna Ludwig, Philipp Schnabel, Hans Hoffmann, Thomas Muley, Michael Brockmann, Walburga Engel-Riedel, Lucia A Muscarella, Vito M Fazio, Harry Groen, Wim Timens, Hannie Sietsma, Erik Thunnissen, Egbert Smit, Daniëlle AM Heideman, Peter JF Snijders, Federico Cappuzzo, Claudia Ligorio, Stefania Damiani, John Field[33], Steinar Solberg, Odd Terje Brustugun, Marius Lund-Iversen, Jörg Sänger, Joachim H Clement, Alex Soltermann, Holger Moch, Walter Weder**,** Benjamin Solomon, Jean-Charles Soria, Pierre Validire, Benjamin Besse, Elisabeth Brambilla, Christian Brambilla, Sylvie Lantuejoul, Philippe Lorimier, Peter M Schneider**,** Michael Hallek, William Pao, Matthew Meyerson, Julien Sage, Jay Shendure, Robert Schneider, Reinhard Büttner, Jürgen Wolf[3,4], Peter Nürnberg[10,17,54], Sven Perner[7], Lukas C Heukamp, Paul K Brindle, Stefan Haas, Roman K Thomas
   Nature Genetics 2012, Sep 2. doi: 10.1038/ng.2396.

4. Rationale for treatment of metastatic squamous cell carcinoma of the lung using FGFR Inhibitor
   Friederike Goeke, Alina Franzen, **Roopika Menon,** Diane Goltz, Robert Kirsten, Diana Boehm, Wenzel Vogel, Antonia

Goeke, Veit Scheble, Joerg Ellinger, Ulrich Gerigk, Falko Fend, Patrick Wagner, Andreas Schroeck, Sven Perner.
CHEST, Apr 12

5. Rearrangement of the ETS genes ETV-1, ETV-4, ETV-5 and ELK-1 is a clonal event during prostate cancer progression
Zaki Shaikhibrahim,, Martin Braun, Pavel Nikolov, Diana Boehm, Veit Scheble, **Roopika Menon**, Falko Fend, Glen Kristiansen, Sven Perner, Nicolas Wernert.
Human Pathology. 2012 Nov;43(11):1910-6.

6. The HOPE fixation technique - a promising alternative to common prostate cancer biobanking approaches**.**
Martin Braun*, **Roopika Menon***, Pavel Nikolov, Karen Petersen, David Schilling, Christina Schott, Falko Fend, Karl-Friedrich Becker, Sven Perner
BMC Cancer. 2011 Dec 7;11:511.
*Equally contributed

7. SOX2 amplification is a common event in squamous cell carcinomas of different organ sites.
Sebastian Maier, Theresia Wilbertz, Martin Braun, Veit Scheble, Markus Reischl, Ralf Mikut, **Roopika Menon**, Pavel Nikolov, Karen Petersen, Christine Beschorner, Holger Moch, Christoph Kakies, Chris Protzel, Jurgen Bauer, Alex Soltermann, Falko Fend, Annette Staebler, Claudia Lengerke, Sven Perner.
Human Pathology. 2011 Aug;42(8):1078-88

8. Relevance of cohort design for studying the frequency of ERG rearrangement in prostate cancer.
Martin Braun, Veit Scheble, **Roopika Menon**, Gregor Scharf, Theresia Wilbertz, Karen Petersen, David Schilling, Rainer Kuefer, Falko Fend, Glen Kristiansen, Marl Rubin, Sven Perner.
Histopathology, **2011** Jun;58(7):1028-1036

9. Frequency and Clinicopathologic Correlates of *KRAS* Amplification in Non-Small Cell Lung Carcinoma
Patrick L. Wagner, Ann-Cathrin Stiedl, Theresia Wilbertz, Karen Petersen, Veit Scheble, **Roopika Menon**, Markus Reischl, Ralf Mikut, Mark A. Rubin, Falko Fend, Holger Moch Alex Soltermann, Walter Weder, Nasser K. Altorki, Sven Perner
Lung Cancer. 2011 Oct;74(1):118-23. Epub 2011 Apr 8.

10. Frequent and focal FGFR1 amplification associates with therapeutically tractable FGFR1 dependency in squamous cell lung cancer.
Jonathan Weiss, Martin Sos, Danila Seidel, Martin Peifer,

Thomas Zander, Johannes Heuckmann, Roland Ullrich, **Roopika Menon**, Sebastian Maier, Alex Soltermann, Holger Moch, Patrick Wagener, Florian Fischer, Stefanie Heynck , Mirjam Koker, Jacob Schöttle, Frauke Leenders, Franziska Gabler, Ines Dabow, Silvia Querings, Lukas Heukamp, Hyatt Balke-Want, Sascha Ansén, Daniel Rauh, Ingelore Baessmann, Janine Altmüller, Zoe Wainer, Matthew Conron, Gavin Wright, Prudence Russell, Ben Solomon, Elizabeth Brambilla, Christian Brambilla, Philipe Lorimier, Steinar Sollberg, Odd Terje Brustugun, Walburga Engel-Riedel, Corinna Ludwig, Iver Petersen, Jorg Sänger, Joachim Clement, Harry Groen, Wim Timens, Hannie Sietsma, Erik Thunnissen, Egbert Smit, Danielle Heideman, Federico Cappuzzo, Claudia Ligorio, Stefania Damiani, Michael Hallek, Rameen Beroukhim , William Pao, Bert Klebl, Mathias Baumann, Reinhard Buettner, Karen Ernestus, Erich Stoelben, Jurgen Wolf , Peter Nürnberg, Sven Perner, Roman Thomas.
Sci Transl Med. 2010 Dec 15;2(62):62ra93.

11. ERG (v-ets erythroblastosis virus E26 oncogene like (avian))
Roopika Menon, Martin Braun, Sven Perner
Atlas Genet Cytogenet Oncol Haematol. November 2010

12. ERG rearrangement as a clonal expansion marker for prostate cancer.
Martin Braun, **Roopika Menon**, Pavel Nikolov, Sven Perner.
The Open Prostate Cancer Journal, 2010, Volume 3, 63-68.

Meeting Abstracts:

1. Somatic copy number alterations by whole exome sequencing reveals *YWHAZ* and *PTK2* as potential therapeutic targets in castration resistant prostate cancer
R. Menon, M. Deng, K. Ruenauver, F. Kunze, D. Boehm, W. Vogel, F. Schaeble, F. Fend, G. Kristiansen, N. Wernert, D. Beohm, S. Biskup, M. Rubin, Z. Shaikhibrahim, S. Perner.
Tumor Invasion and Metastasis
American Association of Cancer Research (AACR)
San Diego, USA 2013. Poster Presentation

2. Whole Exome Sequencing Identifies Potential Therapeutic Targets For Castration Resistant Prostate Cancer
R. Menon, M. Deng, D. Beohm, M. Braun, F. Fend, D. Boehm, S Biskup, S Perner
Advances in Prostate Cancer Research
American Association of Cancer Research (AACR)
Florida, USA 2012. Poster Presentation

3. Whole Exome Sequencing Identifies Potential Therapeutic Targets For Castration Resistant Prostate Cancer

R. Menon, M. Deng, D. Beohm, M. Braun, F. Fend,
D. Boehm, S Biskup, S Perner
Advances in Prostate Cancer Research
American Association of Cancer Research (AACR)
Florida, USA 2012. Poster Presentation

4. Somatic copy number alterations by whole exome sequencing reveals *YWHAZ* and *PTK2* as potential therapeutic targets in castration resistant prostate cancer
R. Menon, M. Deng, K. Ruenauver, F. Kunze, D. Boehm, W. Vogel, F. Schaeble, F. Fend, G. Kristiansen, N. Wernert, D. Beohm, S. Biskup, M. Rubin, Z. Shaikhibrahim, S. Perner.
European Congress for Pathology (ECP),
Prague, Czech Republic 2012. Platform presentation.

5. Whole Exome Sequencing Identifies Potential Therapeutic Targets For Castration Resistant Prostate Cancer
R. Menon, M. Deng, D. Beohm, M. Braun, F. Fend,
D. Boehm, S Biskup, S Perner
From Basic Research to Personalized Cancer Treatment
European Association of Cancer Research (EACR)
Barcelona, Spain 2012. Poster Presentation

6. Whole Exome Sequencing Identifies Potential Therapeutic Targets For Castration Resistant Prostate Cancer
R. Menon, M. Deng, D. Beohm, M. Braun, F. Fend,
D. Boehm, S Biskup, S Perner
Kongress der Deutschen Gesellschaft für Pathologie (DGP),
Berlin, Germany 2012. Platform presentation

7. Whole Exome Sequencing Identifies Potential Therapeutic Targets For Castration Resistant Prostate Cancer
R. Menon, S.Perner,
Bonner Forum Biomedizin (BFB)
Bonn, Germany 2012. Platform Presentation

8. Exome Sequencing of Hormone Refractory Prostate Cancer Samples using the SOLiD^{TM} 4 platform.
R. Menon, S.Perner.
Deutsches Prostatakarzinomkonsortium (DPKK),
Herne, Germany 2011. Platform presentation

9. Next Generation Sequencing**.**
R Menon.
63. Deutschen Gesellschaft für Urologie (DGU),
Hamburg 2011, Platform Presentation.

10. Genome-wide Massively Parallel Sequencing using SOLiD^{TM} 4 of formalin fixed paraffin embedded prostate cancer tissue
R. Menon, P. Nikolov, M Braun, V Scheble, F Fend, D

Boehm, S Biskup, S Perner
96 Jahrestagung der Deutschen Gesellschaft fur Pathologie (DGP), Leipzig, 2011, Platform Presentation.

11. Genome-wide Massively Parallel Seqencing using SOLiD™ of formalin fixed paraffin embedded prostate cancer tissue
R. Menon, P. Nikolov, M Braun, V Scheble, F Fend, D Boehm, S Biskup, S Perner
Changing Landscape of the Cancer Genome, Keystone Symposium, Boston, USA, 2011. Poster Presentation

12. Determining the Protein Profile of Prostate Cancer Samples harboring the ERG rearrangement using MADI Imaging Mass Spectrometry
R. Menon, K Schwamborn, P NIkolov, M Braun, R Caprioli, S Perner
96 Jahrestagung der Deutschen Gesellschaft fur Pathologie (DGP), Leipzig, 2011. Poster presentation.

13. Determining the Protein Profile of Prostate Cancer samples harboring the *ERG* rearrangement using MALDI Imaging Mass Spectrometry
R. Menon, K Schwamborn, P NIkolov, M Braun, R Caprioli, S Perner
Congress of the United States and Canadian Academy of Pathology (USCAP),
San Antonio, USA 2011. Platform presentation.

14. NKX3.1, ERG and AR define genetic alteration patterns correlating with tumor progression in prostate cancer
R Menon, V Scheble, G Scharf, P Nikolov, K Petersen, F Fend, M Reischl, S Perner
96 Jahrestagung der Deutschen Gesellschaft fur Pathologie (DGP), Leipzig, 2011. Poster presentation.

15. Introducing a Next Generation Sequencing Pipeline to Study Molecular Biology of Prostate Cancer (PCa).
R. Menon, S.Perner.
Deutsches Prostatakarzinomkonsortium (DPKK),
Saarland, Germany 2010. Platform presentation.

Grants and Scholarships:

1. **GlaxoSmithKline Grant** for attending the 'Tumor Invasion and Metastasis' Meeting- AACR
   San Diego, USA 2013

2. **International Graduate School of Theoretical and Experimental Medicine – THEME**- The Best Talk Award'
   Bonn, Germany 2012

3. **Bonner Forum Biomedizin** Grant for 'The Best Talk Award'
   Bonn, Germany 2012

4. **GlaxoSmithKline Grant** for attending the 'Advances in Prostate Cancer Research' Meeting- AACR
   Florida, USA 2012

5. **Scholar-In-Training Award** by the American Association of Cancer Research for attending the 'Advances in Prostate Cancer Research' Meeting
   Florida, USA 2012

6. **GlaxoSmithKline Grant** for attending the 'Changing Landscape of the Cancer Genome – Keystone Symposium',
   Boston, USA 2011

7. **Bonner Forum Biomedizin** Grant for attending the 96 Jahrestagung der Deutschen Gesellschaft fur Pathologie (DGP), Leipzig, Germany 2011

8. **Erasmus Mundus European Master Scholar** for a Masters in Animal Breeding and Genetics, Germany, France and Netherlands, 2007-2009

9. **Bangalore University 5th Rank**,
   M.Sc. Biotechnology
   India, 2007- 2009